Tettonica a zolle, il sistema e i tipi di margini di placche

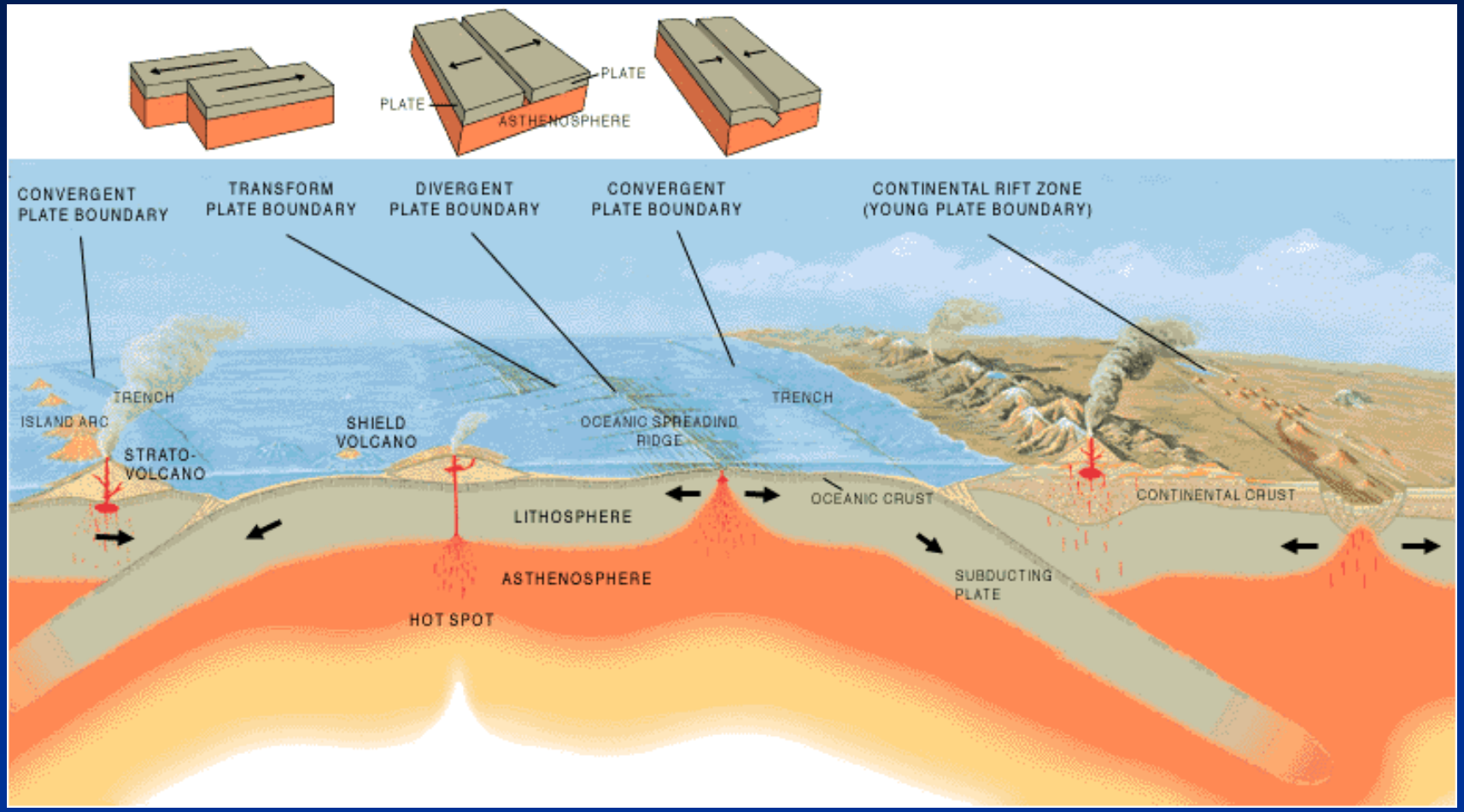

Da "The dynamic Earth" in USGS Web Site

Immagini e fotografie tratte da:

- Armijo R., Lacassin R., Coudurier-Curveur A., Carrizo D., 2015. Coupled tectonic evolution of Andean orogeny and global climate. Earth-Science Reviews, 143, 1–35
- Catuneanu O., Sweet A.R., Miall A.D., 2000. Reciprocal stratigraphy of the Campanian-Paleocene Western Interior of North America. Sedimentary Geology, 134, 235-255.
- Chen W.-P., Brudzinski M.R., 2001. Evidence for a Large-ScaleRemnant of SubductedLithosphere Beneath Fiji. Science, 292.
- Doglioni C., 1994. Elementi di Tettonica. Editrice Il Salice.
- Doglioni C., Harabaglia P., Merlini S., Mongelli F., Peccerillo A., Piromallo C., 1999. Orogens and slabs vs. their direction of subduction. Earth-Science Reviews, 45, 167–208.
- Guinot D., Segonzac M., 2018. A review of the brachyuran deep-sea vent community of the western Pacific, with two new species of Austinograea Hessler & Martin, 1989 (Crustacea, Decapoda, Brachyura, Bythograeidae) from the Lau and North Fiji Back-Arc Basins. Zoosystema, 40, 75-107.
- Homza T.X., Wallace W.K., 1995. Geometric and kinematic models for detachment folds with fixed and variable detachment depths. Journal of Structural Geology, 17, 575-588.
- Horton B.K., 2018. Sedimentary record of Andean mountain building. Earth-Science Reviews, 178, 279–309
- Lillie R.J., 2005. Parks and Plates: The Geology of our National Parks, Monuments and Seashores. W. W. Norton and Company.
- Marshak S., 2001. Earth: Portrait of a Planet. W. W. Norton & Comp., New York.
- McClay K.R., Coward M.P., 1981. The Moine Thrust Zone: an overview. Geological Society, London, Special Publications, 9, 241-260.
- Merle O., 1994. Emplacement Mechanisms of Nappes and Thrust Sheets. Springer.
- Mitra S., 2003. A unified kinematic model for the evolution of detachment folds. Journal of Structural Geology, 25, 1659–1673.
- Moore J.C., Lundberg N., 1986 Tectonic Overview of DSDP transects of forearcs. Geological Society of America Memoir, 166.
- Moore G.F., et al., 2014. IODP Expedition 338: NanTroSEIZE Stage 3: NanTroSEIZE plate boundary deep riser 2. Scientific Drilling, 17, 1-12.
- Moore G.F. et al., 2009. Structural and seismic stratigraphic framework of the NanTroSEIZE Stage 1 transect. In: Proceedings of the Integrated Ocean Drilling Program, Volume 314/315/316.
- Price, R.A., 1981. The Cordilleran foreland thrust and fold belt in the southern Canadian Rocky Mountains. Geological Society, London, Special Publications, 9, 427-448
- Price N.J., Cosgrove J.W., 1990. Analysis of Geological Structures. Cambridge University Press.
- Ramsay J. G., Huber M. I., 1987. The Techniques of Modern Structural Geology. Volume 2: Folds and Fractures. Academic Press Inc.
- Sak P.B. et al., 2012. Unraveling the central Appalachian fold-thrust belt, Pennsylvania: The power of sequentially restored balanced cross sections for a blind fold-thrust belt. Geosphere, 8 (3), 1–18.
- Schmid S.M., Fügenschuh B., Kissling E., Schuster R., 2004. Tectonic map and overall architecture of the Alpine orogen. Eclogae geol. Helv., 97, 93-117.
- Schmid S.M., Pfiffner O.A., Froitzheim N., Schönborn G., 1996. Geophysical-geological transect and tectonic evolution of the Swiss-Italian Alps . Tectonics, 15, 1036-1064.
- Shaw J. & Johnston S.T., 2016. Terrane wrecks (coupled oroclines) and paleomagnetic inclination anomalies. Earth-Science Reviews, 154, 191–209.
- Strasser et al., 2012. Scientific Drilling of Mass-Transport Deposits in the Nankai Accretionary Wedge: First Results from IODP Expedition 333. In: Submarine Mass Movements and Their Consequences, Advances in Natural and Technological Hazards Research 31, 671-681.
- Suppe J., 1985. Principles of Structural Geology. Prentice-Hall Inc.
- van der Pluijm B., Marshak S., 2004. Earth Structure: An Introduction to Structural Geology and Tectonics, Second Edition. WW Norton & Company.
- Zoetemeijer R. (1993) Tectonic Modelling of Foreland Basins: thin skinned thrusting, syntectonic sedimentation and lithospheric flexure. Ph.D. thesis, Free University of Amsterdam.

Tipo di margini di placca e ambienti geodinamici

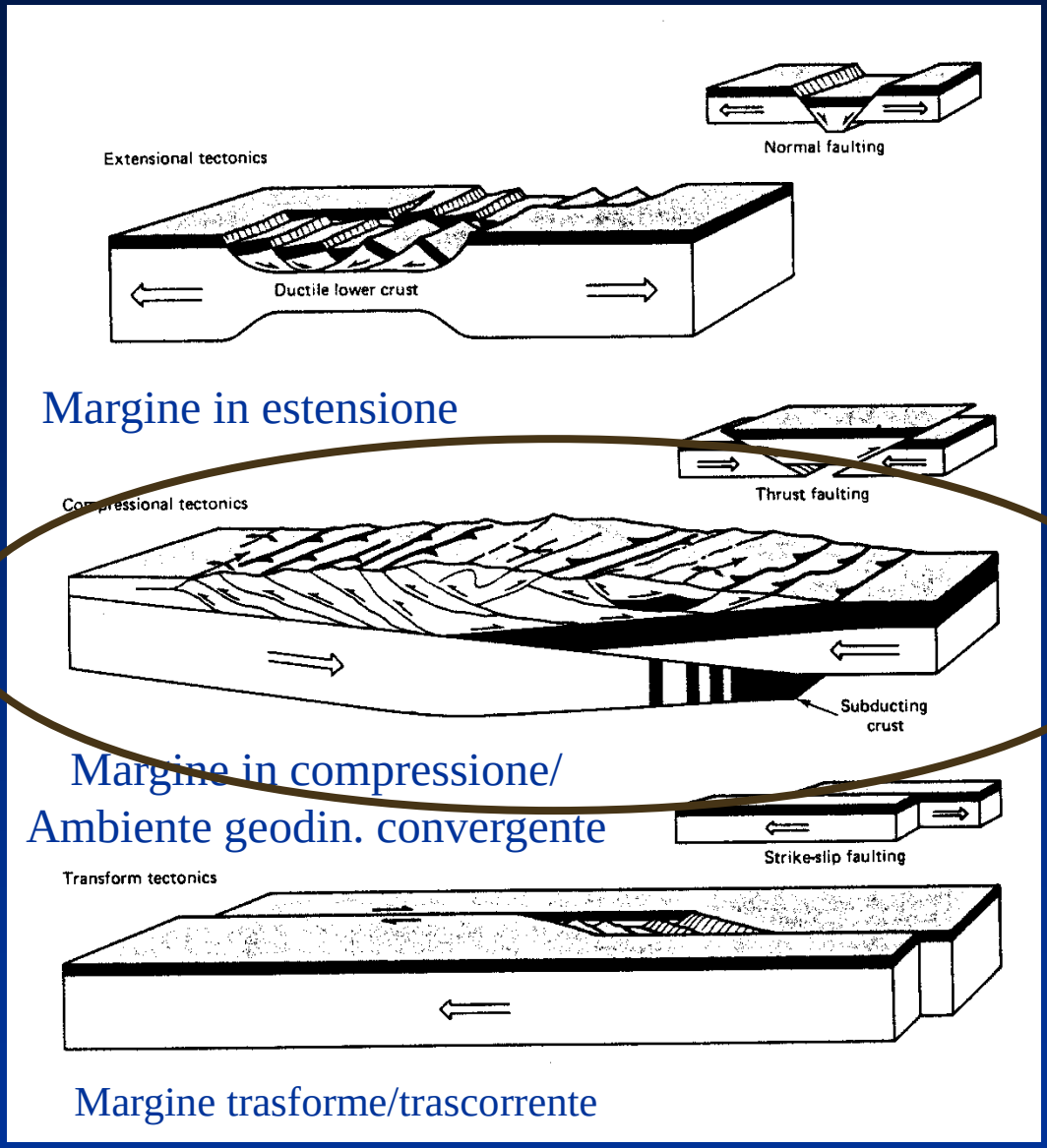

Da Suppe, 1985

Tipi di orogeni

- Catene collisionali

- Prismi di accrezione
  - Tipo cordiliera o andino (margine occidentale delle Americhe)
  - Tipo Barbados-Marianne (arco insulare; es. Barbados, Tonga-Kermadek, Marianne)
  - Tipo ophiolitic back-arc (microcontinente, bacino di retroarco a crosta oceanica; es. Giappone)

Ambiente geodinamico convergente: catene collisionali

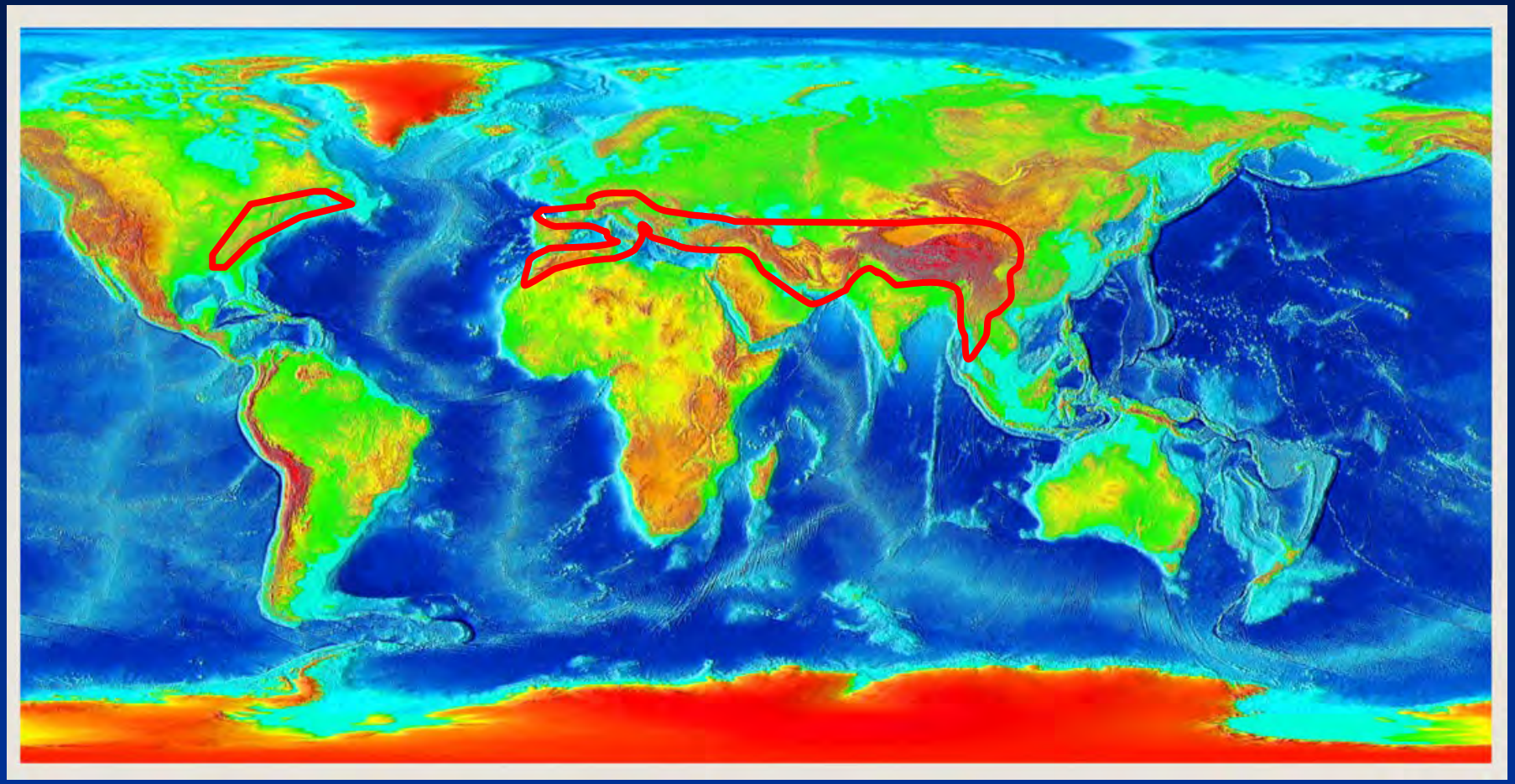

Shaded reliefs e batimetria da NOAA National Centers for Environmental Information (NCEI)

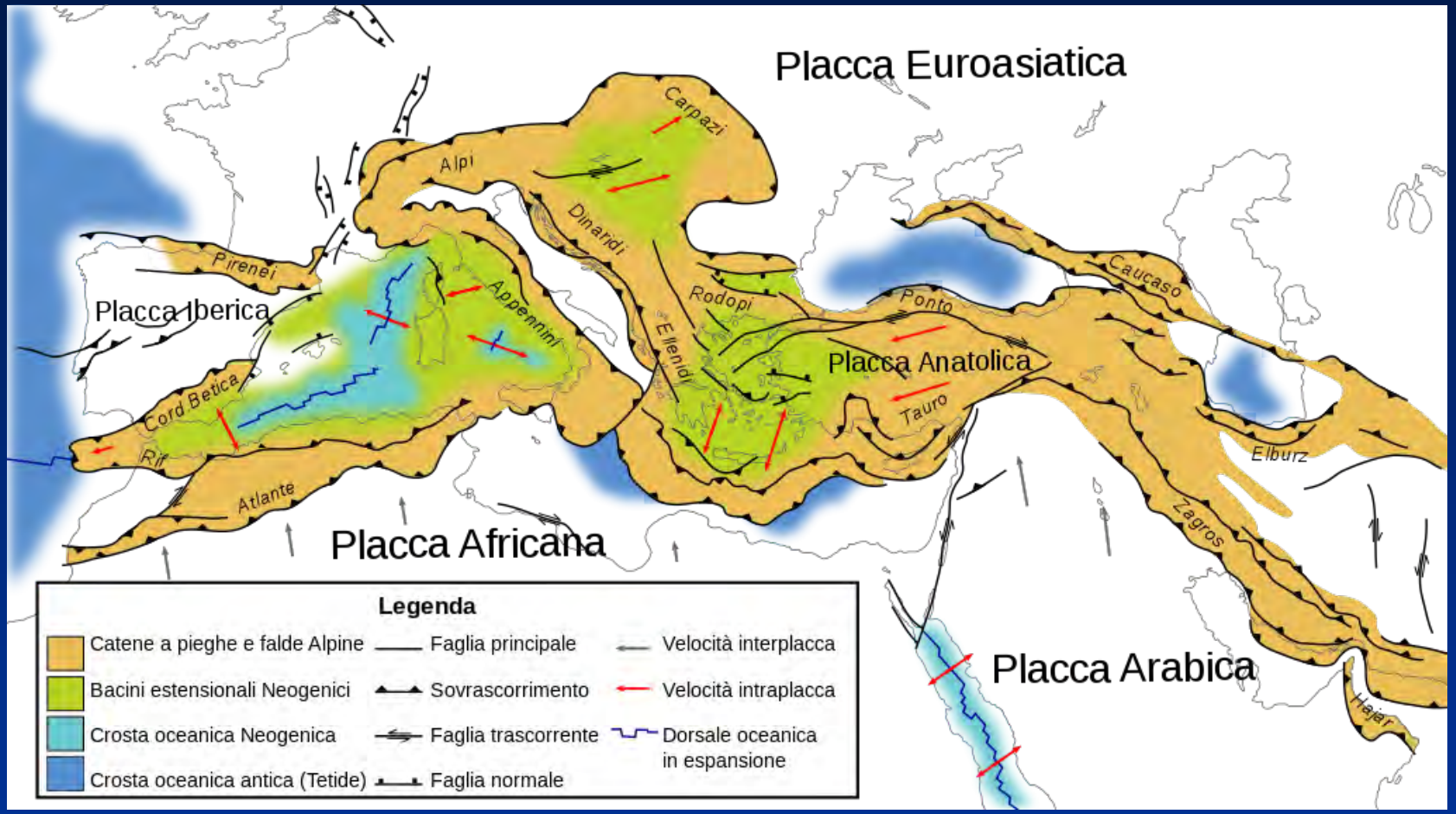

https://it.m.wikipedia.org/wiki/Geologia_delle_Alpi

Catene a doppia polarità: le Alpi

https://it.m.wikipedia.org/wiki/Geologia_delle_Alpi

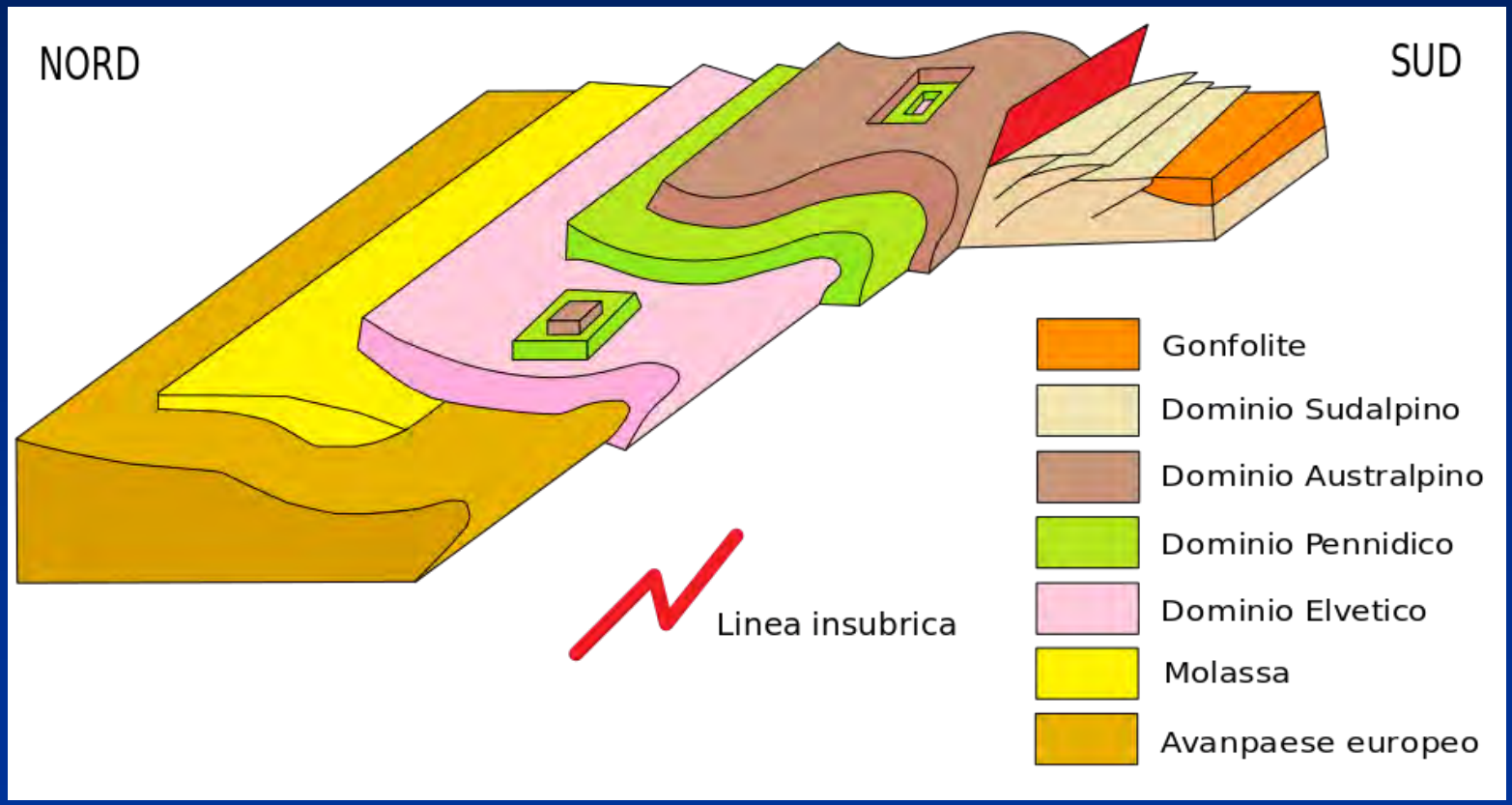

Catene a doppia polarità: le Alpi

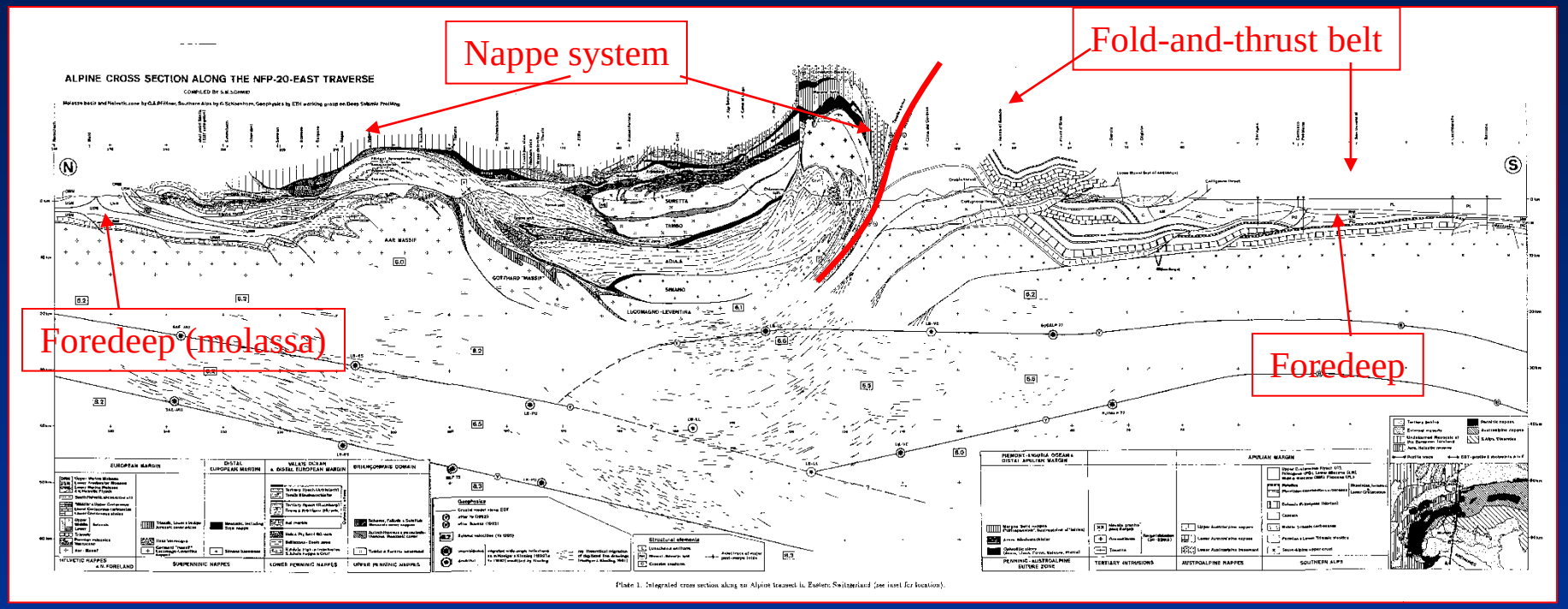

Da Schmid et al., 1996

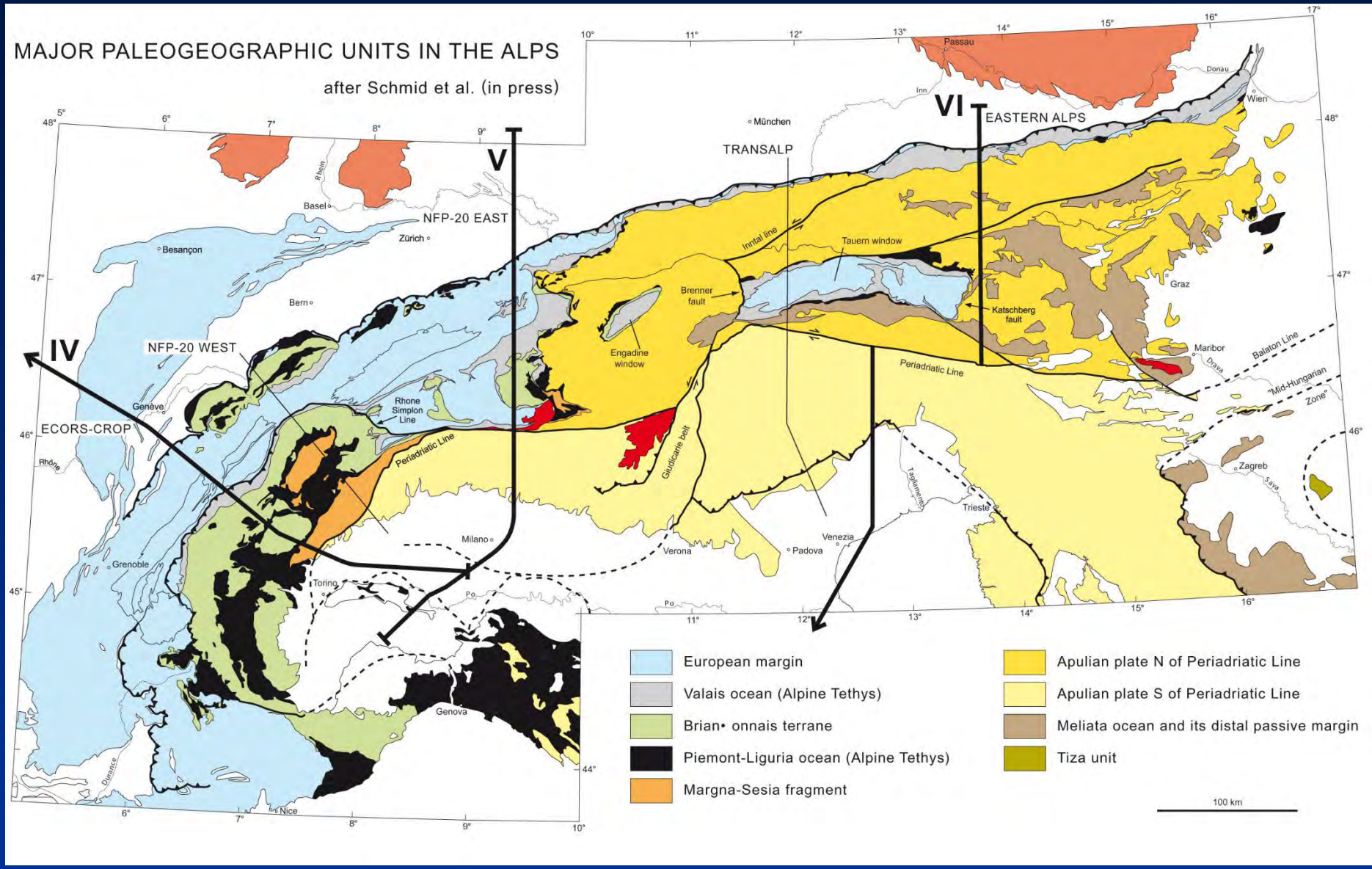

Da Schmid et al 2004

le Alpi: il sistema a falde

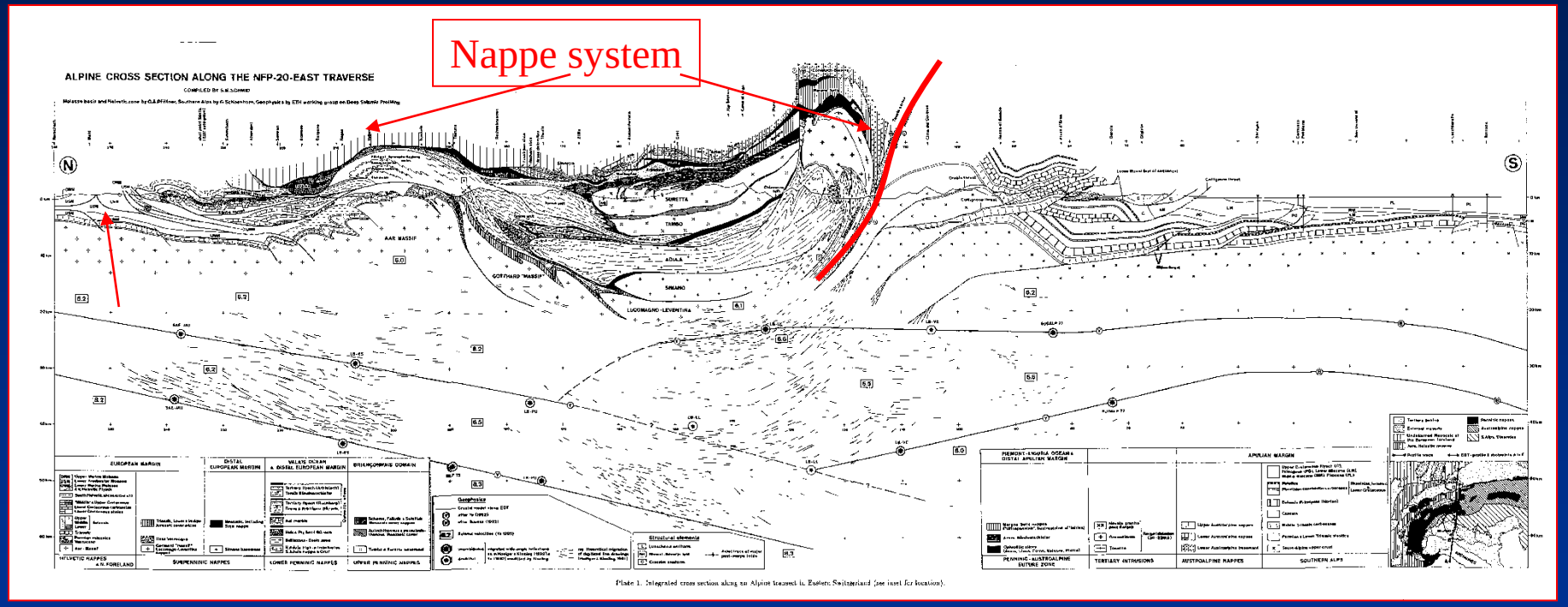

Da Schmid et al., 1996

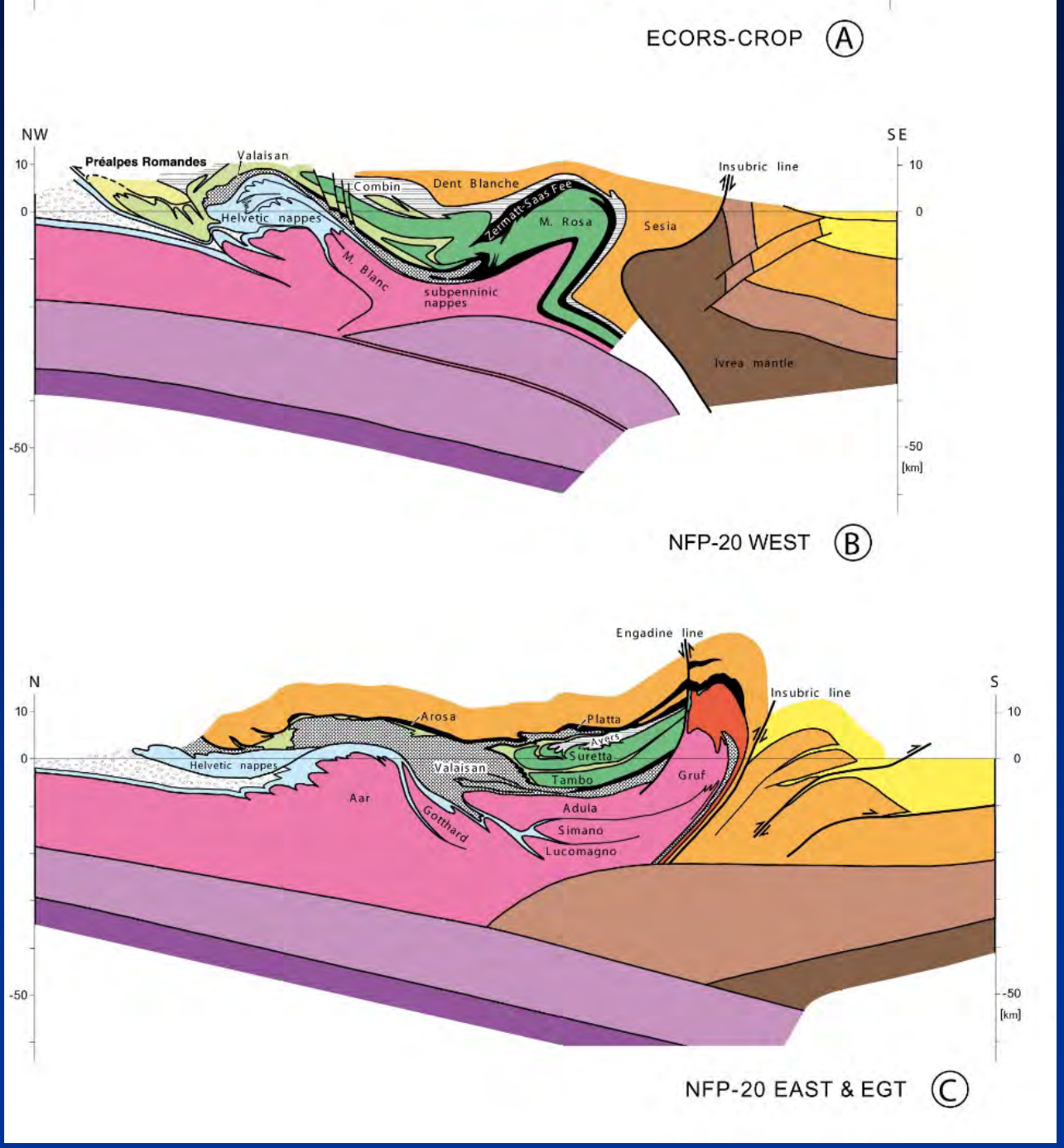

Da Schmid et al 2004

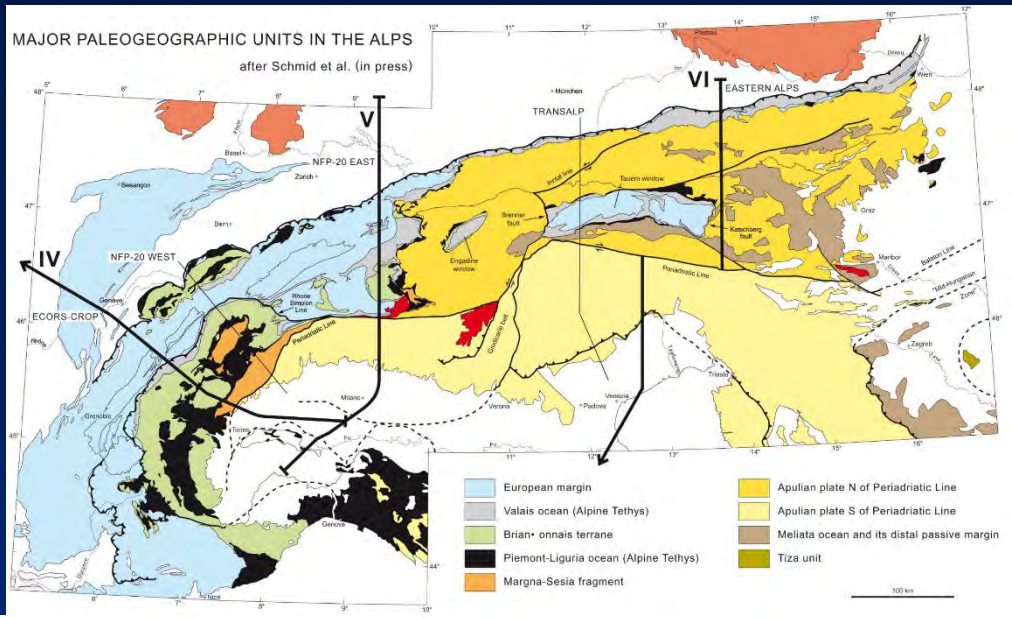

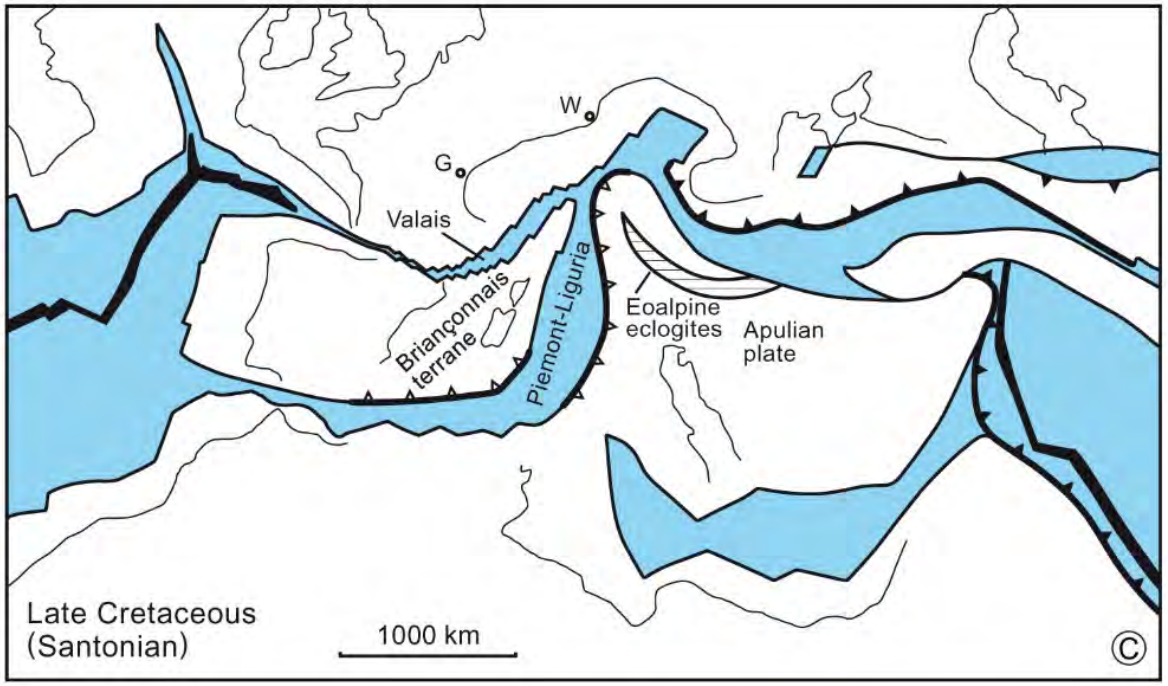

Da Schmid et al 2004

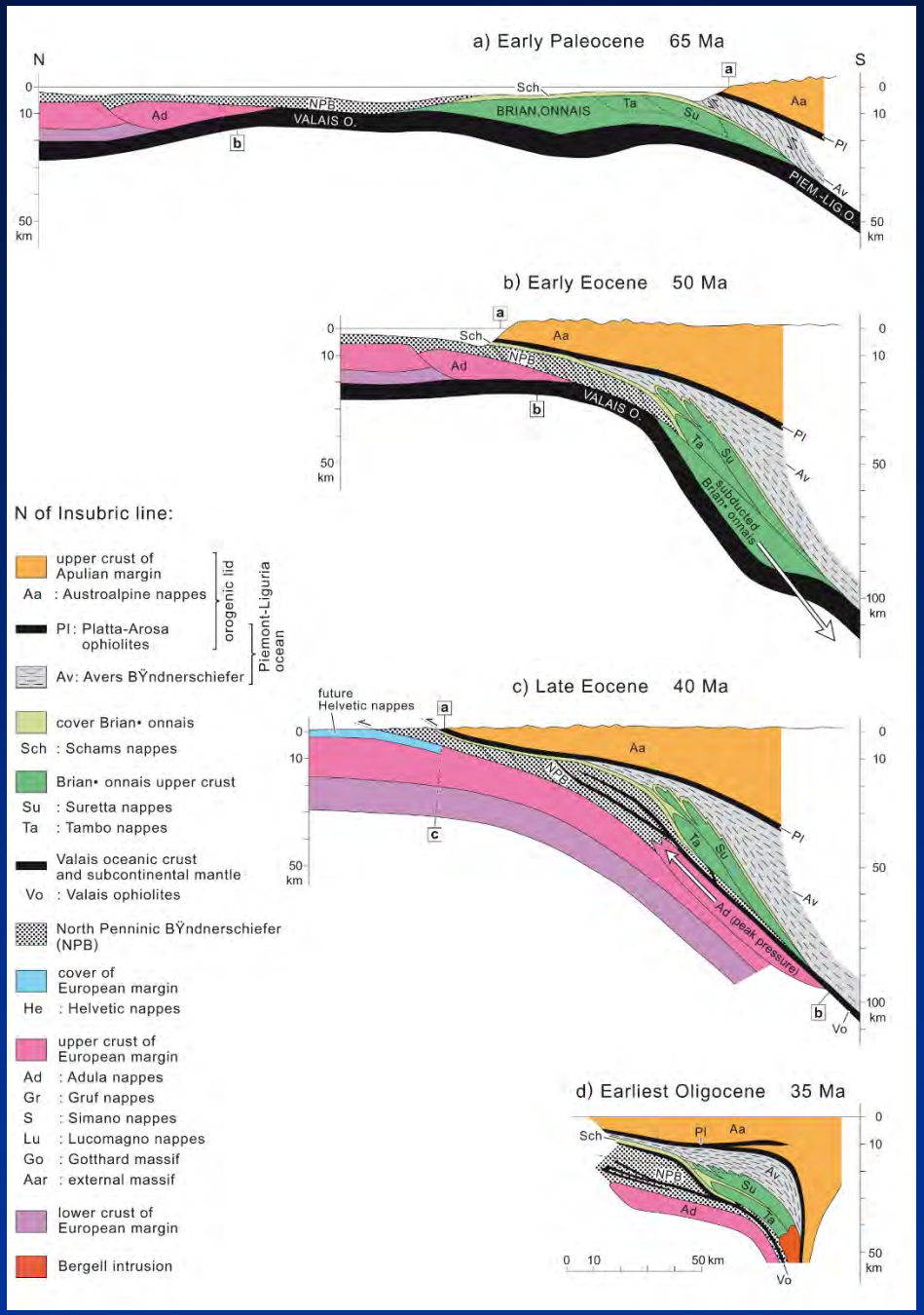

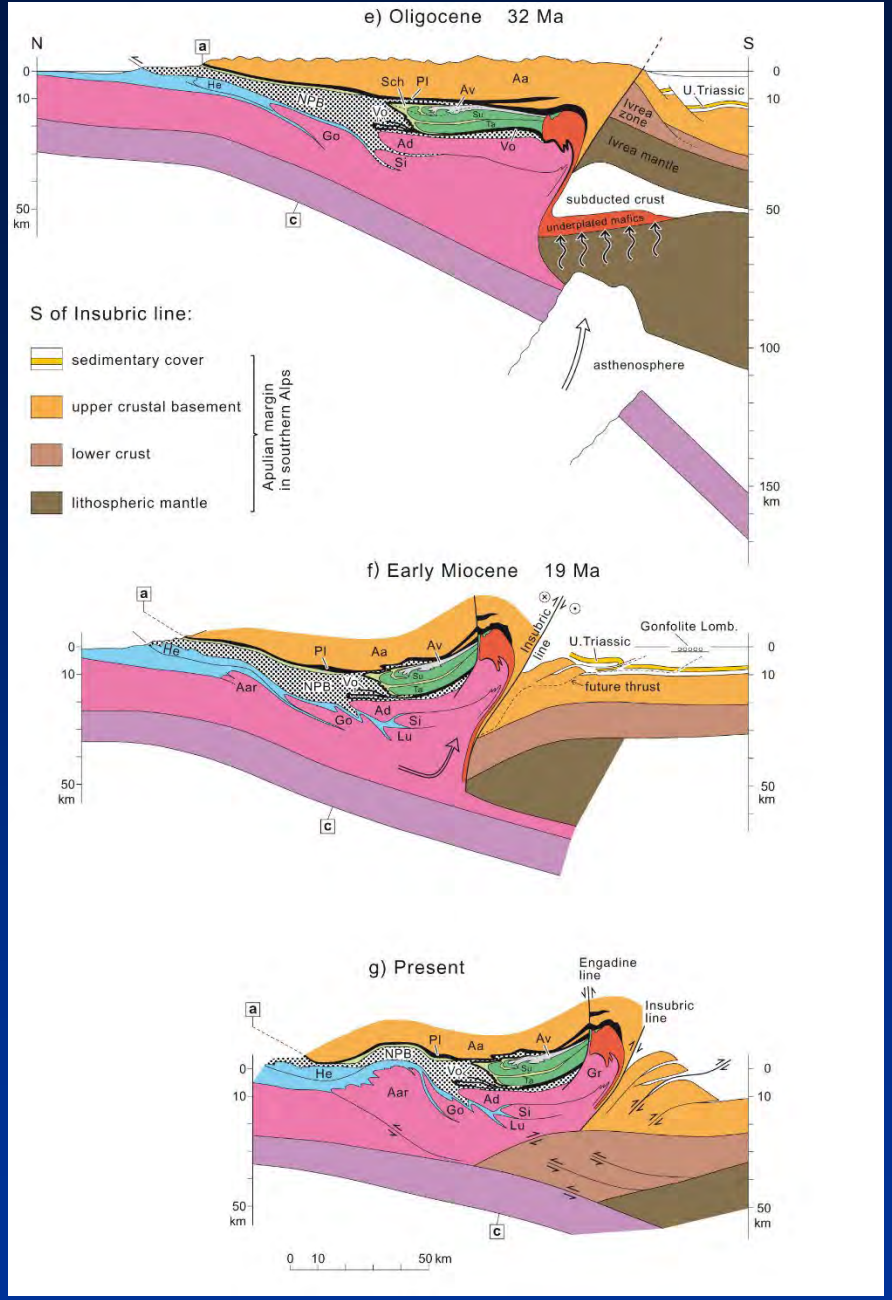

Da Schmid et al 2004

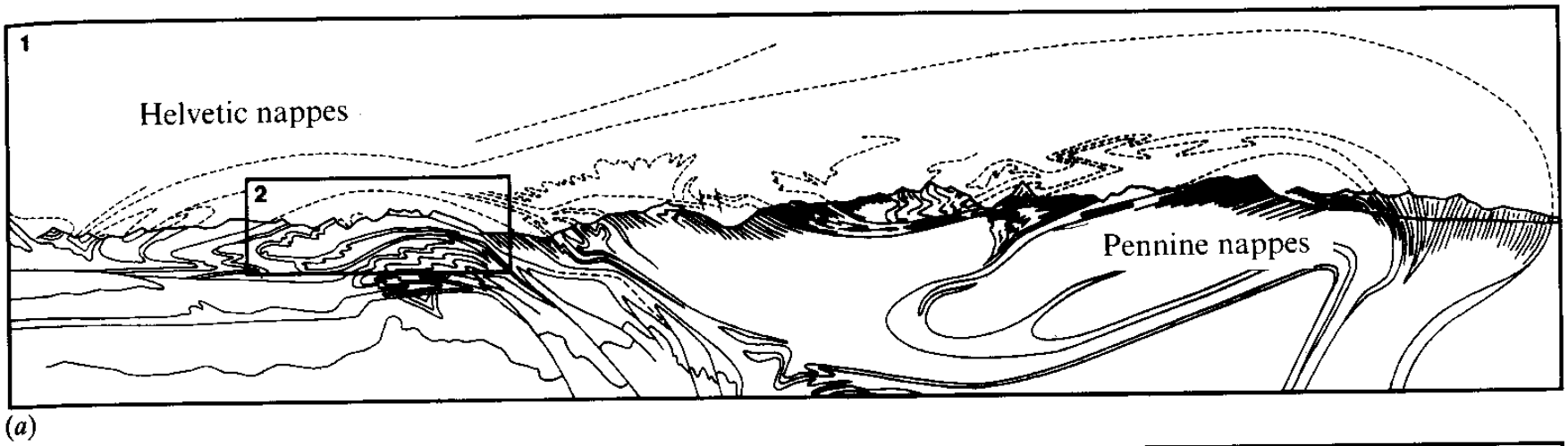

(a)

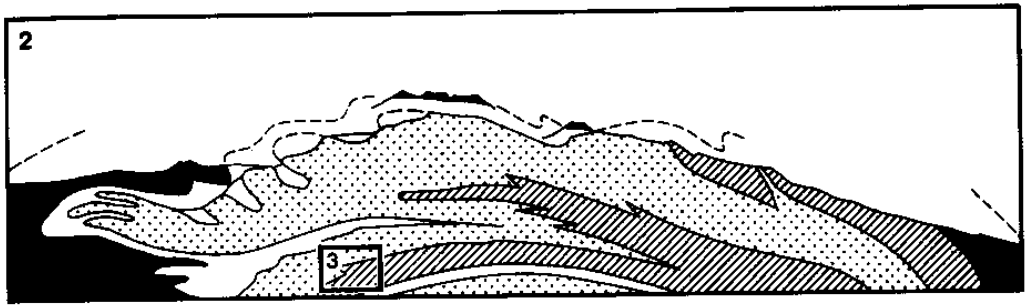

(b)

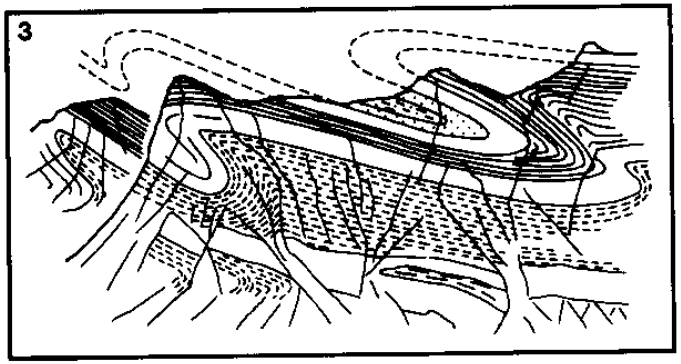

(c)

Da Price and Cosgrove, 1990

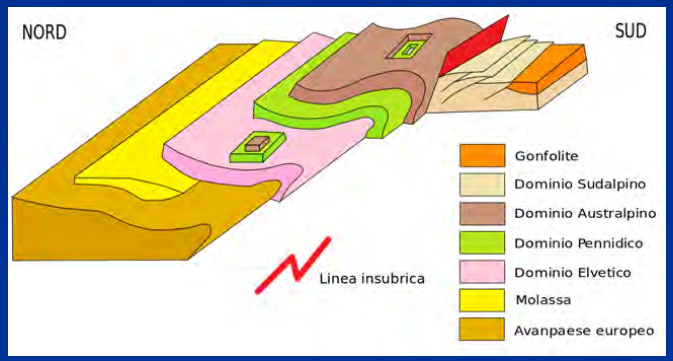

Le Alpi: sistema di falde (nappe system)

https://it.m.wikipedia.org/wiki/Geologia_delle_Alpi

Da Ramsay and Huber, 1987

Da Ramsay and Huber, 1987

Fig 113 _ Evoluzione di una nappe per piega coricata

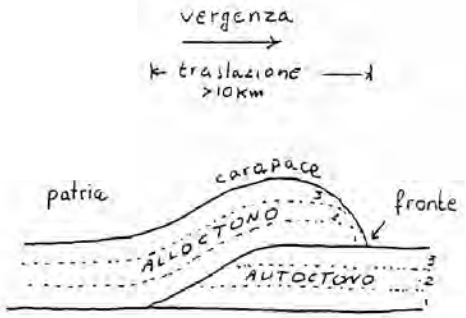

Fig 114 - Nomenclatura delle coltri di ricoprimento.

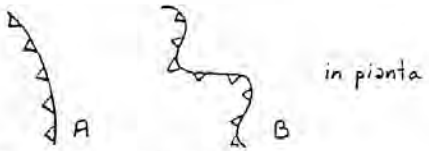

Fig. 115. A_ Fronte cilindrico
B. Digitazioni frontali

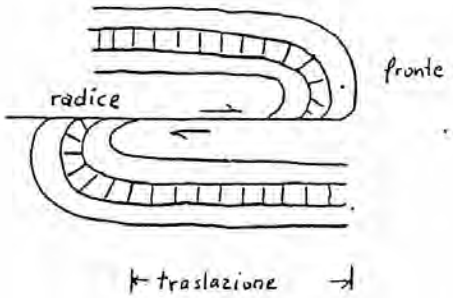

Fig. 116 - Zona di radice in piega-faglia coricata

Da Doglioni, 1994

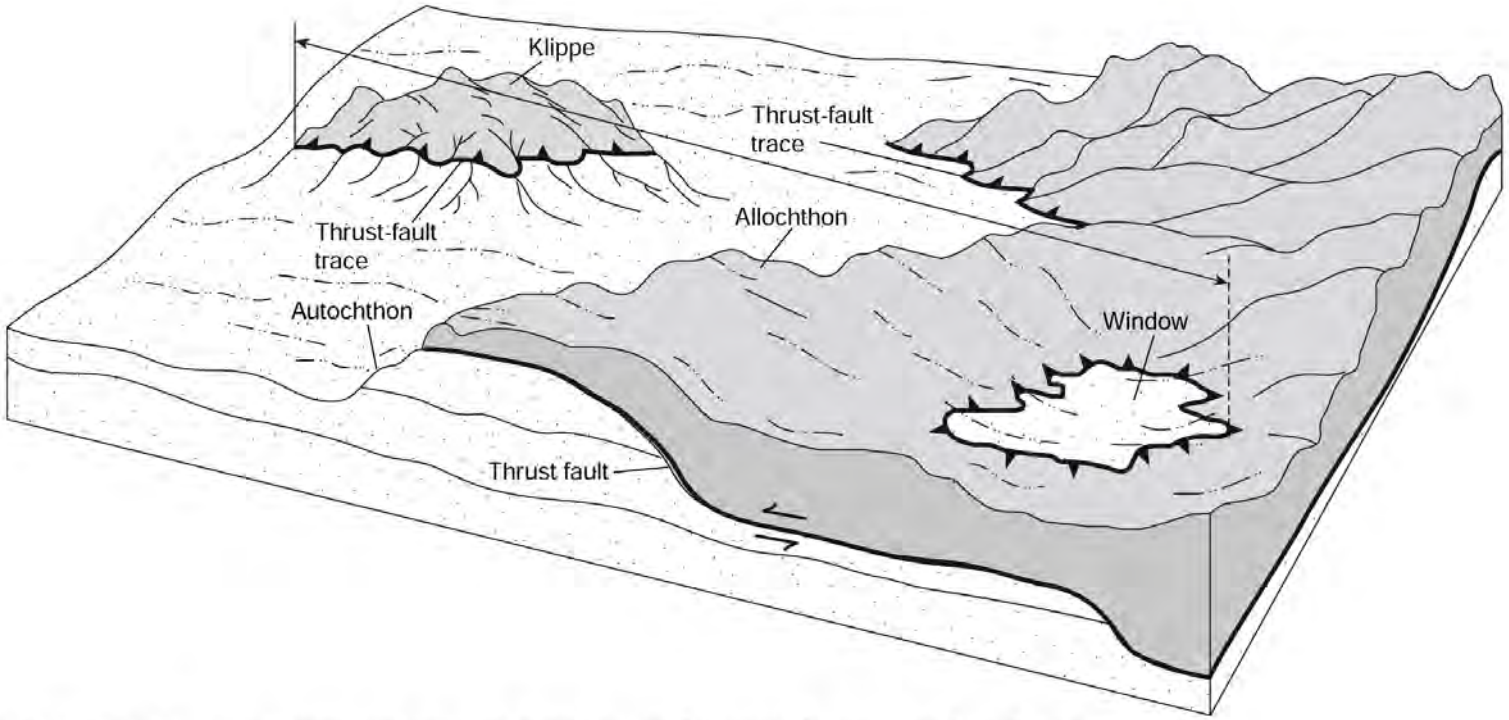

FIGURE 8.8 Block diagram illustrating klippe, window (or fenster), allochthon (gray), and autochthon (stippled) in a thrust-faulted region. Note that the minimum fault displacement is defined by the farthest distance between thrust outcrops in klippe and window.

Da van der Pluim & Marshak, 2004

le Alpi: avanfosse e *foreland fold and thrust belt* meridionale (Alpi Meridionali)

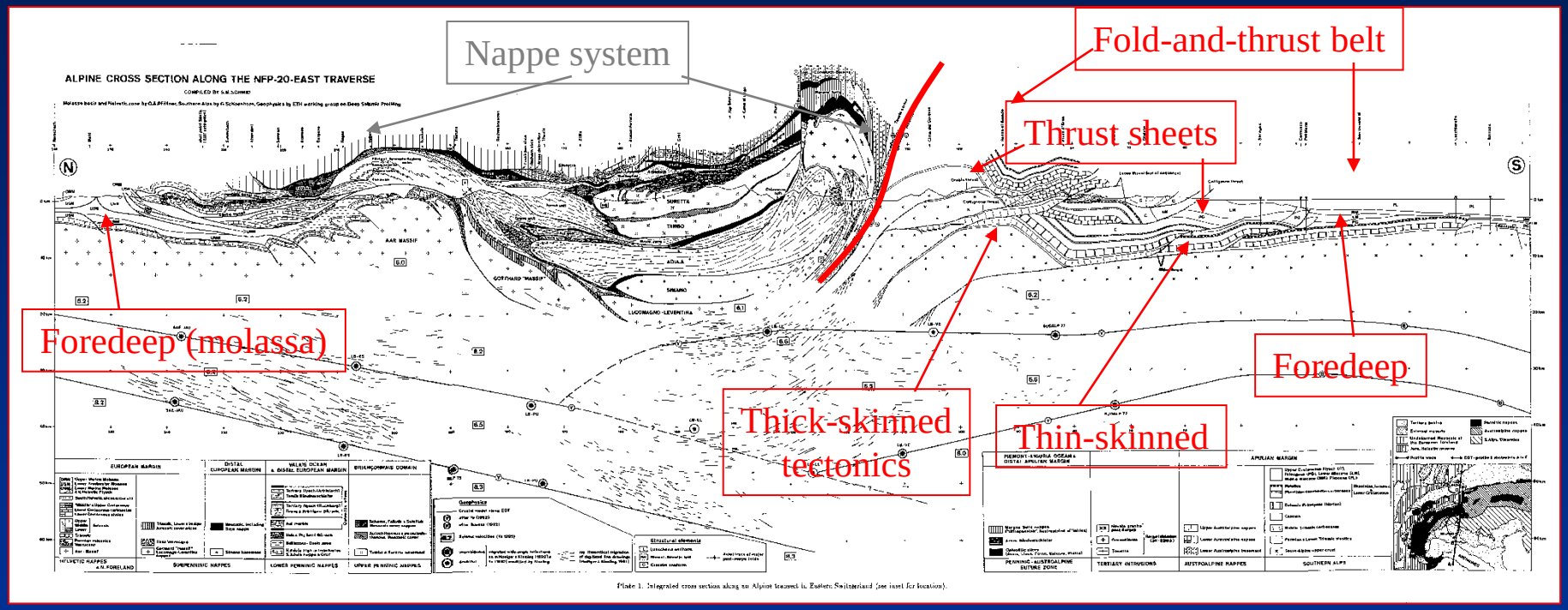

Da Schmid et al., 1996

Thick-skinned e thin-skinned tectonics, sistemi di falde = dicotomia tra basamenti e coperture

Accavallamenti e sovrascorrimenti: Taiwan

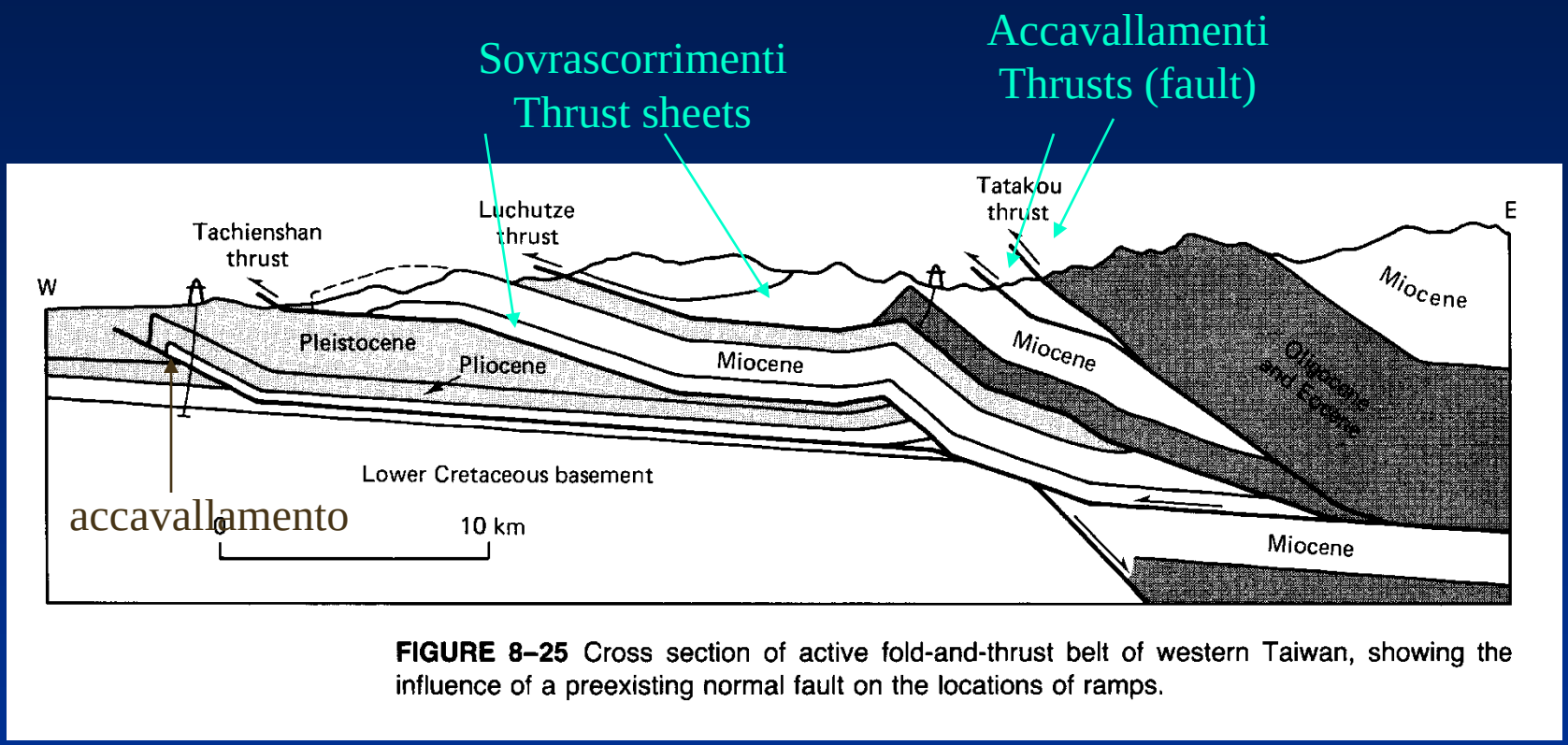

FIGURE 8–25 Cross section of active fold-and-thrust belt of western Taiwan, showing the influence of a preexisting normal fault on the locations of ramps.

Da Suppe, 1985

Accavallamenti, sovrascorrimenti: nomenclatura

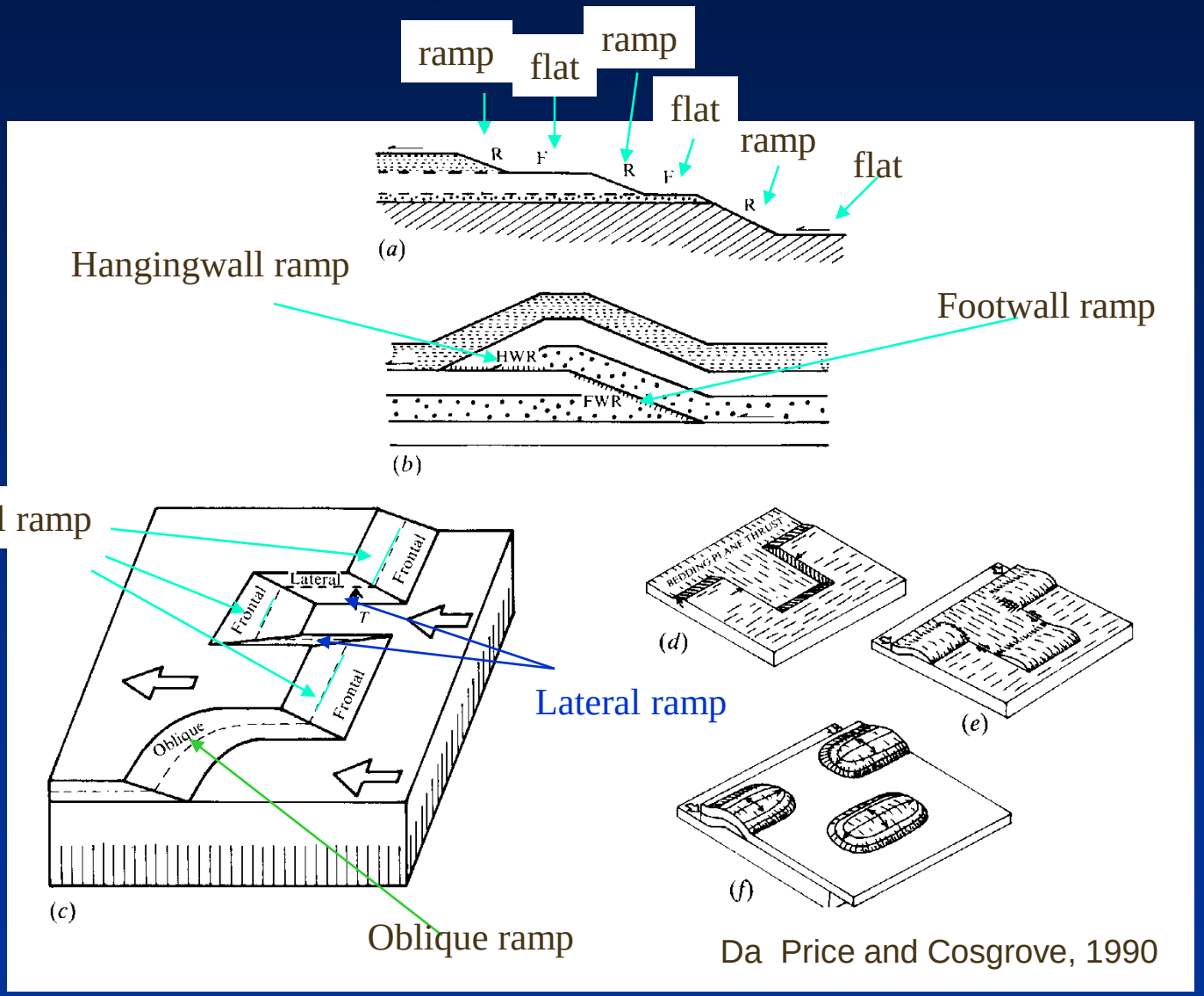

Da Price and Cosgrove, 1990

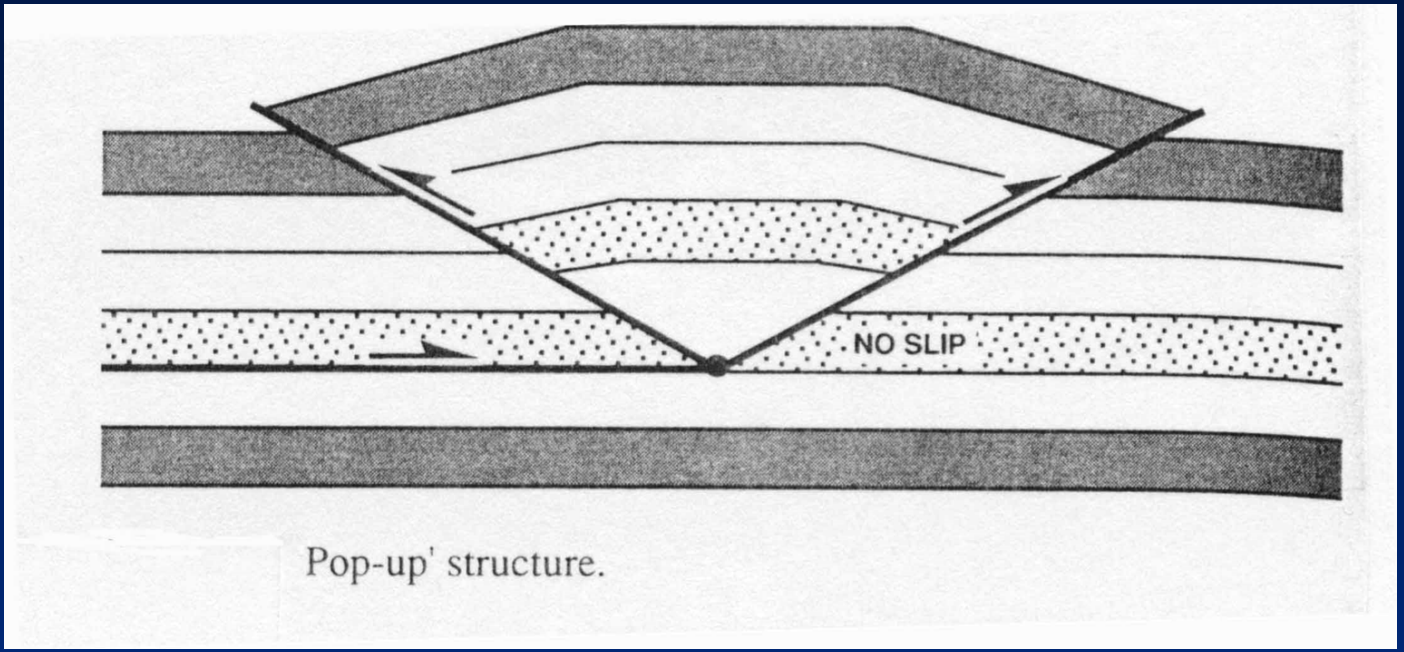

Pop-up' structure.

Da Suppe, 1985

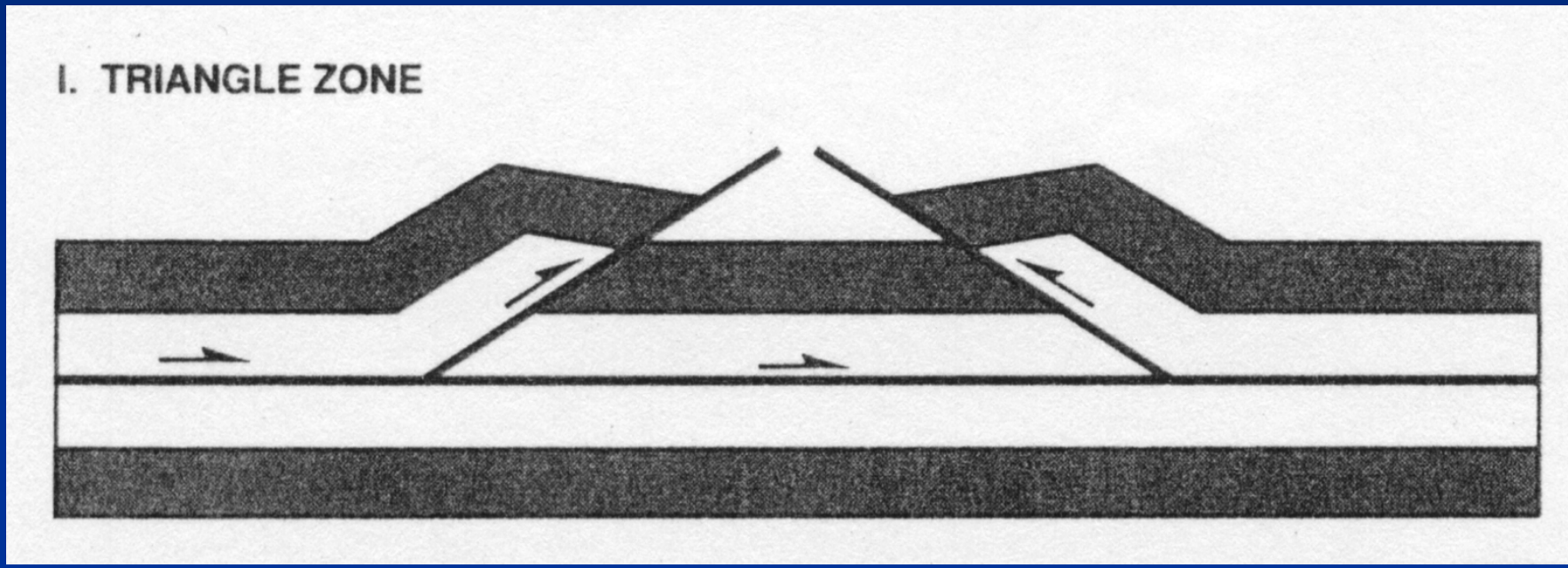

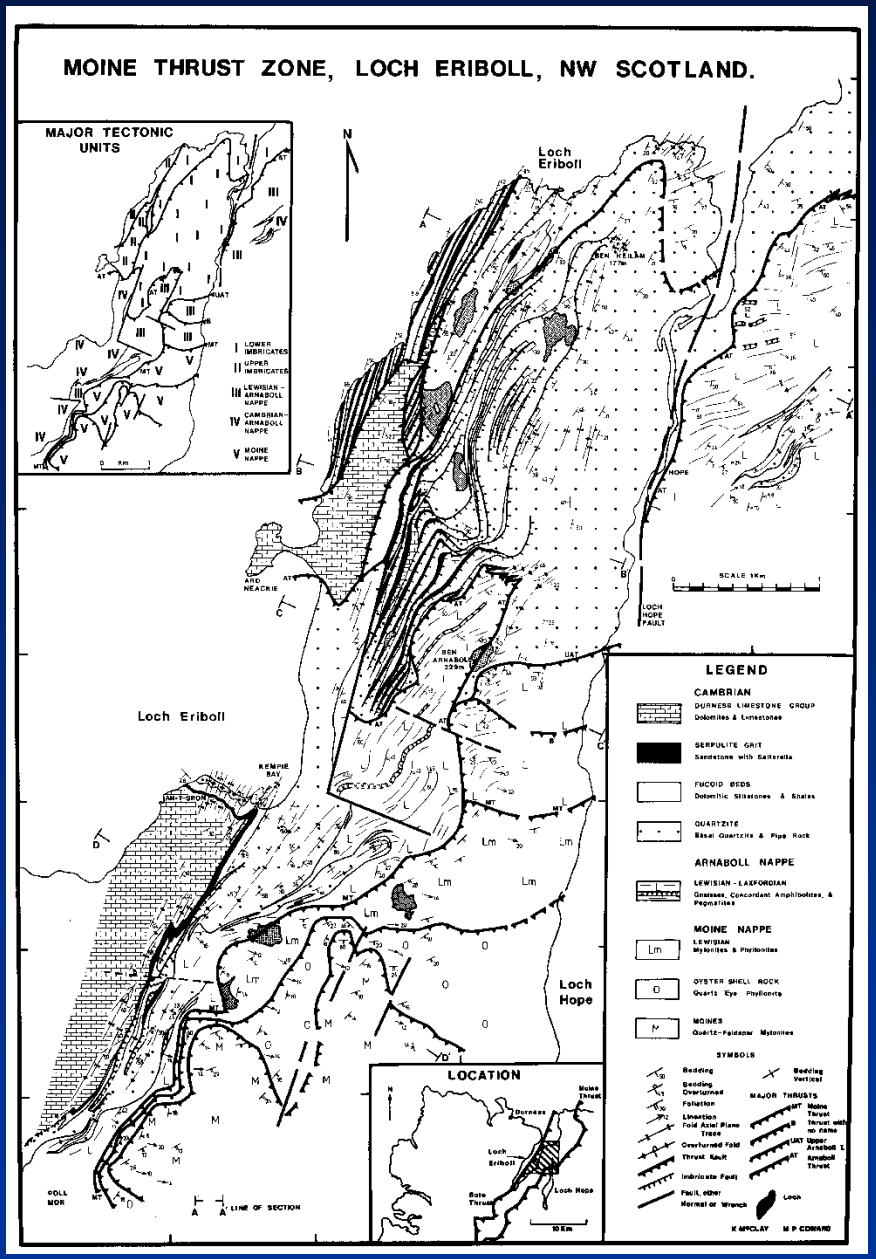

Thrust sheets e
Sistemi di duplex
Moine thrust, Scozia

Da McClay & Coward, 1981

Sistemi di duplex, Moine thrust

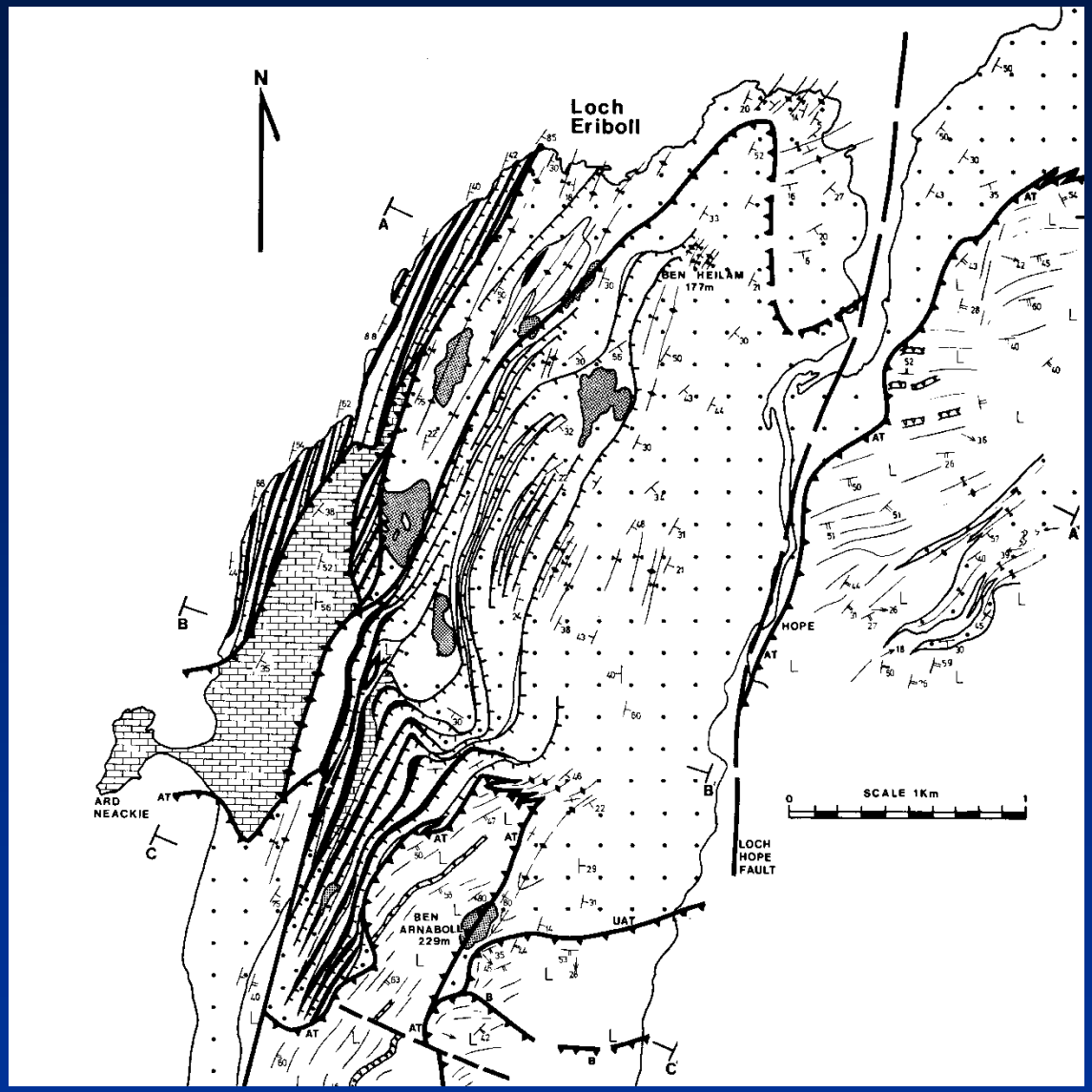

Da McClay & Coward, 1981

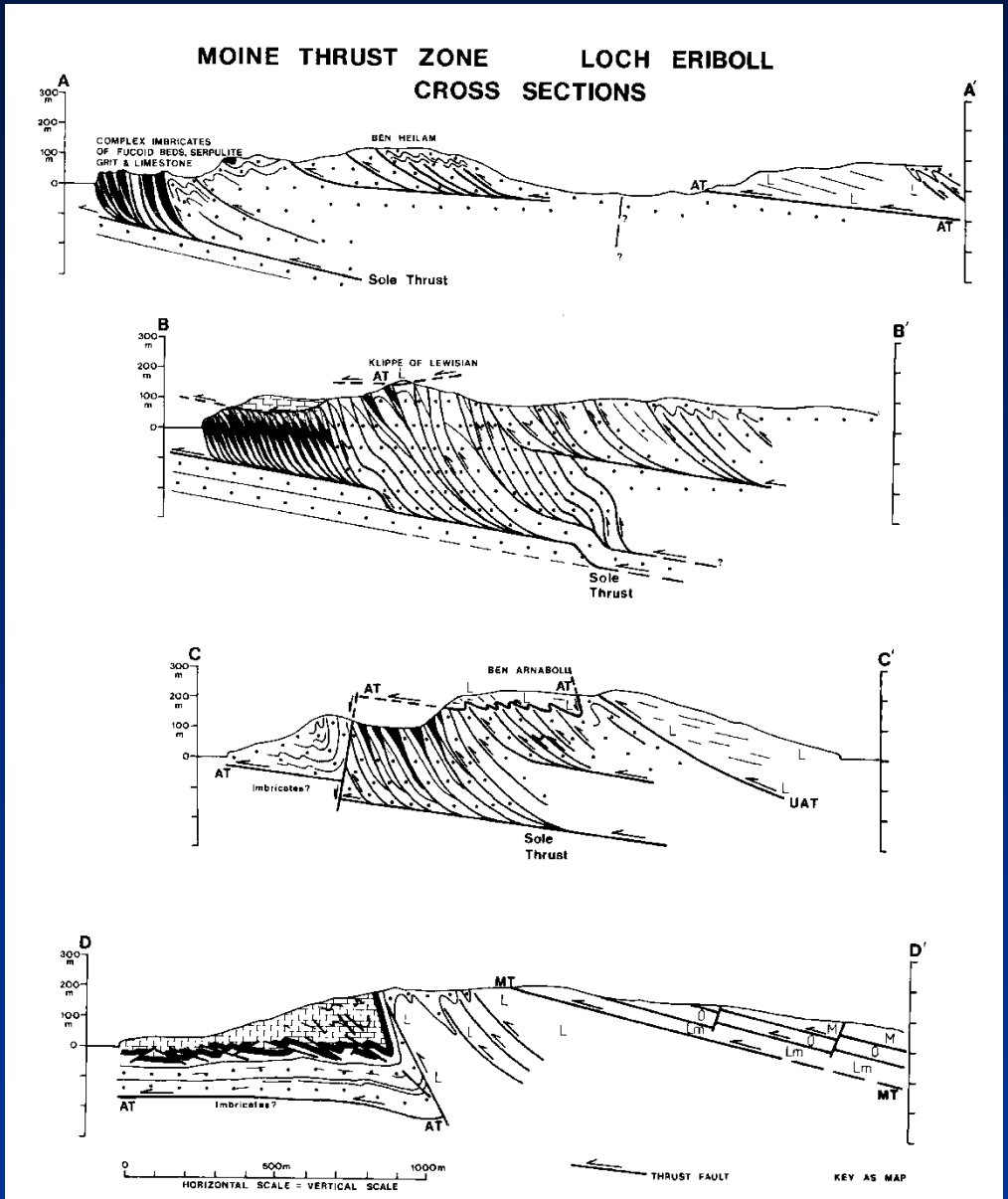

FIG. 3*b*. Cross sections A–D across the Moine Thrust Zone at Loch Eriboll.

Sistemi di duplex, Moine thrust

Da McClay & Coward, 1981

Geometria dei duplex, Moine thrust

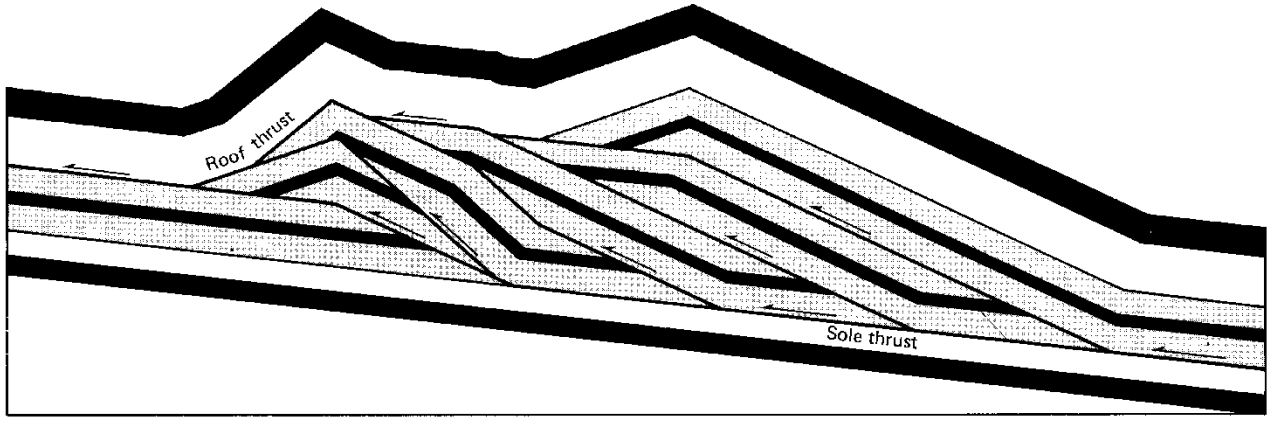

(a) Schematic duplex

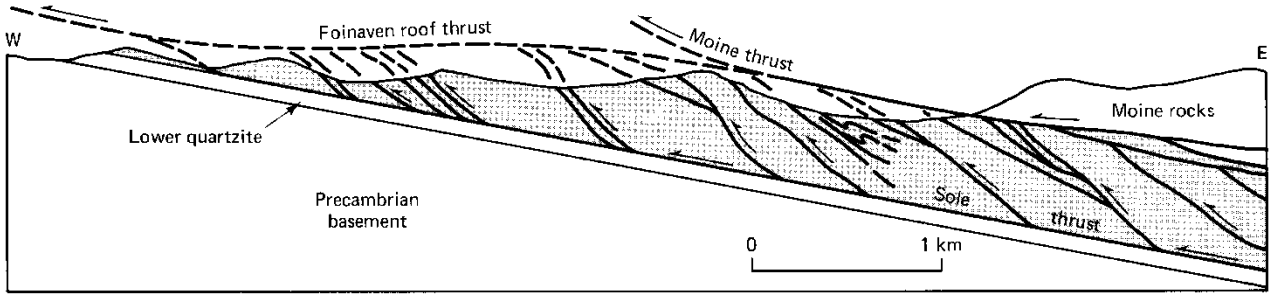

(b) *Eroded duplex, Scotland*

FIGURE 8–27 (a) Schematic drawing of a duplex structure. (b) Example of a duplex structure of the Moine thrust system, Scotland. (Cross section simplified after Elliott and Johnson, Trans. Roy. Soc. Edin., **71**, 69–96, 1980.)

Da Suppe, 1985

Sistemi di duplex: evoluzione

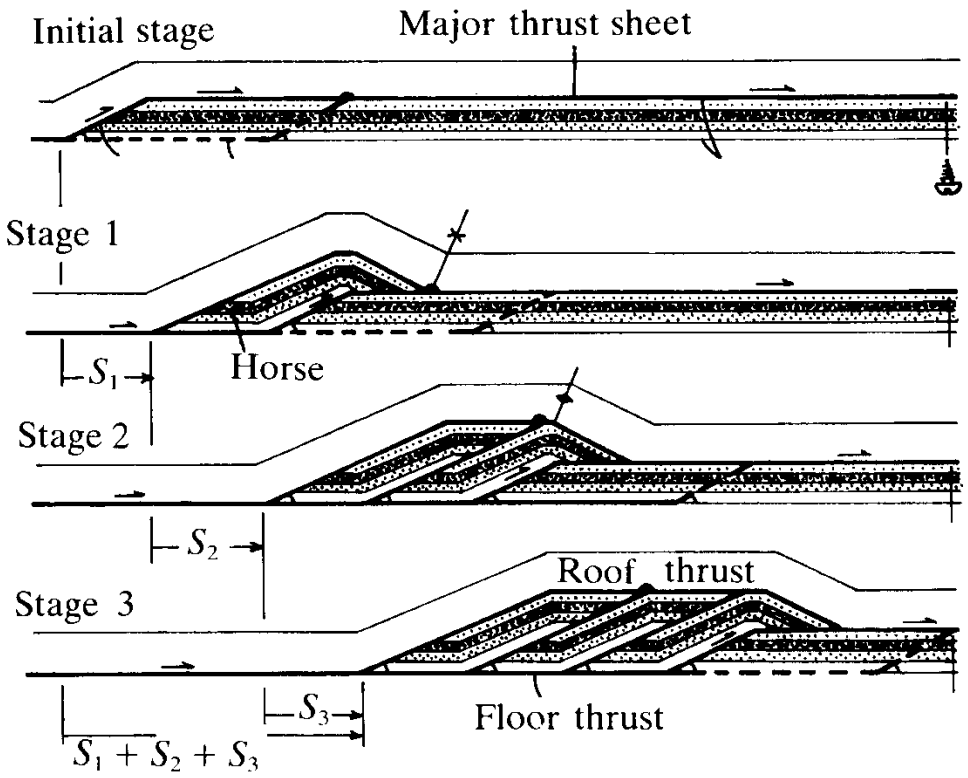

Fig. 7.6. The formation of a duplex by the progressive collapse of a footwall ramp. The roof thrust sheet undergoes a sequence of folding and unfolding. (After Boyer & Elliot, 1982.)

Da Price and Cosgrove, 1990

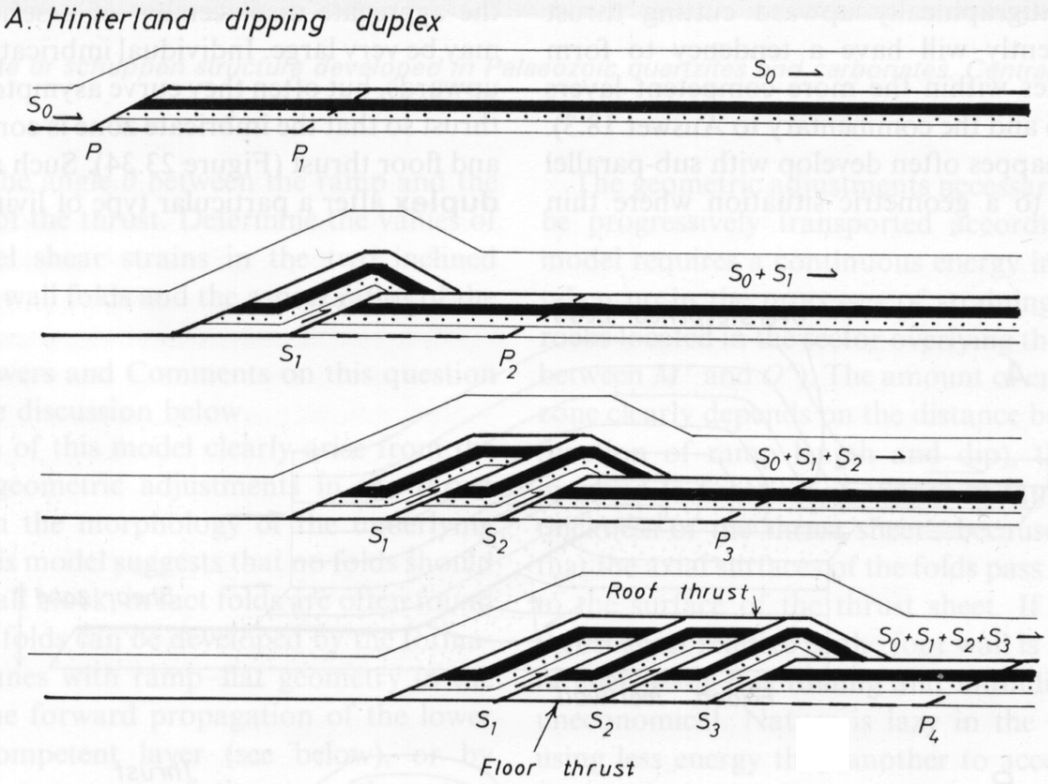

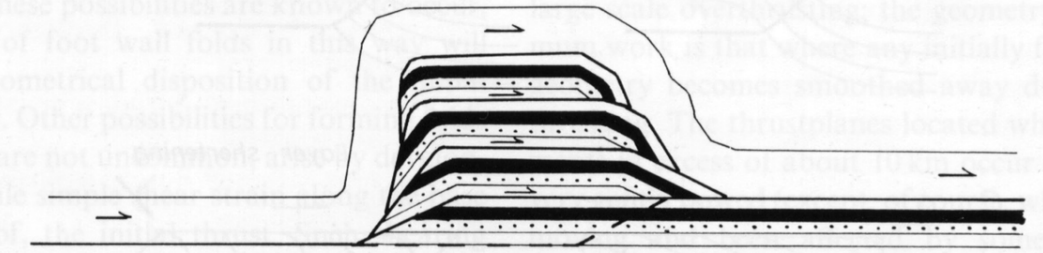

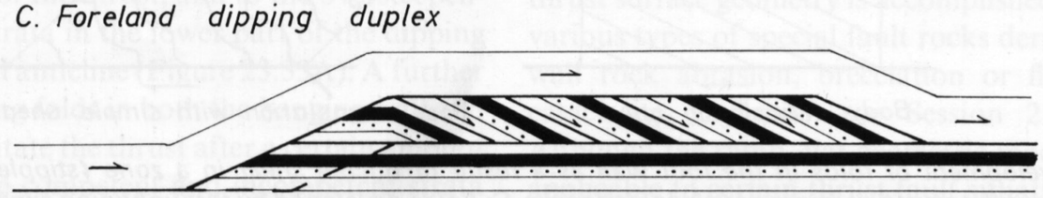

Da Ramsay and Huber, 1987

Associazioni di sovrascorrimenti-accavallamenti: Le Rocky Mountains

Le Rocky Mountains

Da Price, 1981

Cordiliera

Rocky Mountains

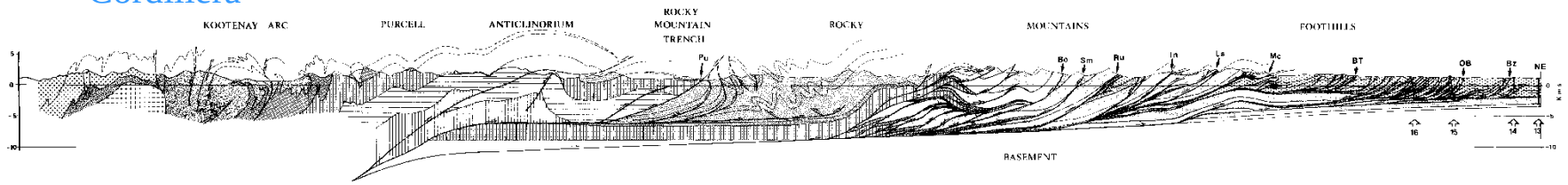

Cordiliera

Rocky Mountains

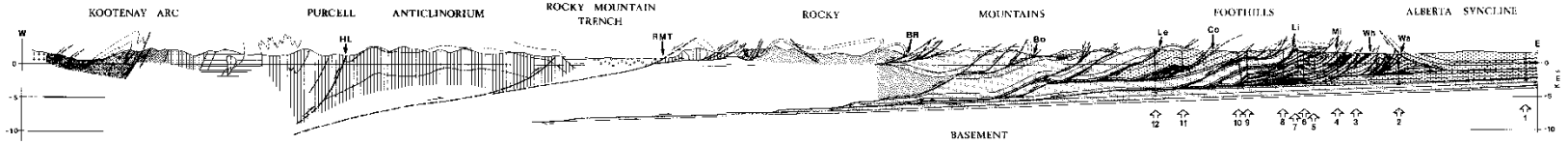

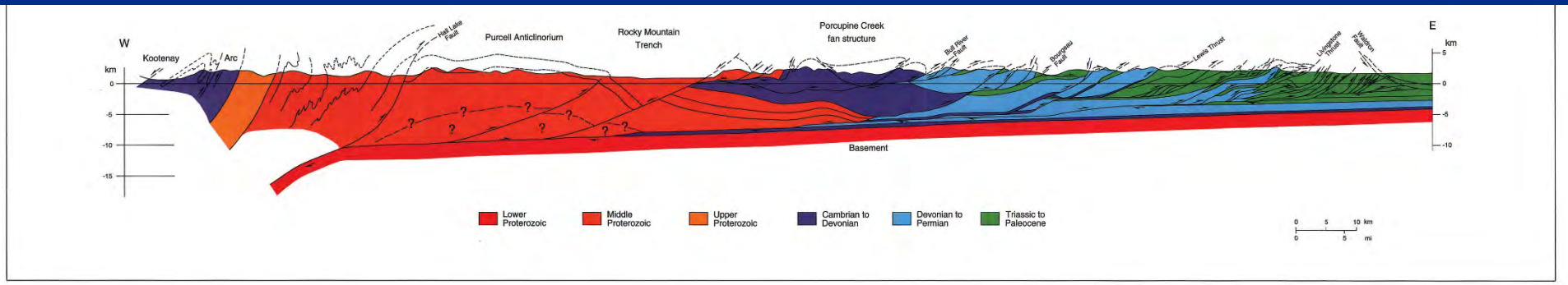

Da Price in Atlas of the Western Canada sedimentary basin, Alberta Geological Survey.

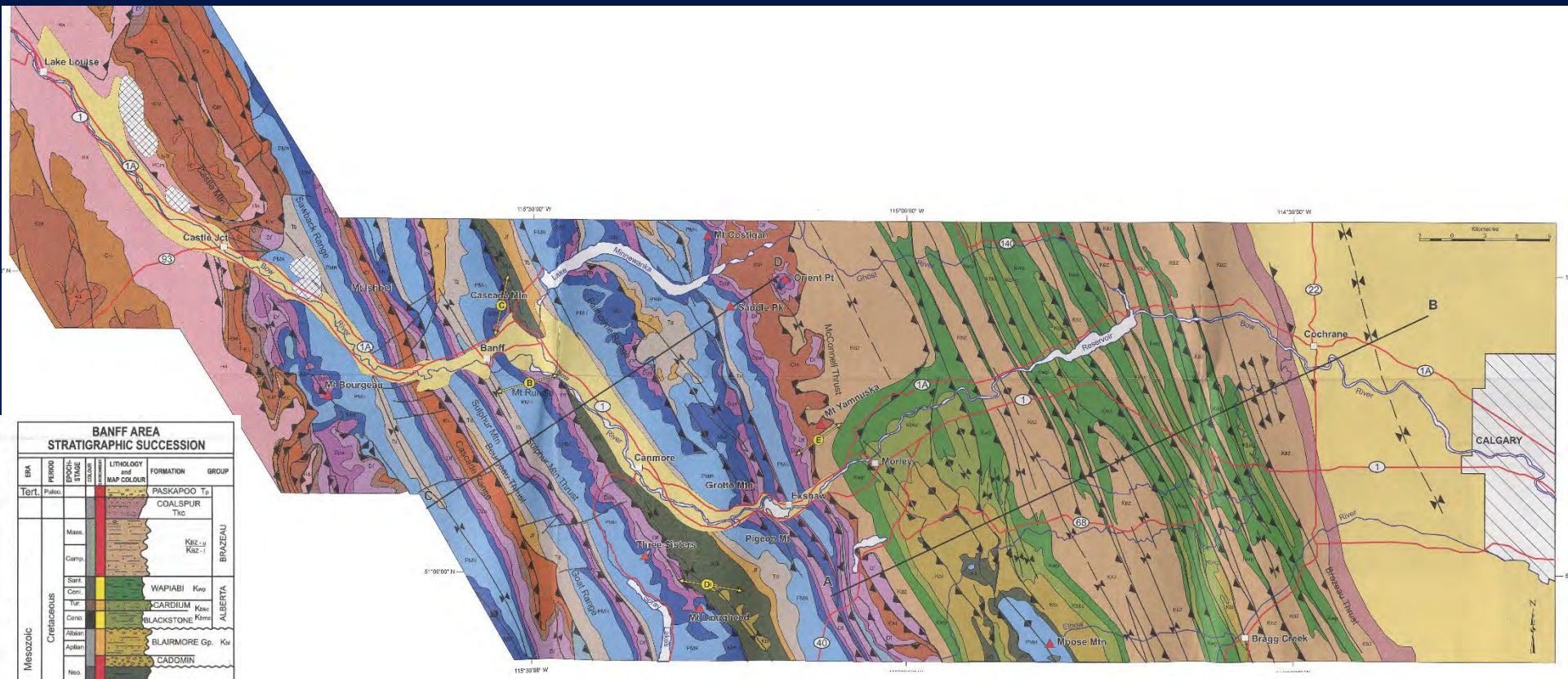

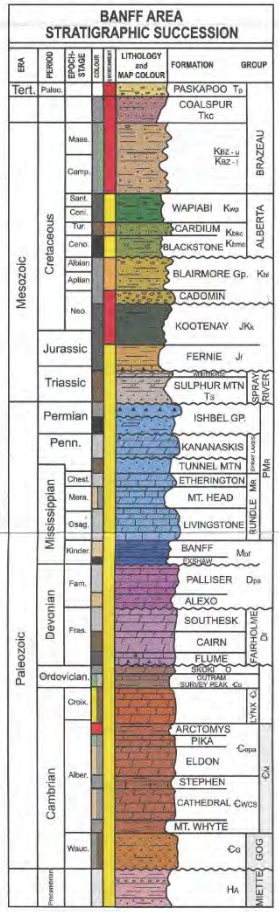

Roadside geology, Calgary - Banff (Trans-Canada Highway). Geological Survey of Canada, 1994

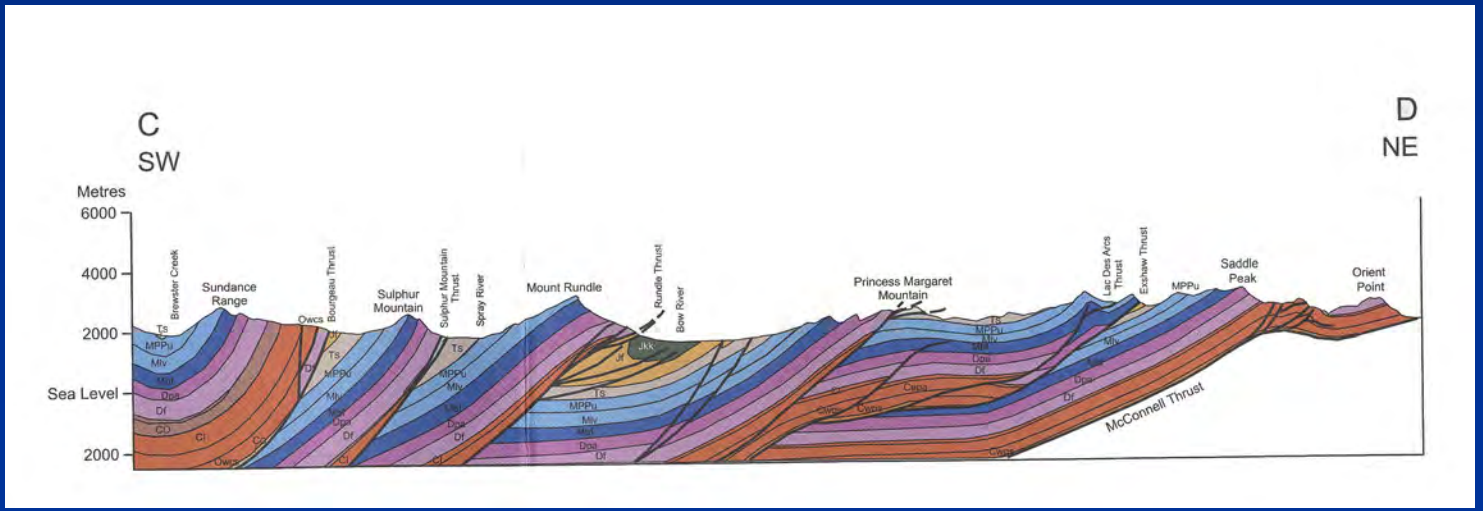

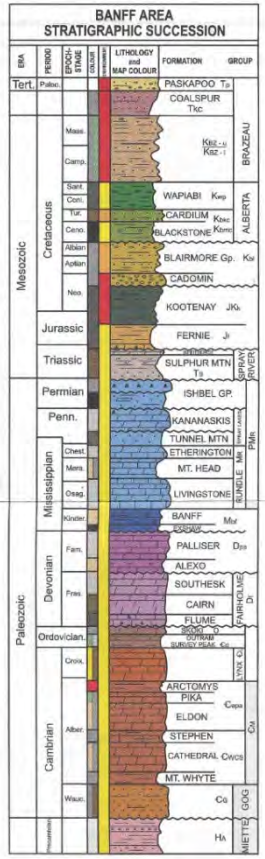

Roadside geology, Calgary - Banff (Trans-Canada Highway). Geological Survey of Canada, 1994

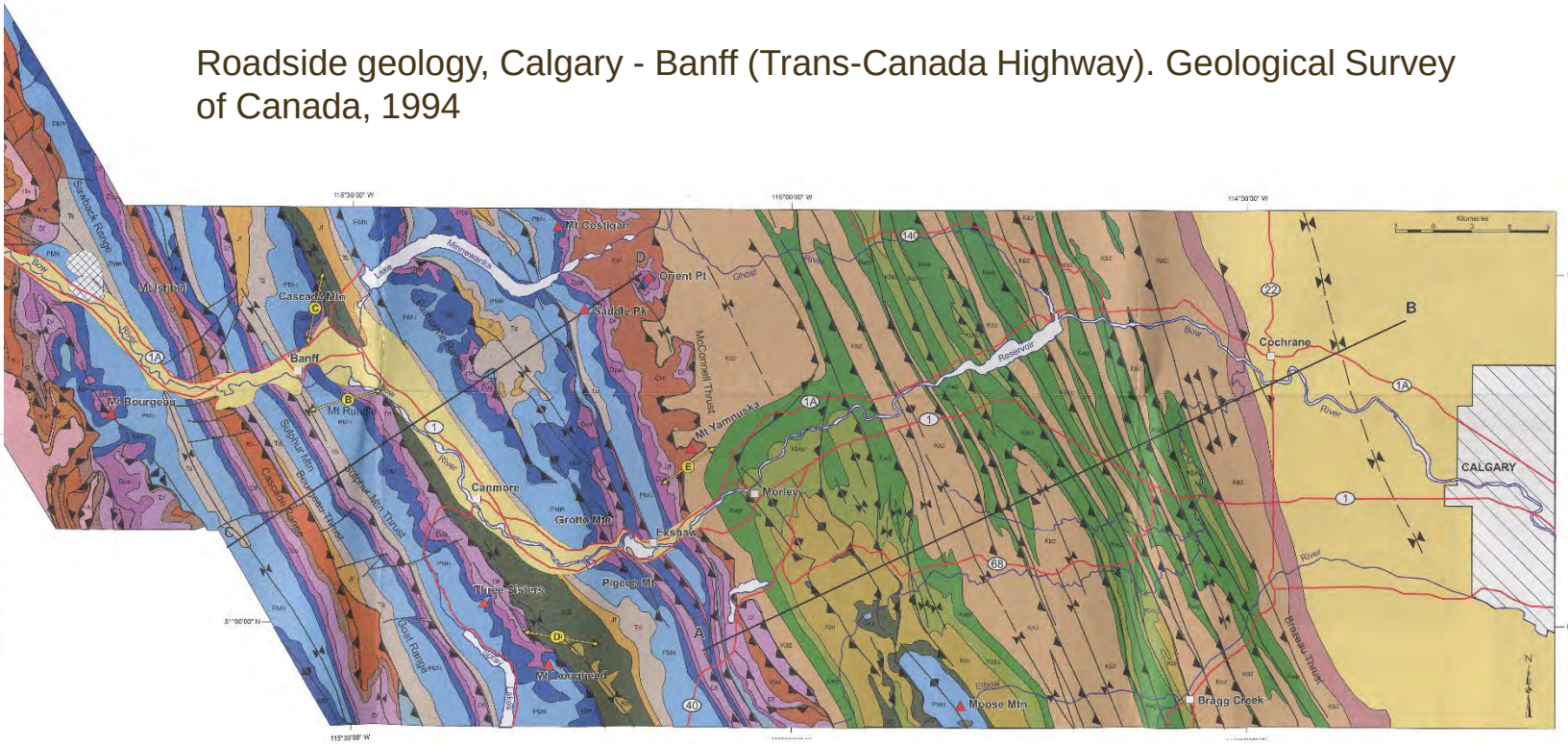

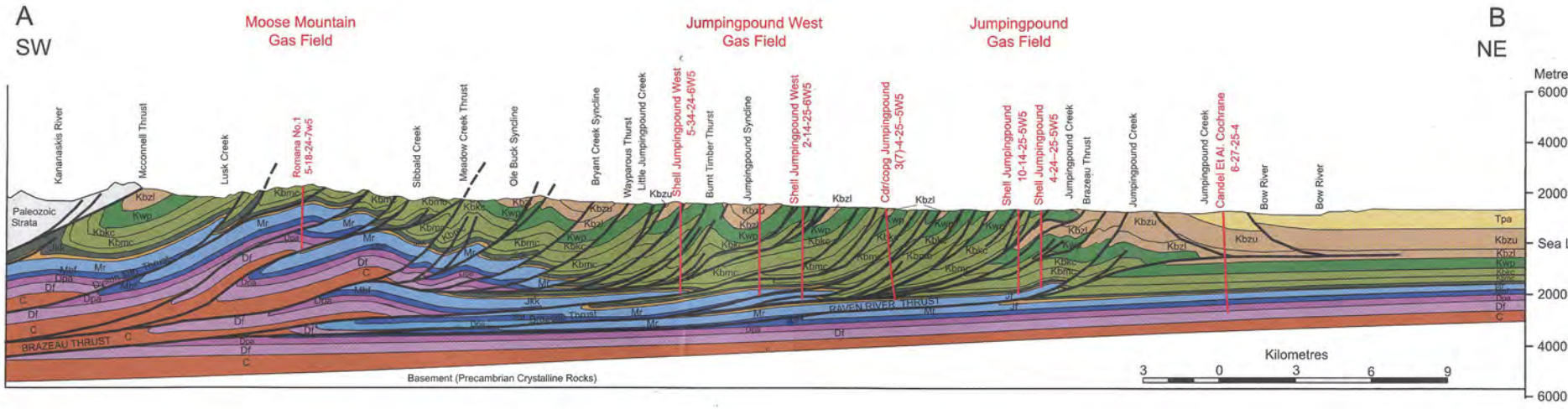

Propagazione degli accavallamenti

“piggy-back”, “overstep (o back-step)”, out-of-sequence

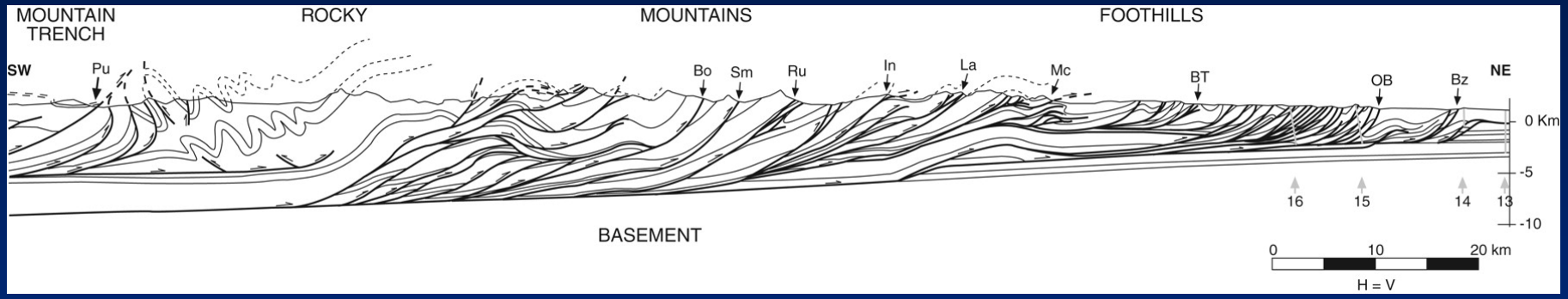

Da Poblet & Lisle, 2011

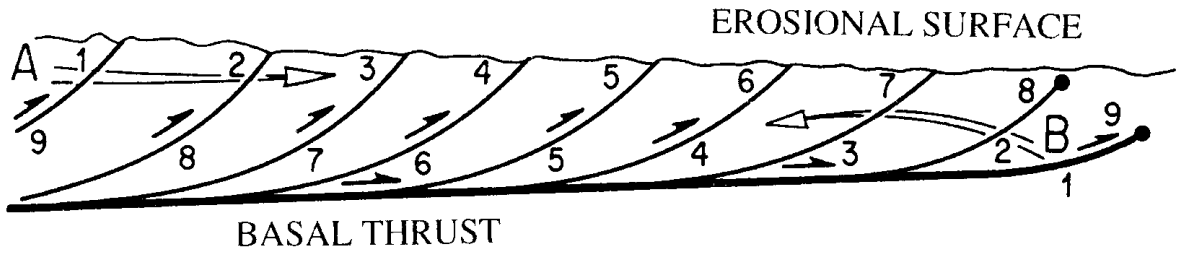

Figure 12 - Imbricate structure and sequential development of thrusts in a piggy-back sequence (foreland propagation; arrow A and numbers indicate the order of development of thrusts). Out of sequence thrust stack (propagation of thrusts in the hanging wall; arrow B and numbers indicating the order of development of thrusts).

Da Merle, 1998

Duplex nelle Rocky Mountains (Mt. Grandell and Lewis Thusts

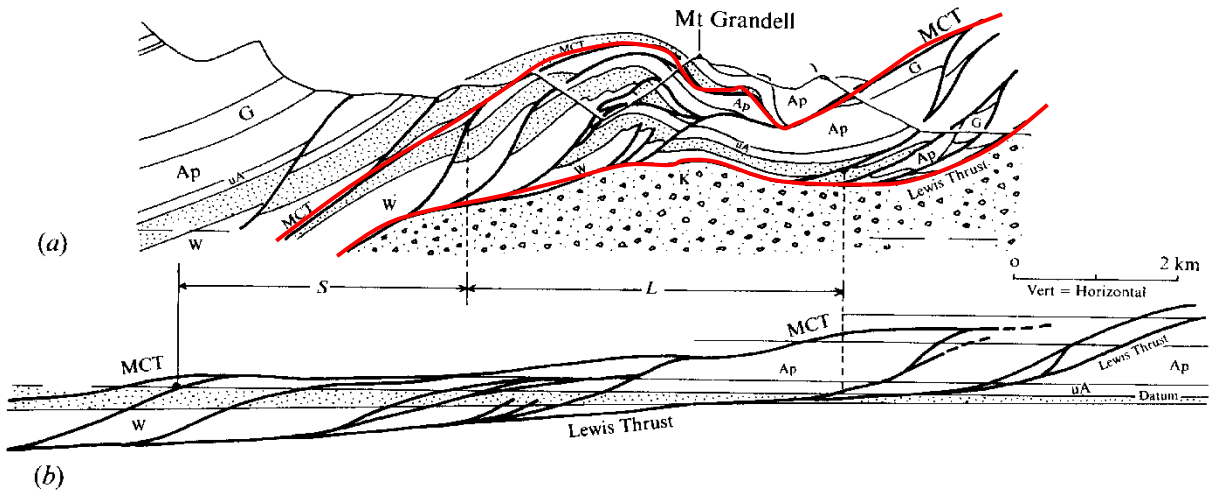

Fig. 7.11. (*a*) Structural profile through structures which have developed above the Lewis Thrust, near Waterton, Alberta, Canada. (*b*) Balanced cross-section of the structures represented in (*a*). (W) Waterton, (uA) Mid and Upper Altyn, (Ap) Appekunny, (G) Grinwell, comprising a Pre-Cambrian Belt supergroup thrust over (K) Cretaceous Siliclastics. *L* is current length and *S* is shortening. MCT = Mt. Crandell Thrust. (From Boyer & Elliot, 1982.)

Da Price and Cosgrove, 1990

Rocky Mountains:
pieghe associate ai sovrascorrimenti e duplex, accavallamenti ciechi

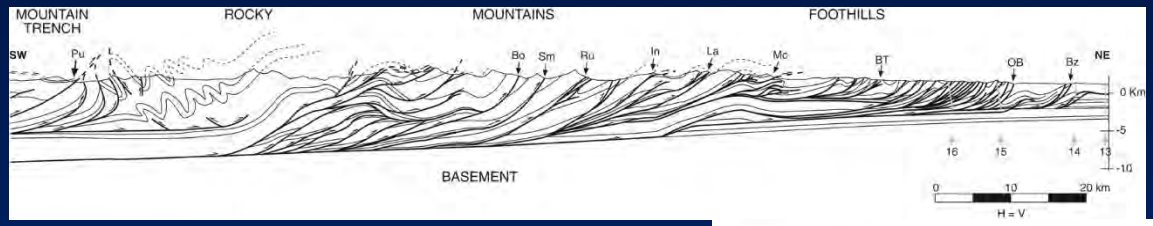

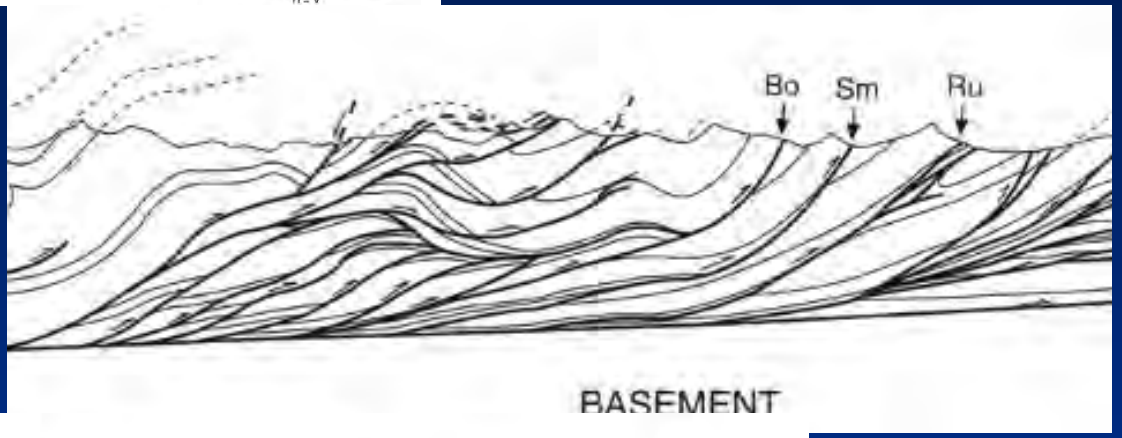

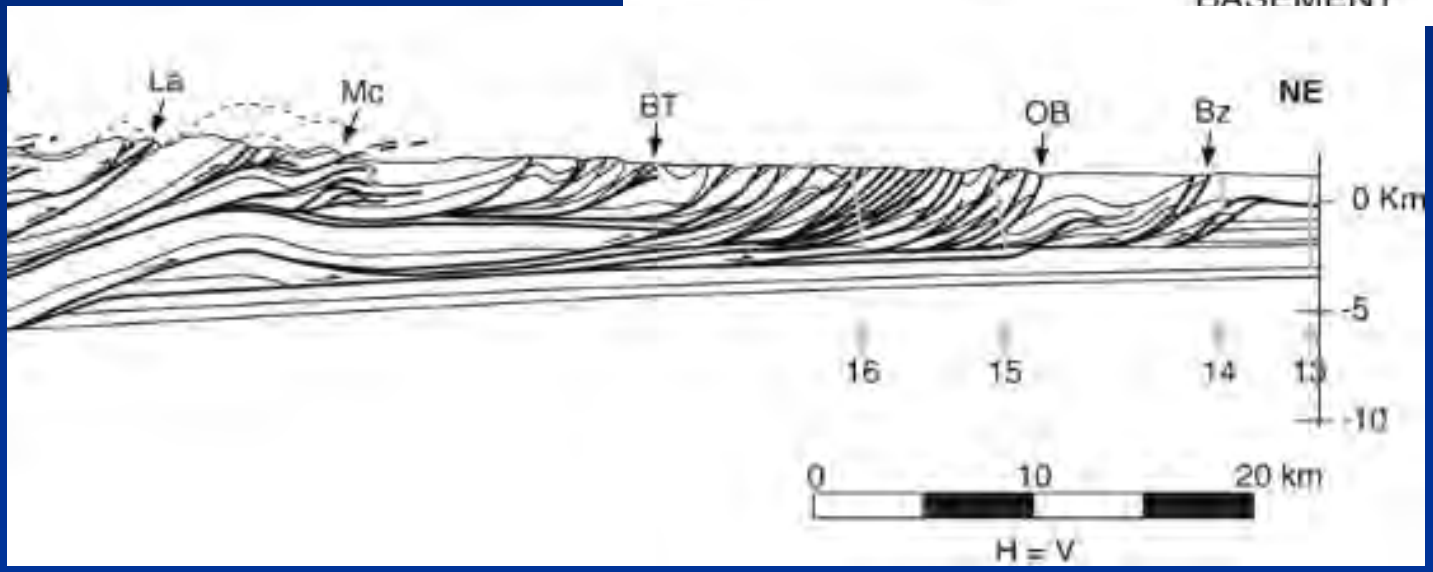

Pieghe, duplex e sovrascorrimenti: Appalachians

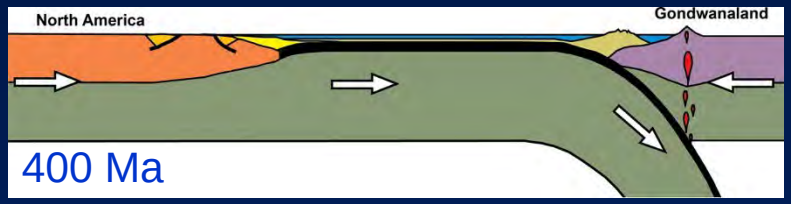

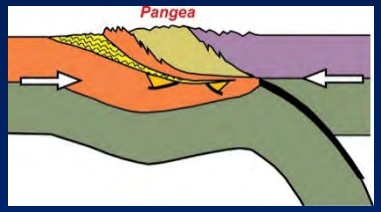

300 Ma

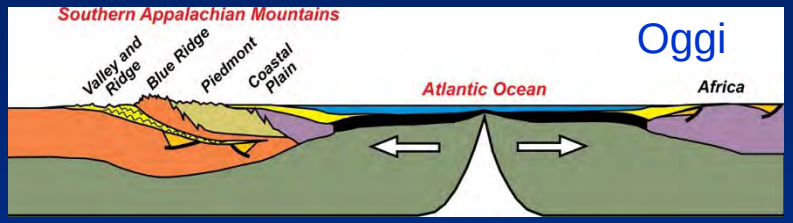

Da National Park Service, tratto da Marshak, 2001

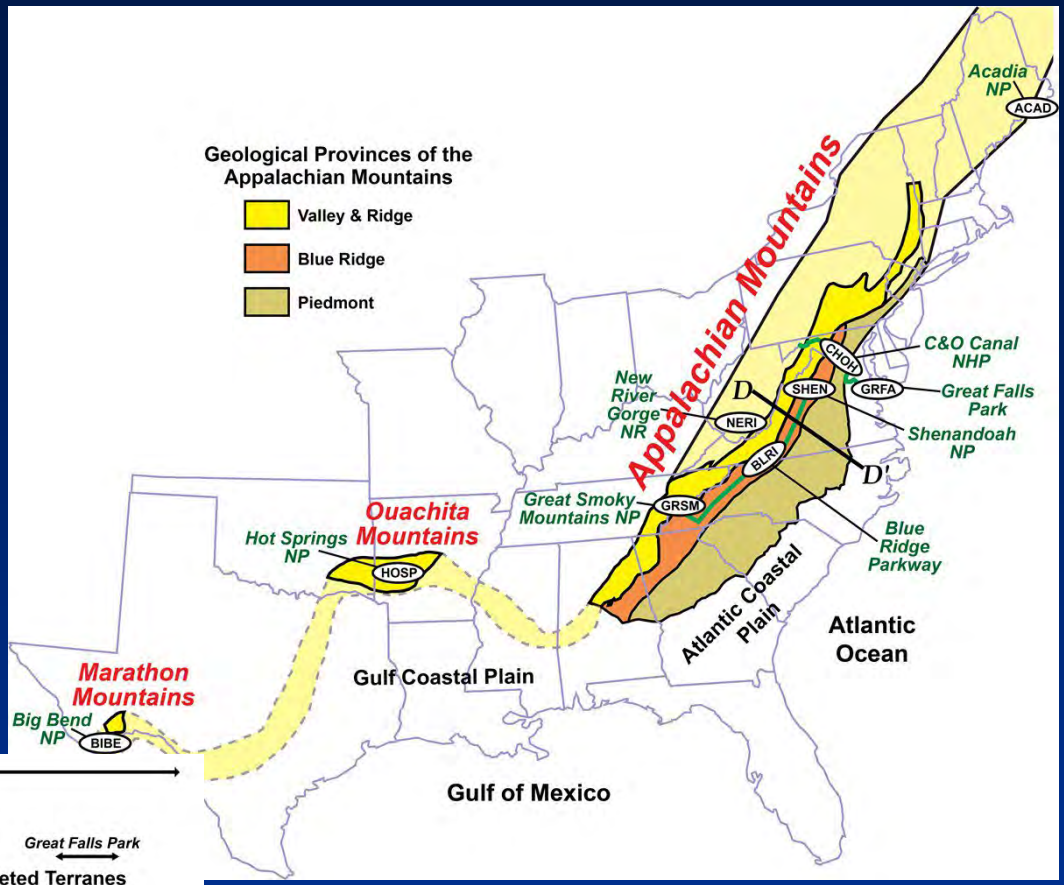

Da National Park Service, tratto da Lillie, 2005

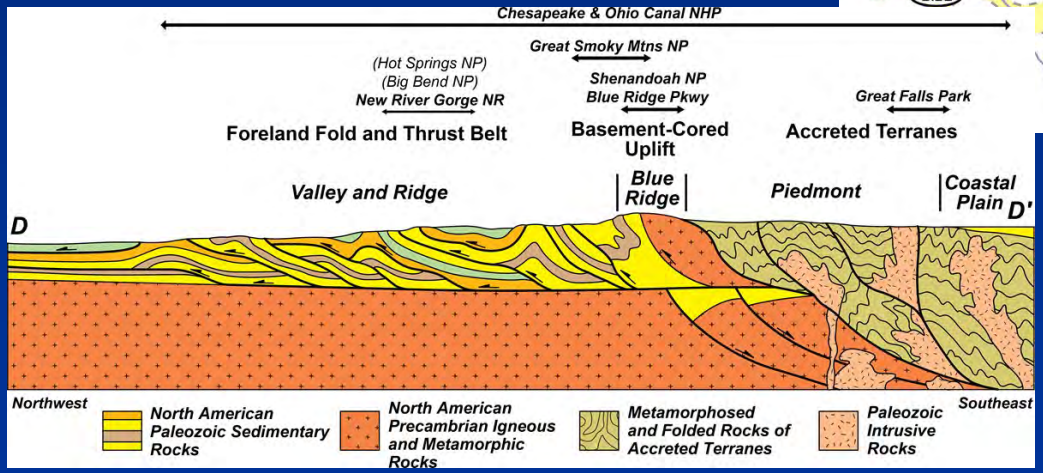

Da National Park Service, tratto da Lillie, 2005

Sistema di catene da prismi di accrezione e collisione continentale (400-300 Ma)

https://www.nps.gov/subjects/geology/plate-tectonics-collisional-mountain-ranges.htm

Pieghe, duplex e sovrascorrimenti: Appalachians

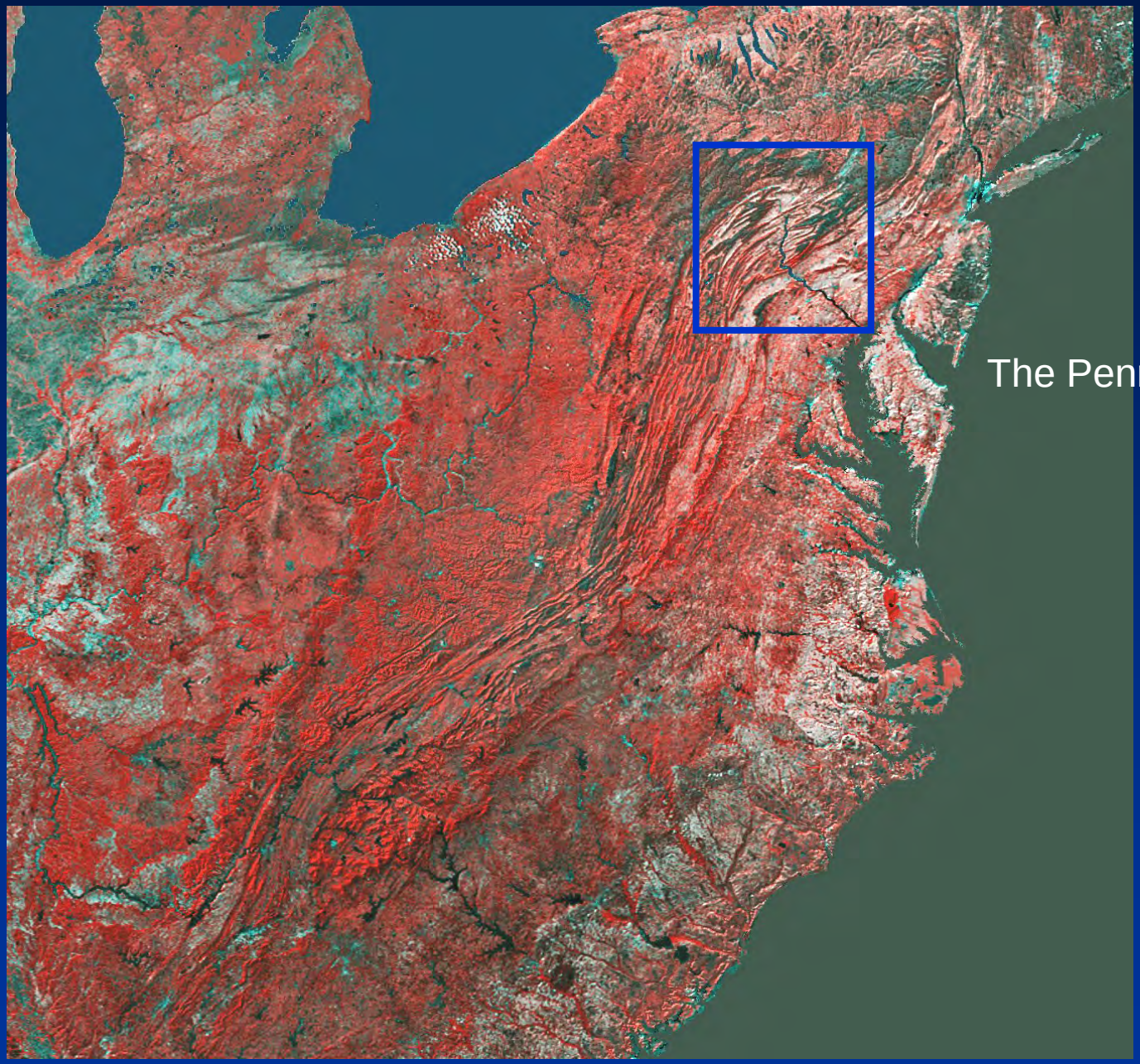

The Pennsylvania Salient

Da USGS
Mosaico dati satellitari AVHRR, falsi colori

Pieghe: Appalachians

Quale origine?

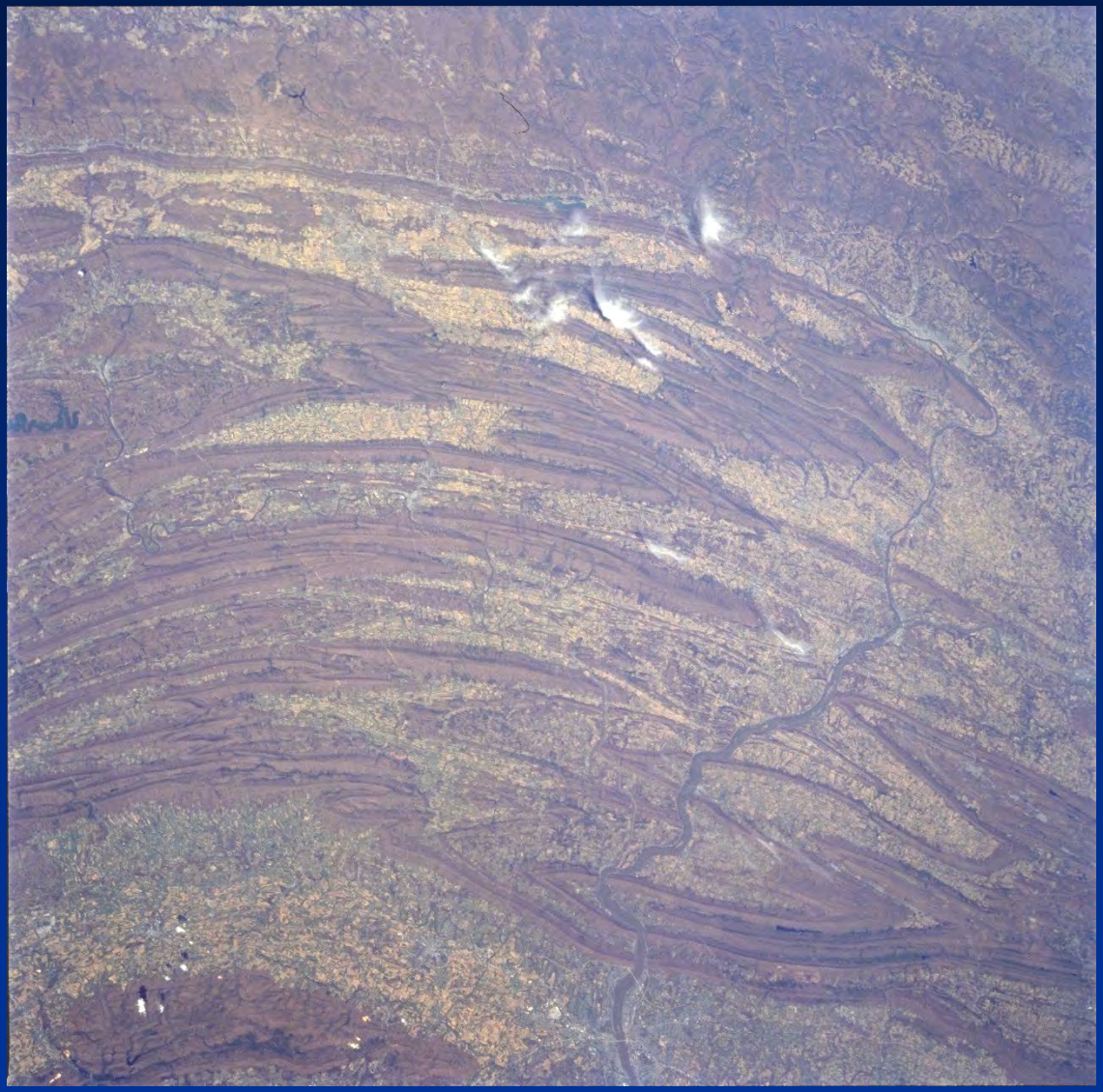

Da NASA-JPL Photo Directory

Pieghe: Appalachians

Quale origine?

Pieghe, duplex e sovrascorrimenti: Appalachians

Da Sak et al., 2012

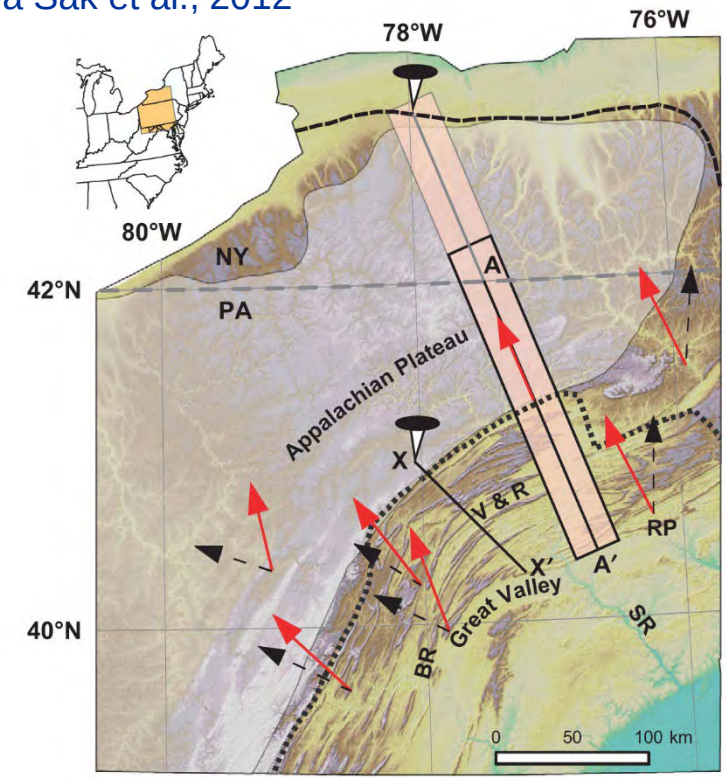

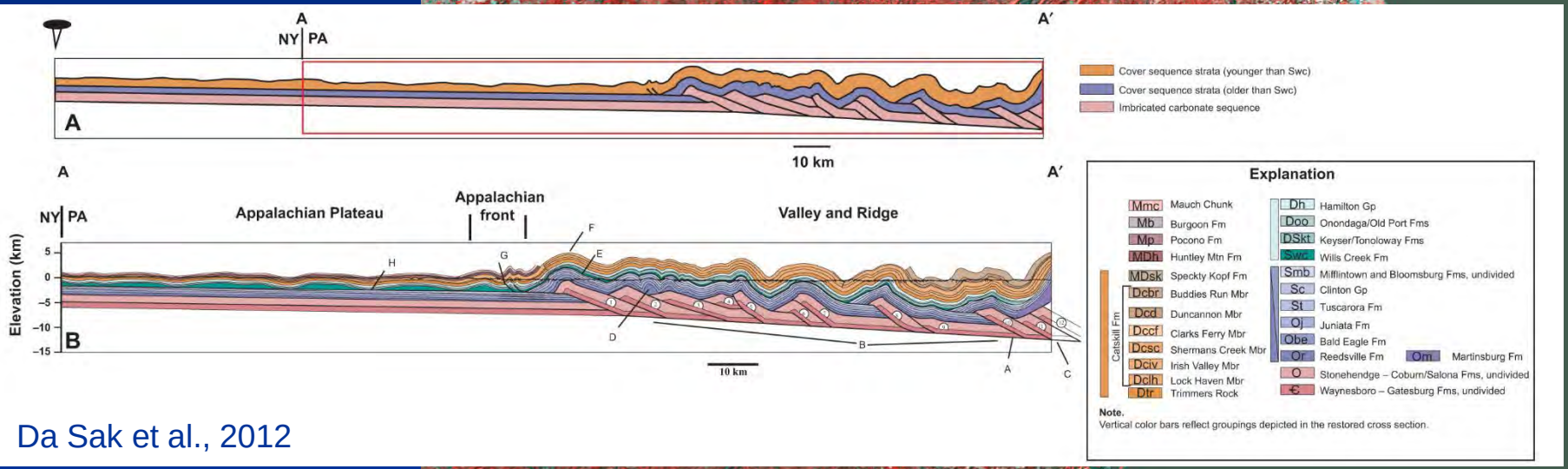

Da Sak et al., 2012

Pieghe e sovrascorrimenti: Appalachians

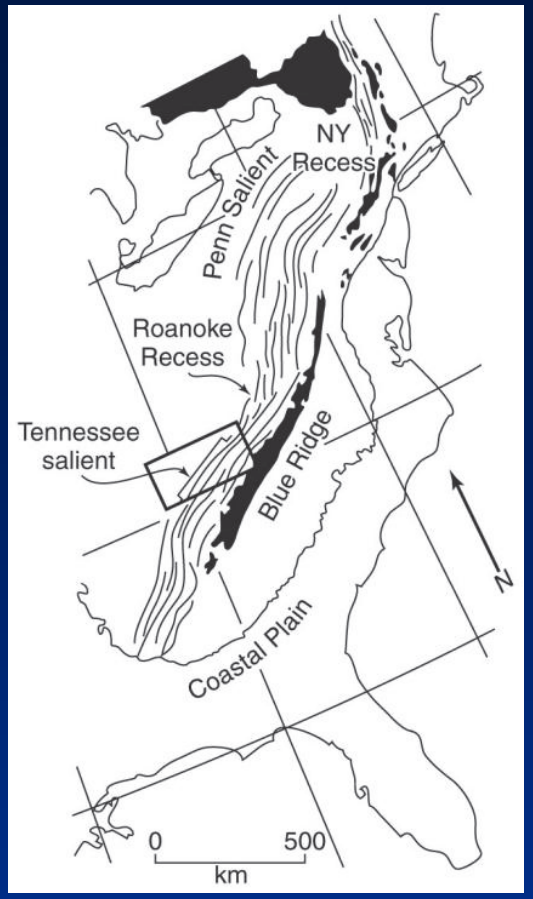

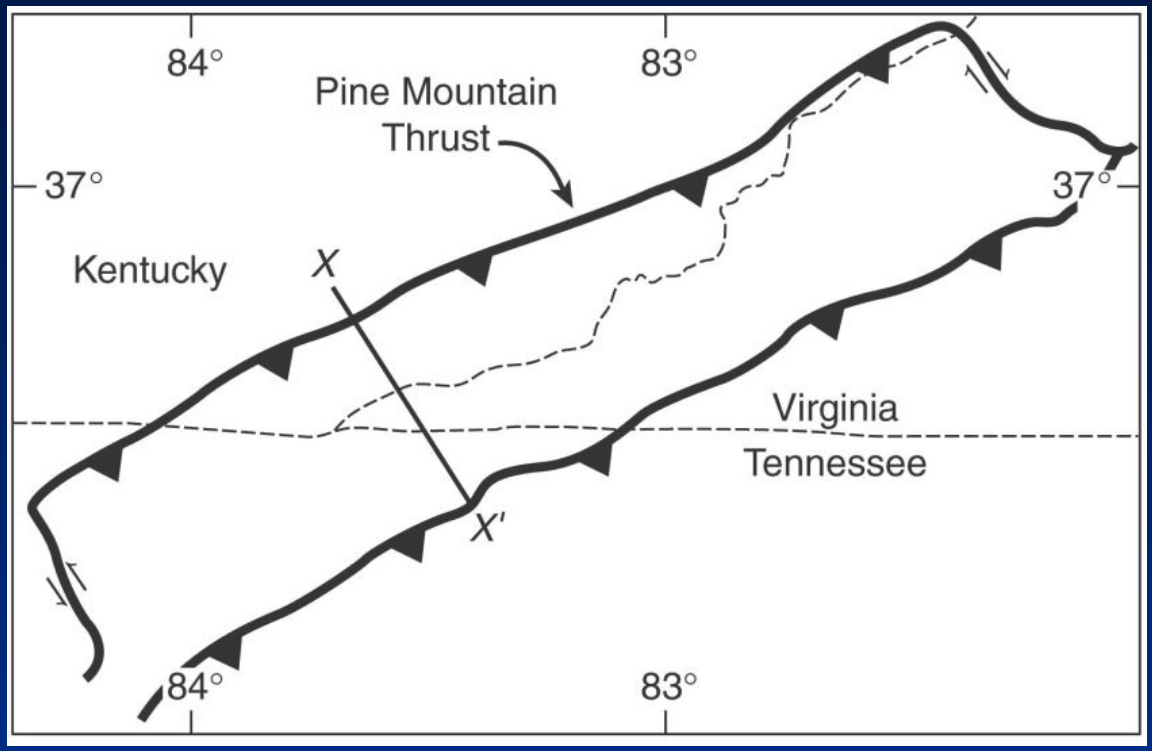

Da van der Pluim & Marshak, 2004

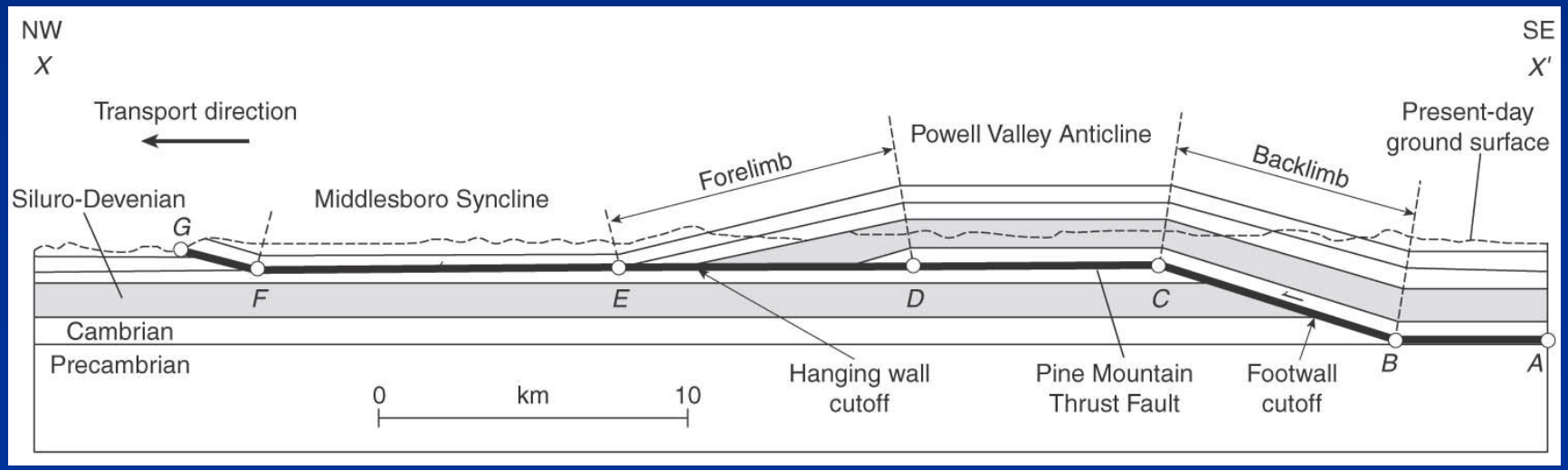

Pieghe, duplex e accavallamenti ciechi: i Pirenei

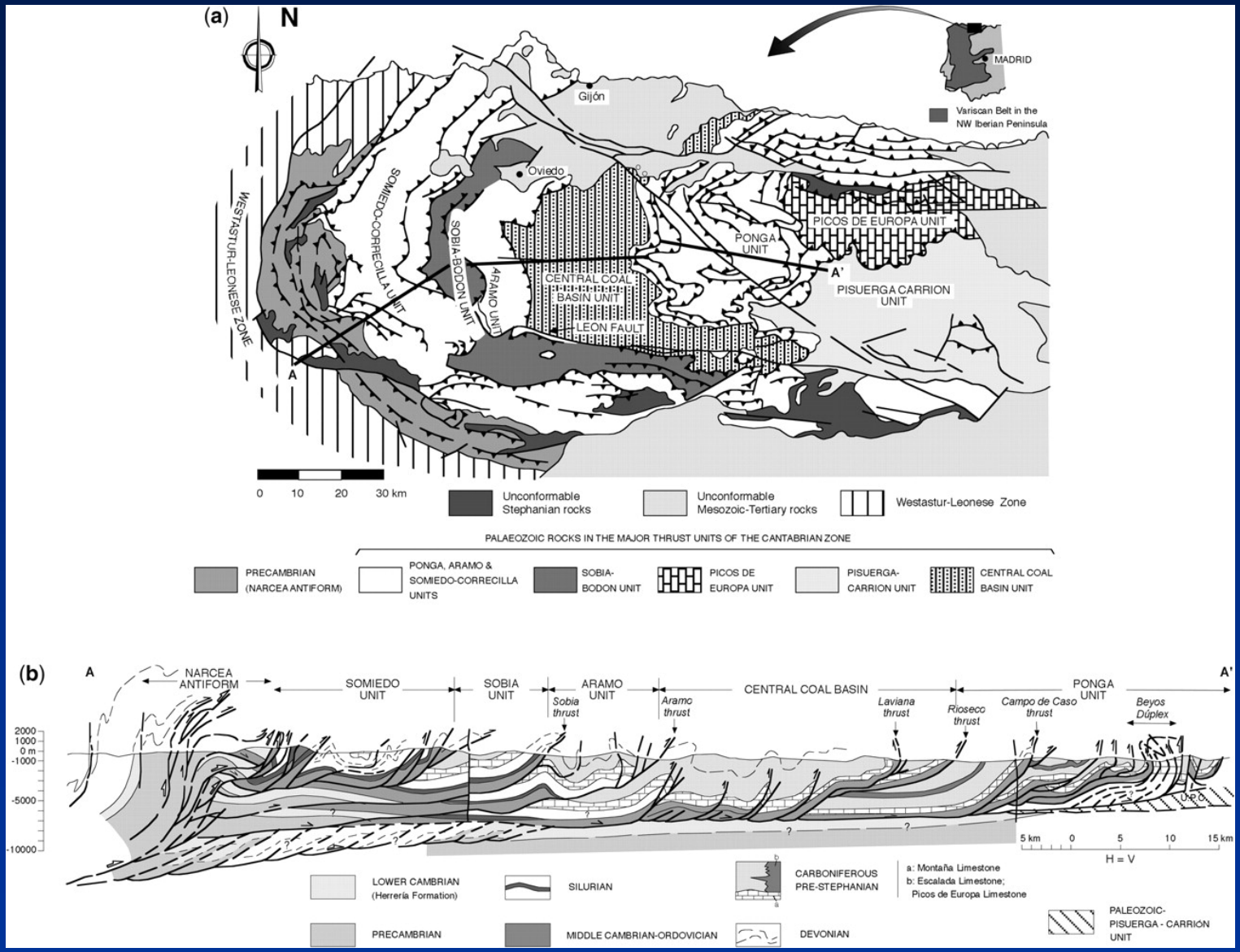

Da Poblet & Lisle, 2011

Accavallamenti e pieghe, altri termini

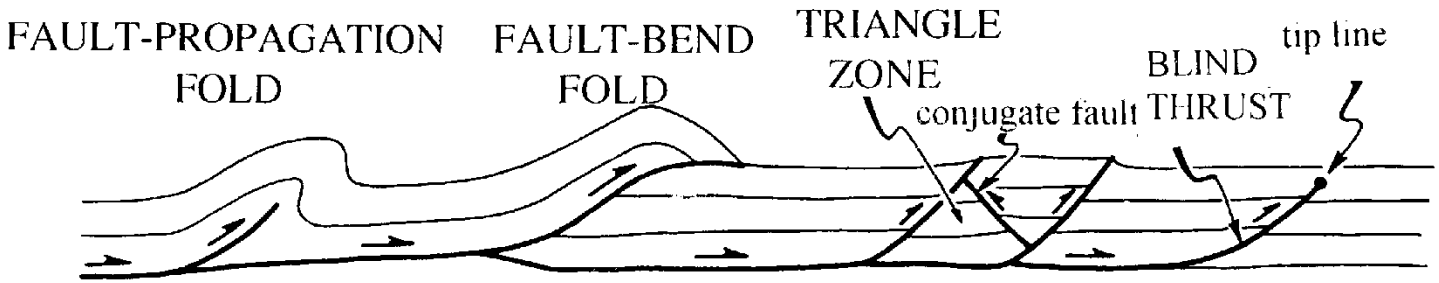

Figure 11 - Structures associated with the formation of reverse faults in thrust belts.

Da Merle, 1998

Pieghe e accavallamenti: tre tipi

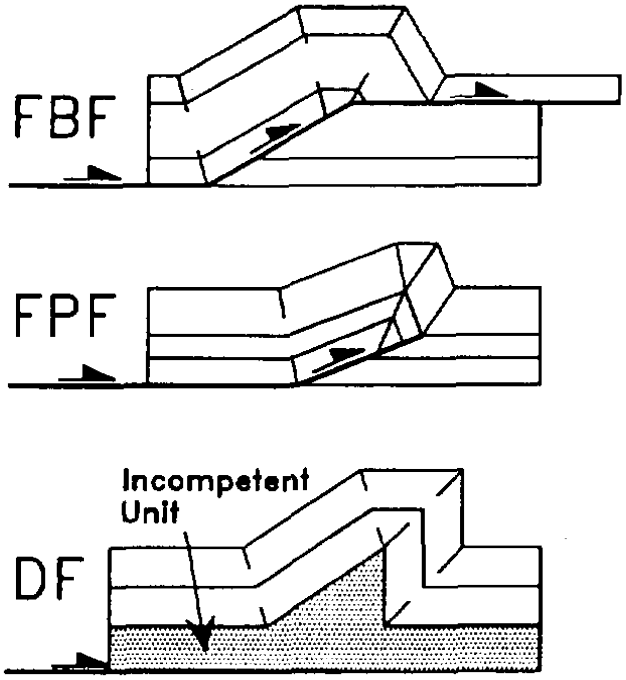

Fig. 1. Three major types of thrust-related folds in fold-and-thrust belts: fault-bend fold (FBF), fault-propagation fold (FPF), and detachment fold (DF).

Da Homza and Wallace, 1995

Pieghe e accavallamenti: fault-bend folds

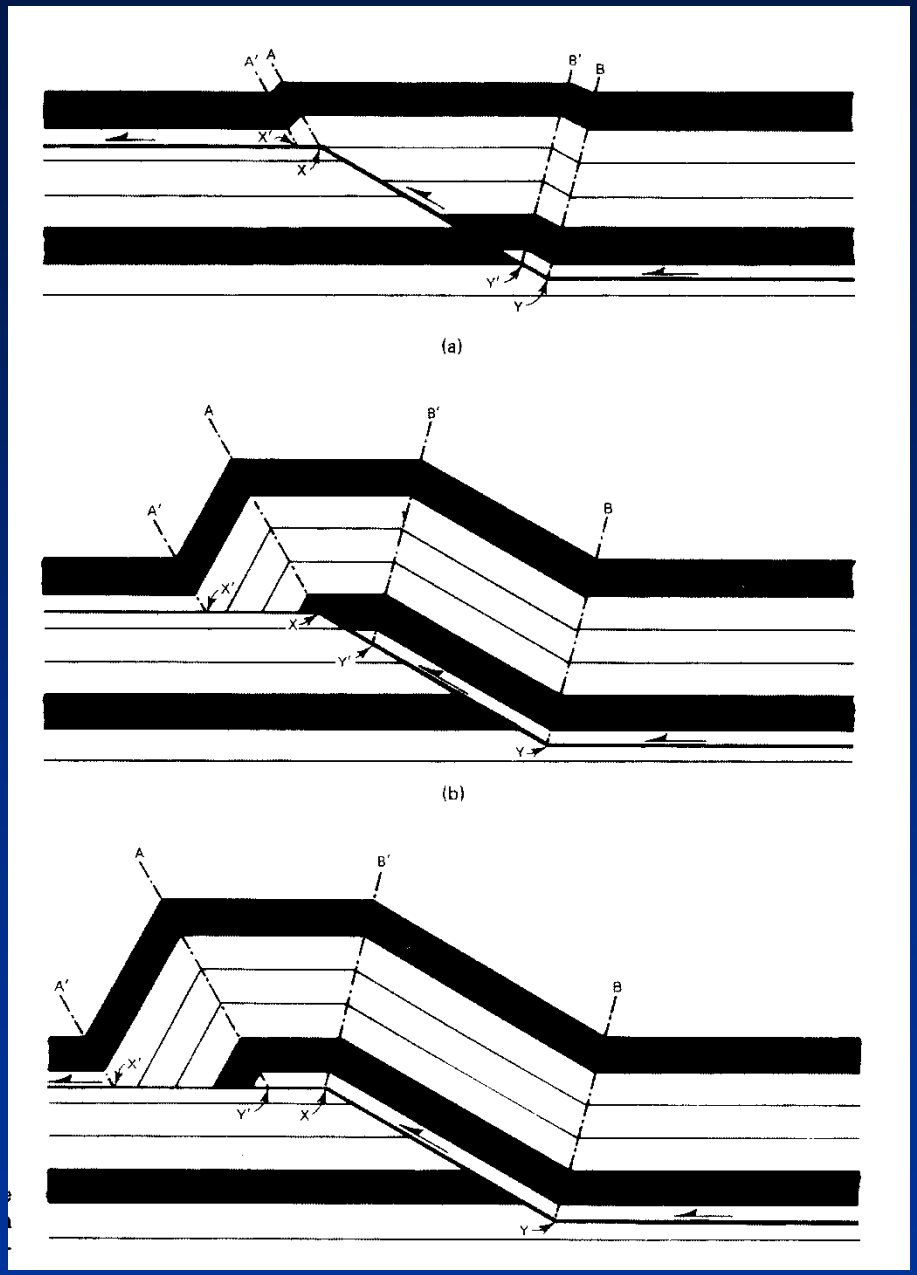

Da Suppe, 1985

Fault-propagation fold, Meilin anticline, Taiwan

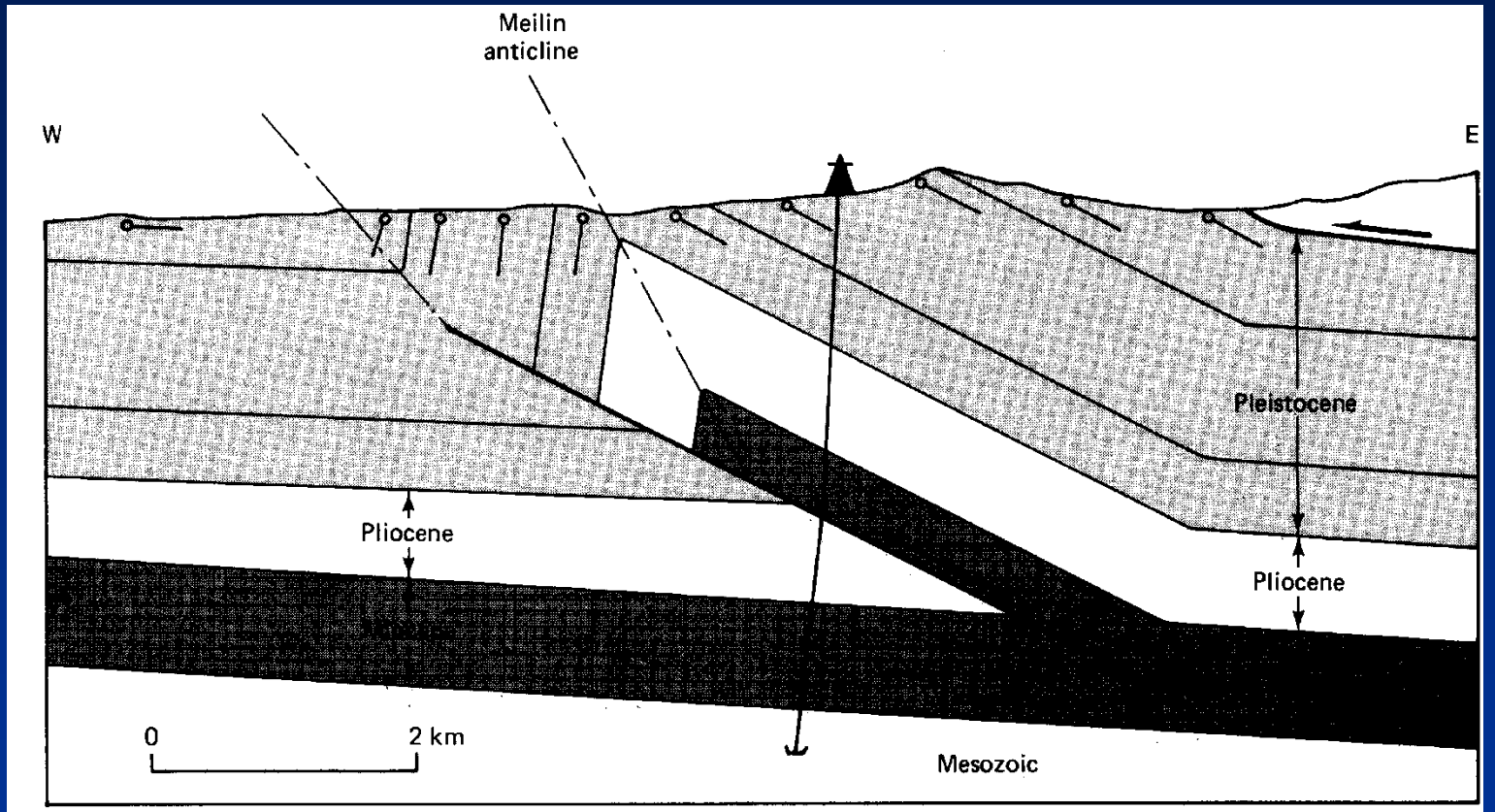

FIGURE 9–48 Cross section of a fault-propagation fold similar to the schematic diagram in Figure 9-47. Meilin anticline, western Taiwan.

Da Suppe, 1985

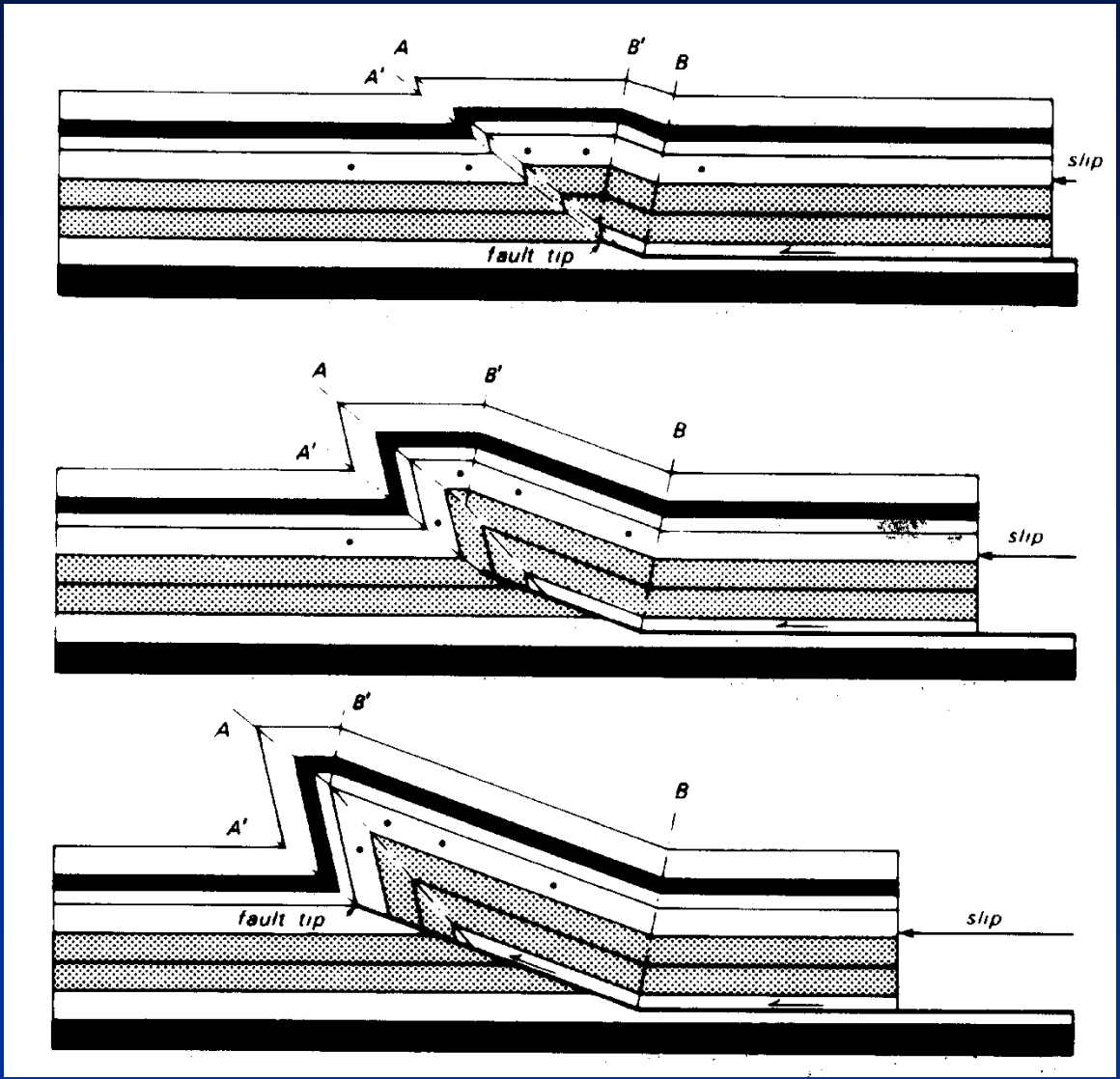

Pieghe e accavallamenti: Fault-propagation folds

Da Suppe, 1985

Pieghe e accavallamenti: detachment folds

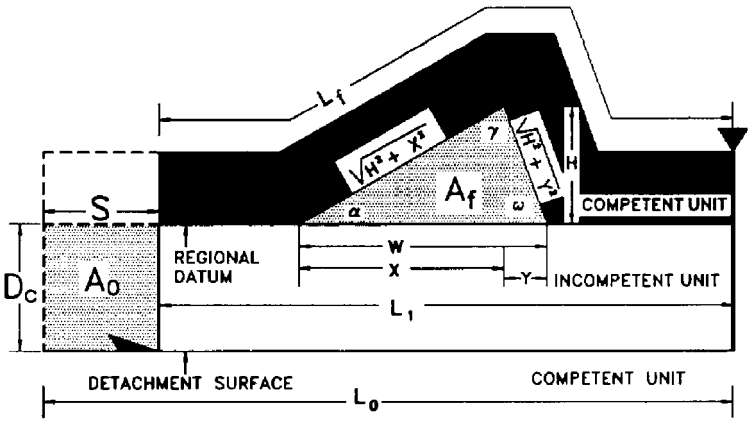

Fig. 2. Geometric basis for the fixed detachment depth model. As the incompetent unit is displaced and shortened, conservation of cross-sectional area requires that the displaced area (A_o) equal the uplifted area (A_f). Conservation of line-length requires the contact between competent and incompetent units to retain its original length ($L_o = L_f$). See text for explanation of other variables.

Da Homza and Wallace, 1995

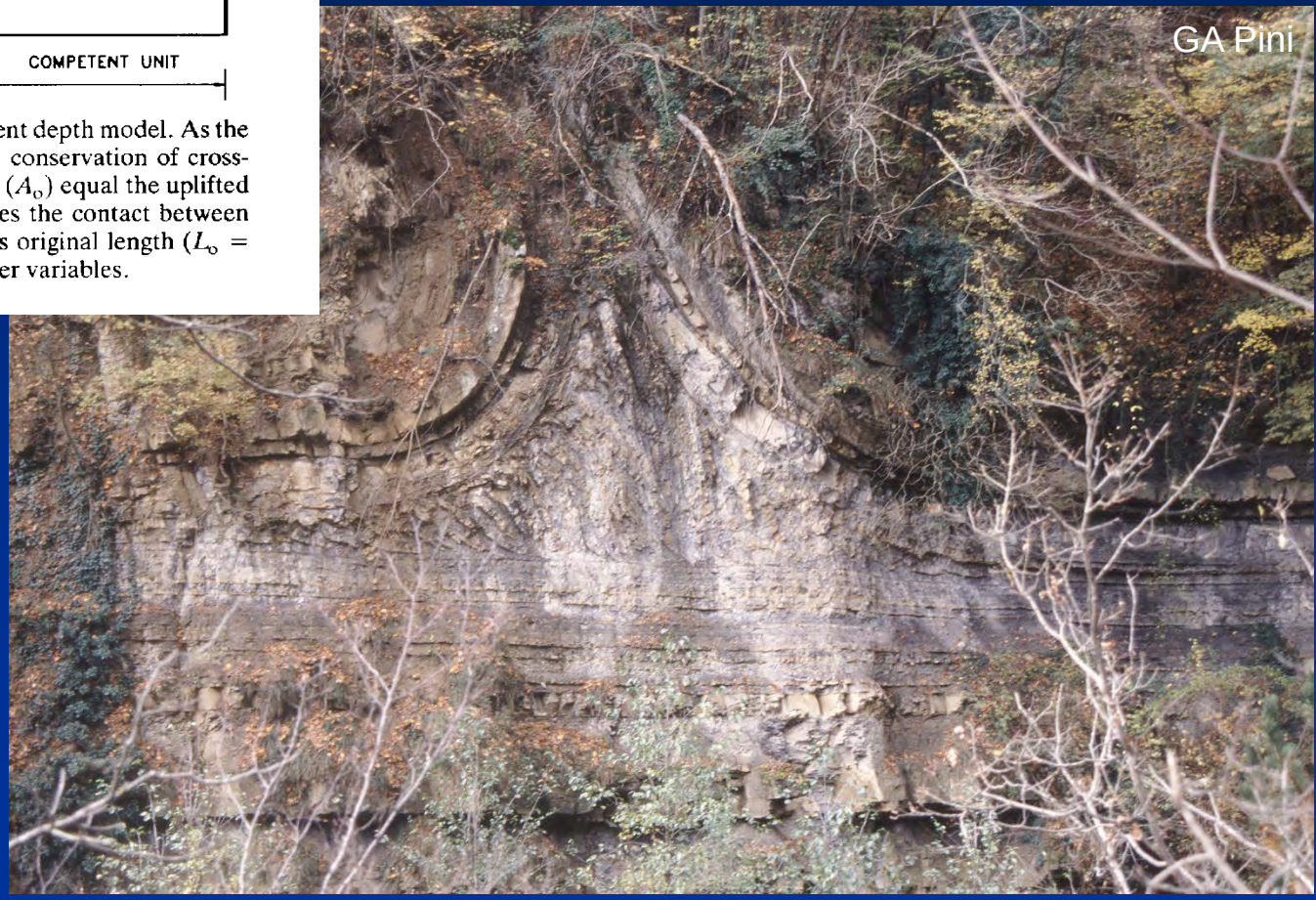

Fault-propagation fold: modello di trishear

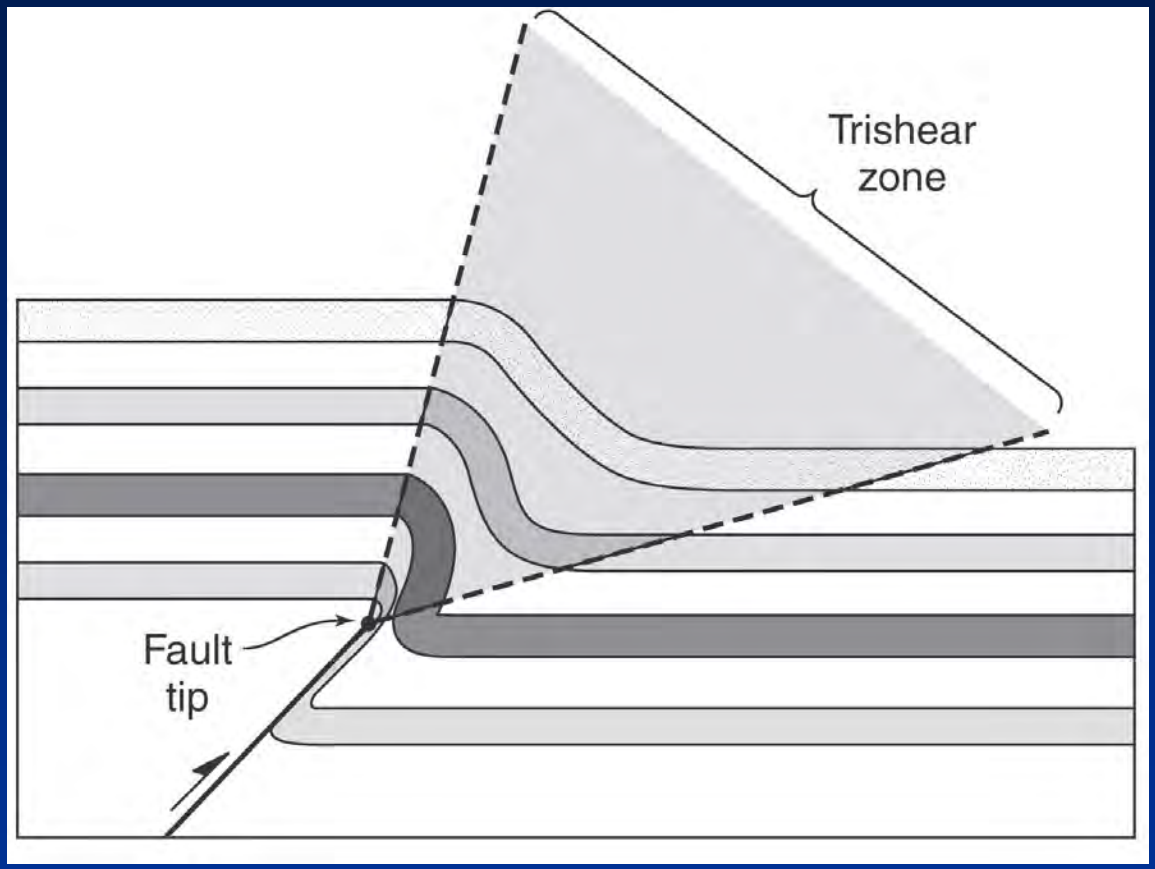

Da van der Pluim & Marshak, 2004

Da NASA-JPL Photo Directory

, la Molassa e il Giura

Foreland fold-and
-thrust belt

Molassa
foredeep

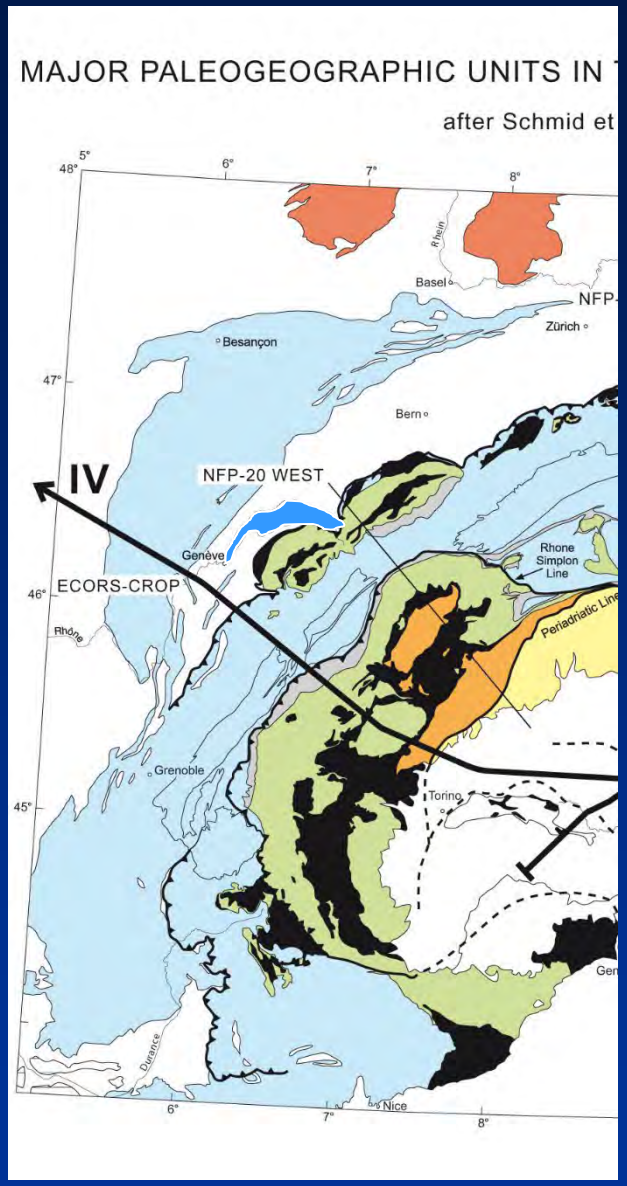

Da Schmid et al., 2004

Il Giura: tettonica di scollamento

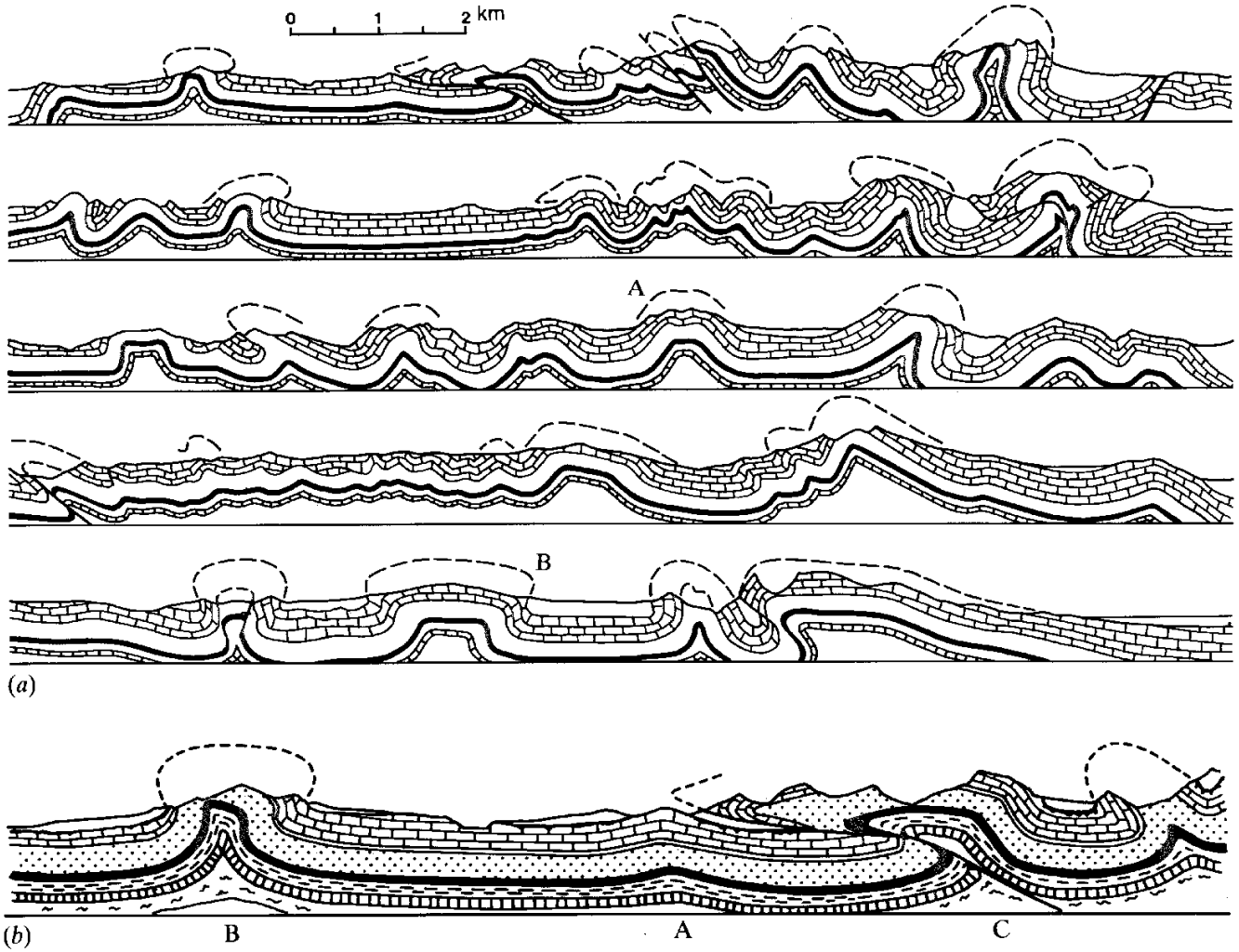

Fig. 13.2. (*a*) Profile sections of fold structures in the Jura Mountains after Heim (1921). (*b*) Detail of (*a*) showing three stages in the formation of a thrust from an originally symmetrical fold.

Da Price & Cosgrove, 1990

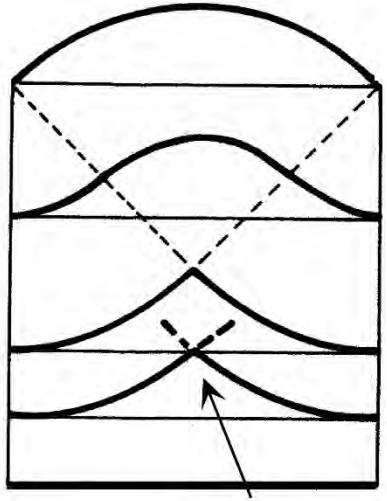

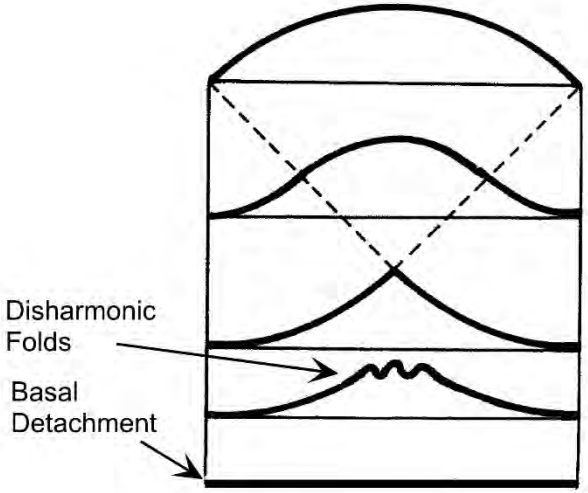

a

Space Problems
in Anticlinal Core

b

JURA MOUNTAINS

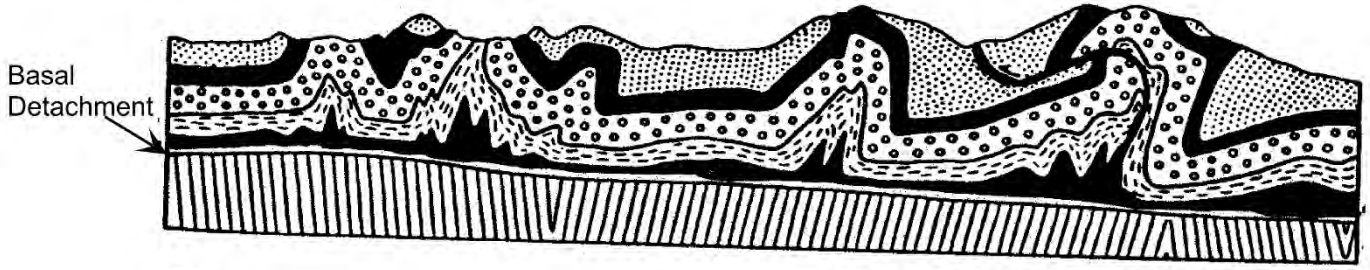

c

Fig. 1. Geometry of disharmonic detachment folds. a. Space problems in the core of a concentric fold resulting from convergence of radii of curvature to form cuspate geometry. b. Space problems resolved by the formation of disharmonic folds (modified from De Sitter, 1964). c. Example of disharmonic detachment folds from the Jura Mountains, Switzerland (modified from Buxtorf, 1916).

Da Mitra, 2003

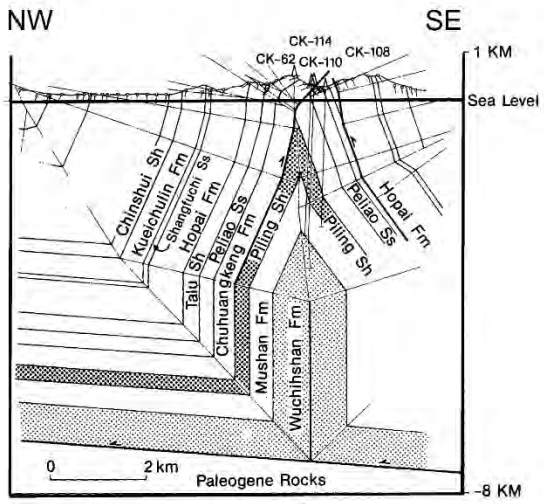

a. Chuhuangkeng Anticline, Taiwan

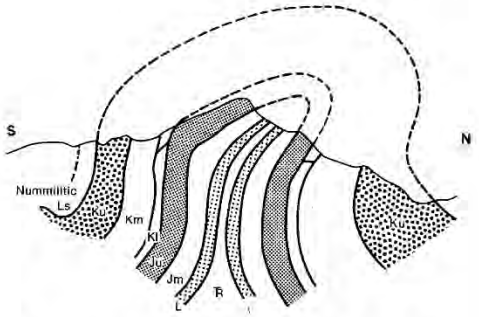

b. Gourdan Anticline, Maritime Alps

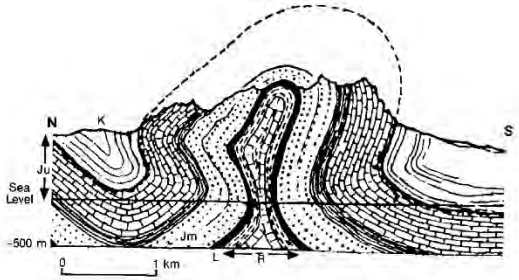

c. Weissenstein Anticline, Jura Mountains

Fig. 2. Examples of lift-off folds from (a) the Taiwan belt (from Namson, 1981), (b) the Maritime Alps (Goguel, 1962), and (c) the Jura Mountains (Buxtorf, 1916).

Da Mitra, 2003

Retrodeformazione delle catene, Rocky Mountains

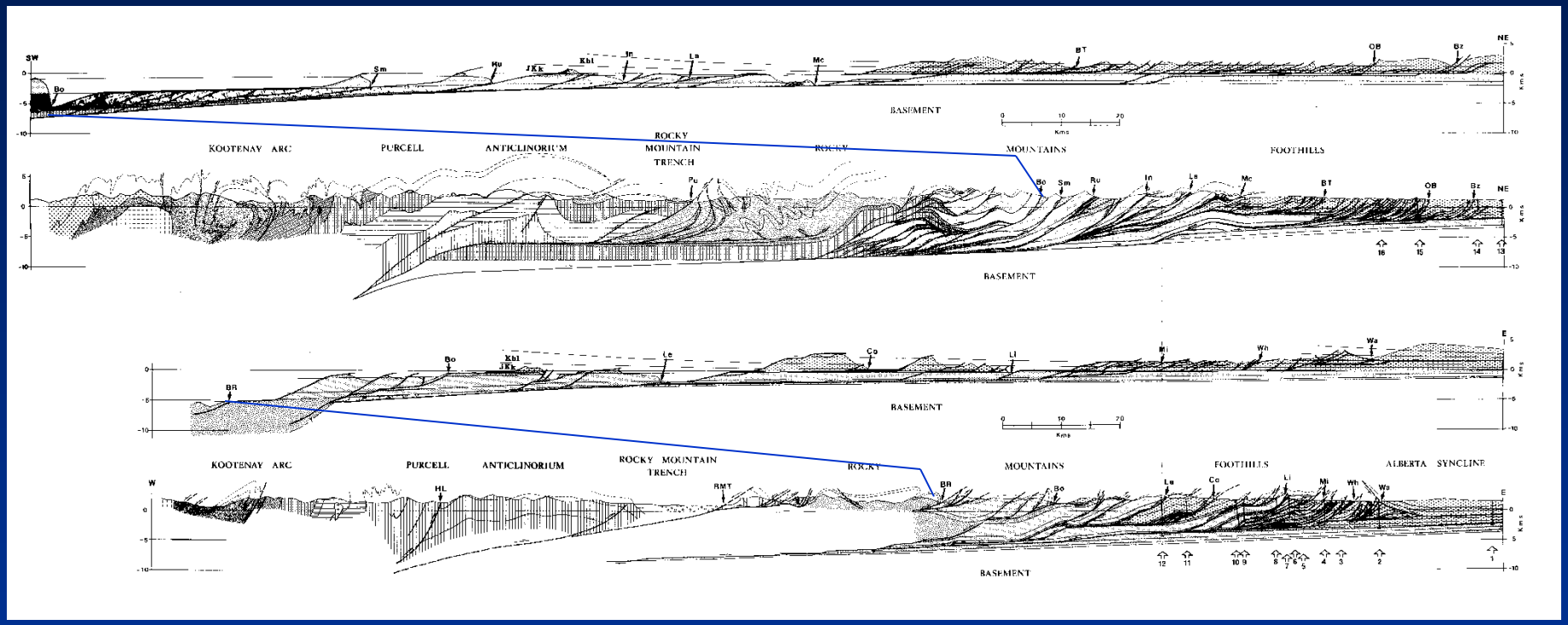

Da Price, 1981

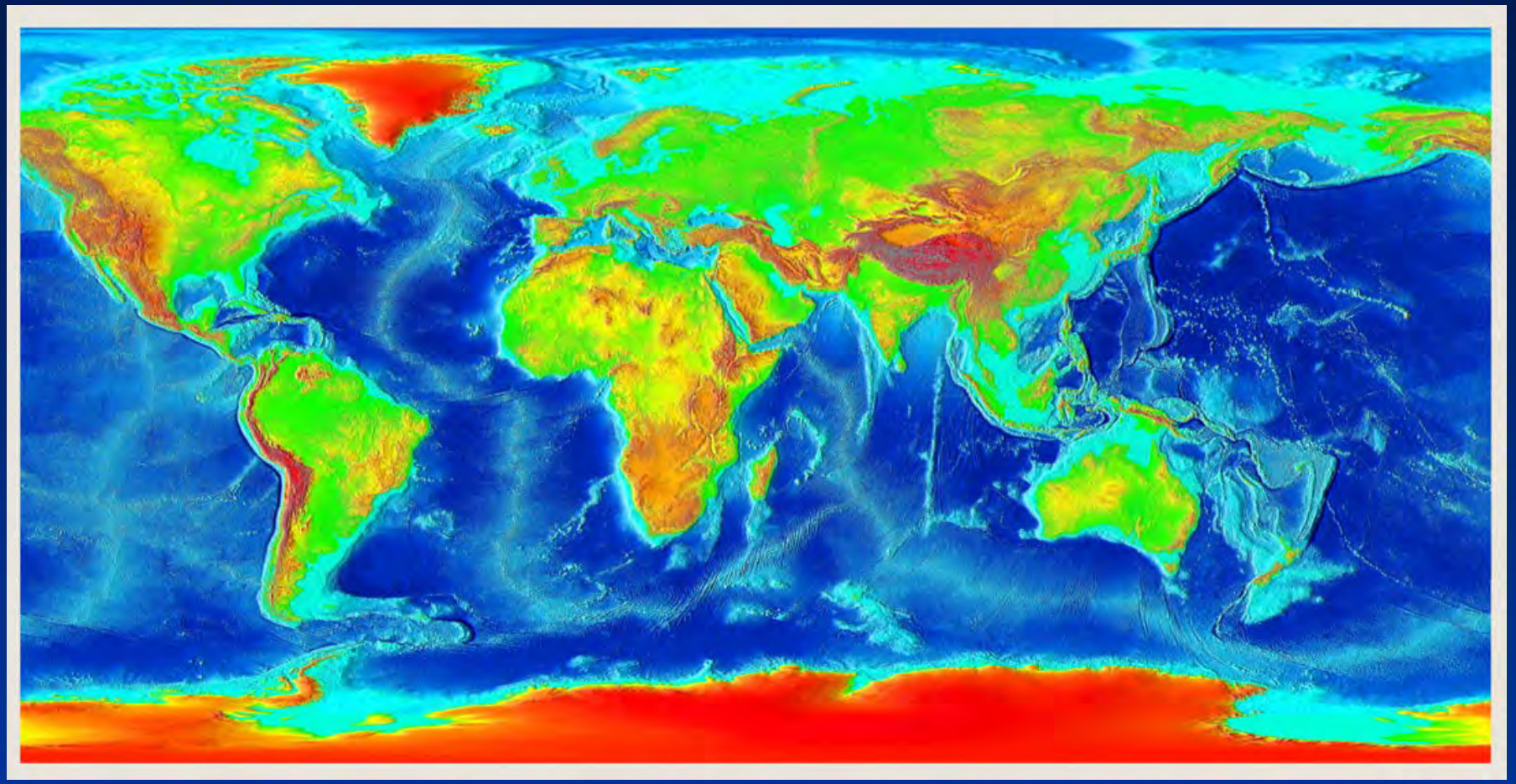

Shaded reliefs e batimetria da NOAA National Centers for Environmental Information (NCEI)

Shaded reliefs e batimetria da NOAA National Centers for Environmental Information (NCEI)

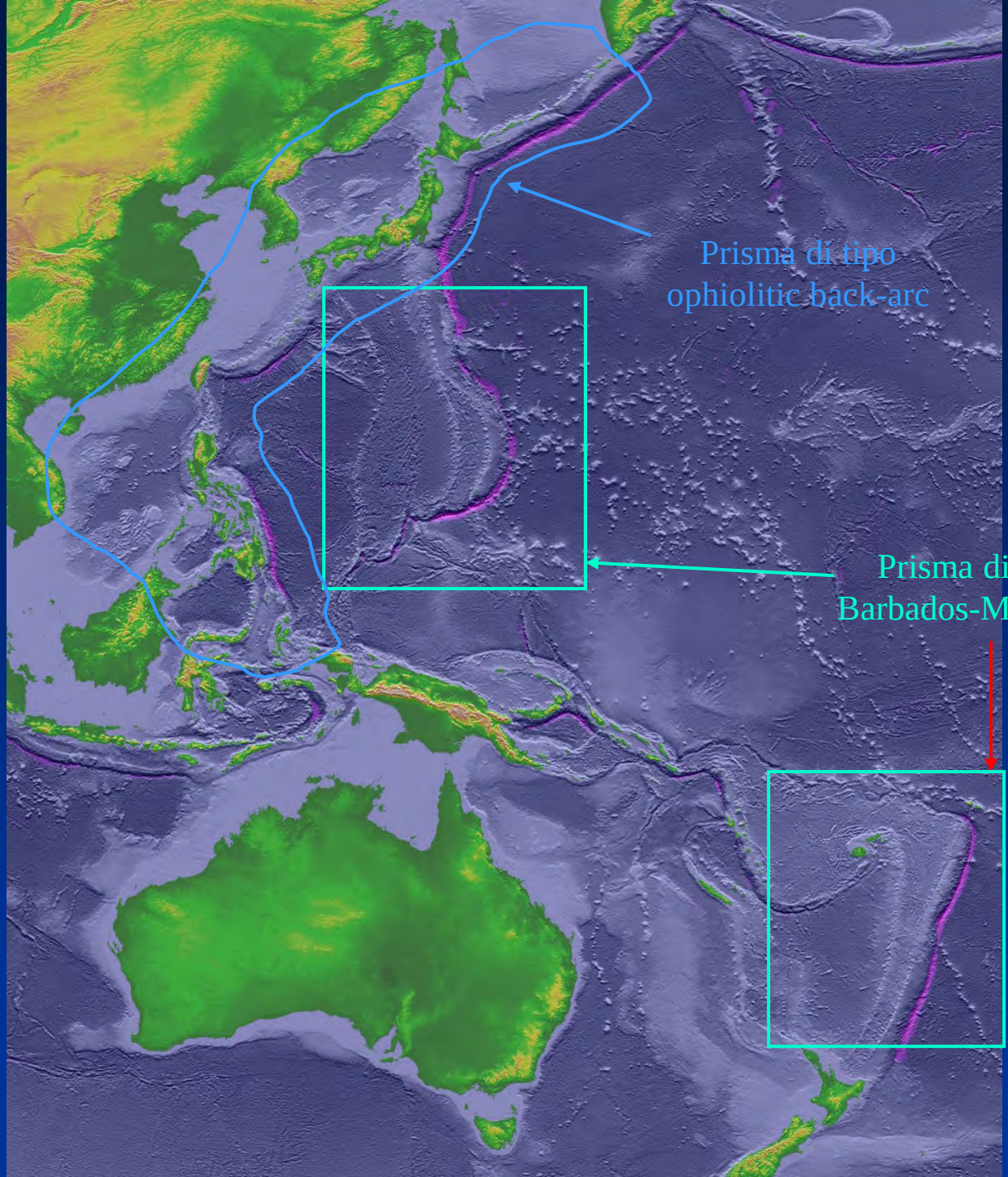

Shaded reliefs e batimetria da NOAA National Centers for Environmental Information (NCEI)

Zona di subduzione delle Piccole Antille - Barbados

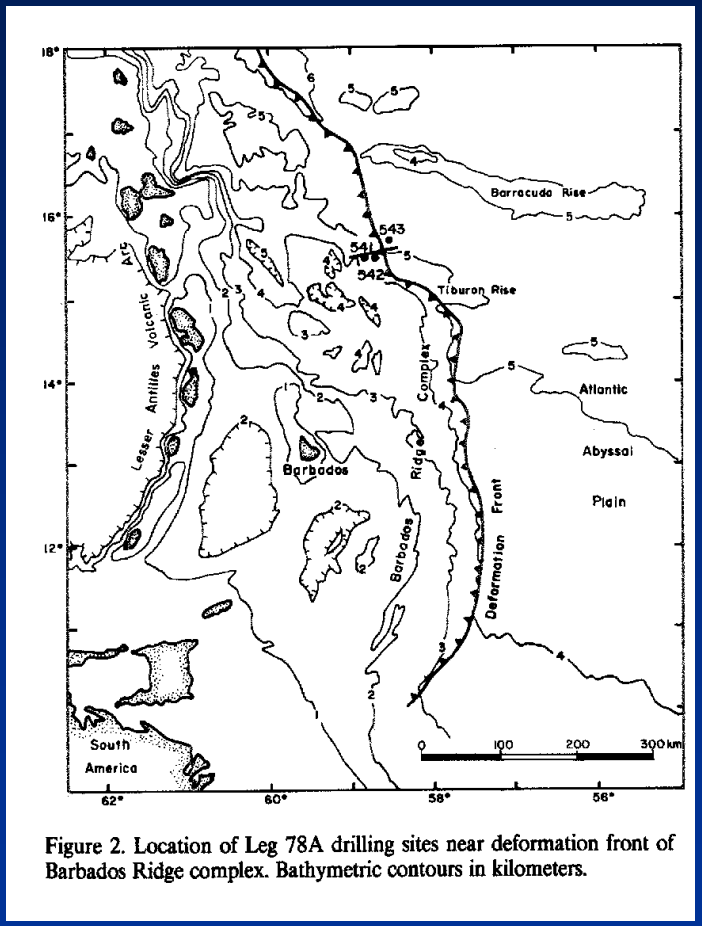

Figure 2. Location of Leg 78A drilling sites near deformation front of Barbados Ridge complex. Bathymetric contours in kilometers.

Moore and Lundberg, 1986

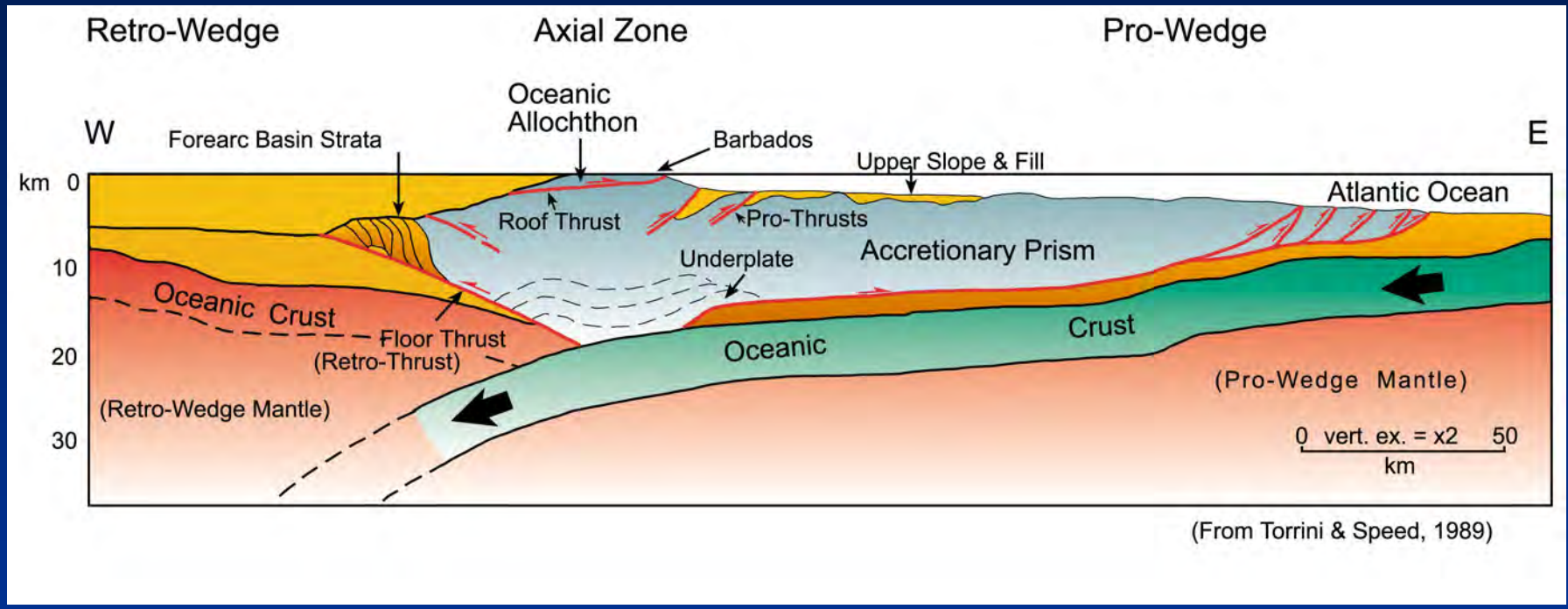

(From Torrini & Speed, 1989)

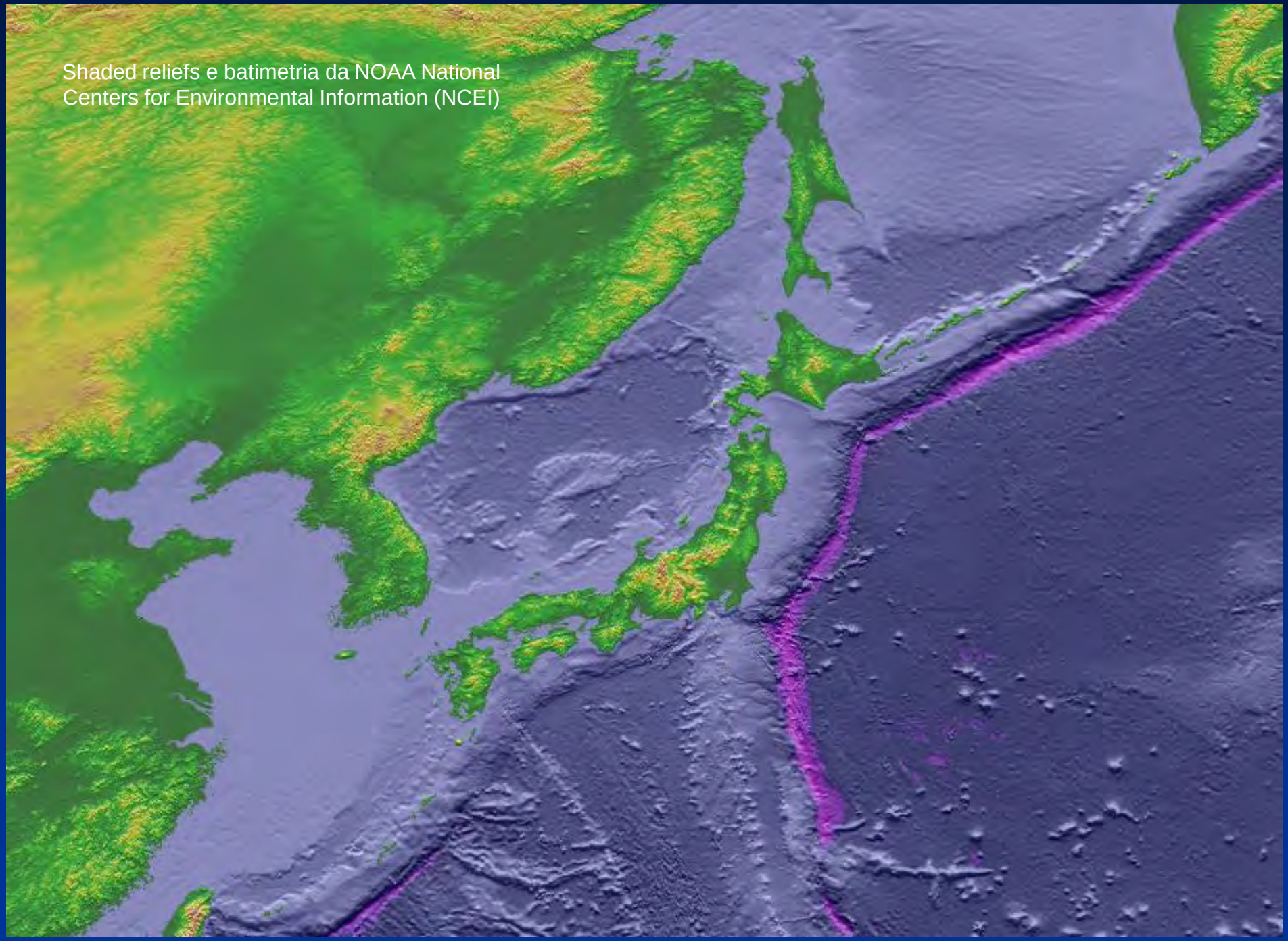
Shaded reliefs e batimetria da NOAA National
Centers for Environmental Information (NCEI)

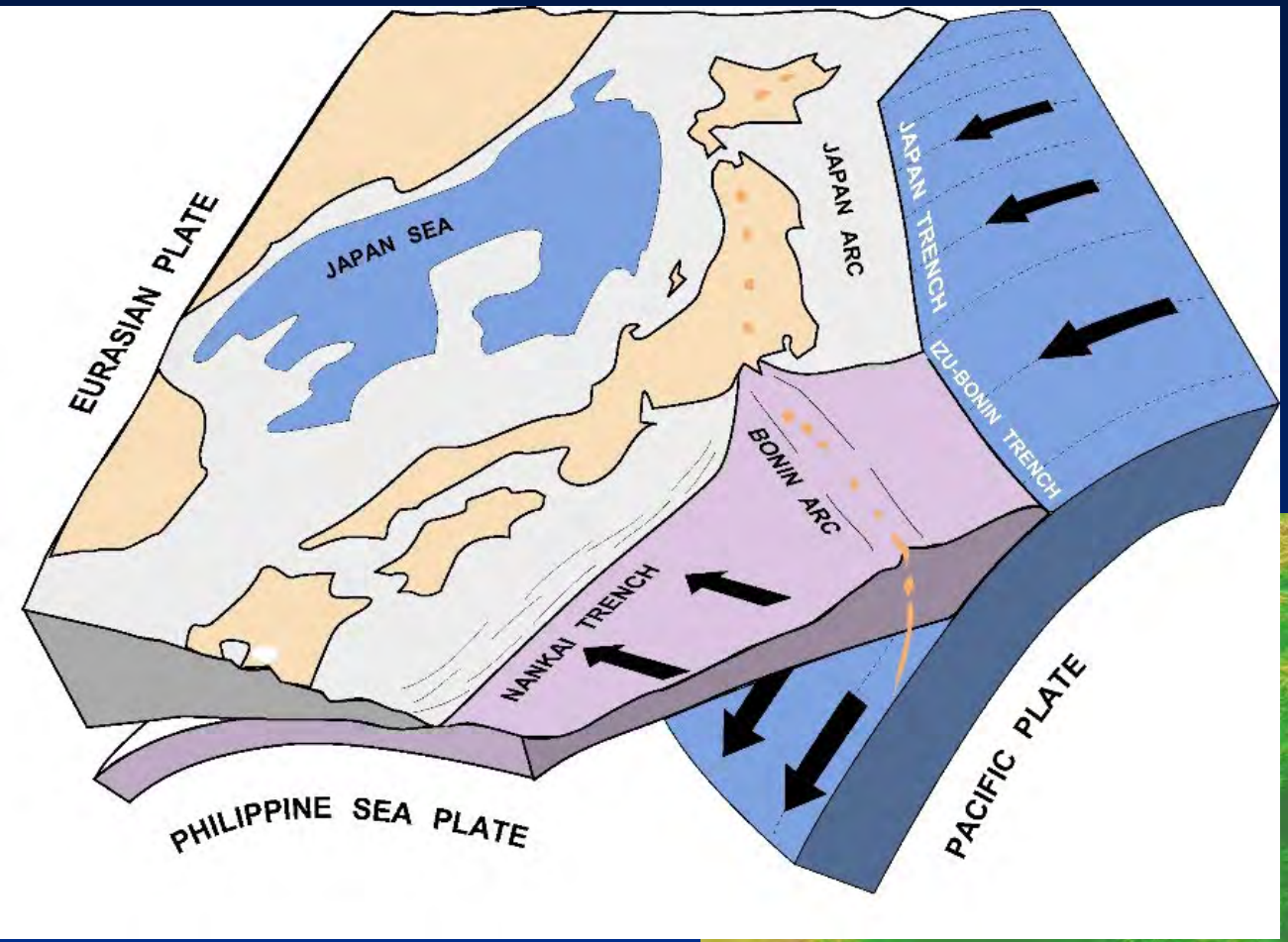

Laurent Jolivet, Sorbonne Université, CNRS-INSU

Shaded reliefs e batimetria da NOAA National Centers for Environmental Information (NCEI)

Figure F1. Map showing locations of Leg 190 and 196 sites. The red box outlines the location of the three-dimensional seismic survey. Yellow numbers indicate sites revisited during Leg 196. Depth contours are in kilometers.

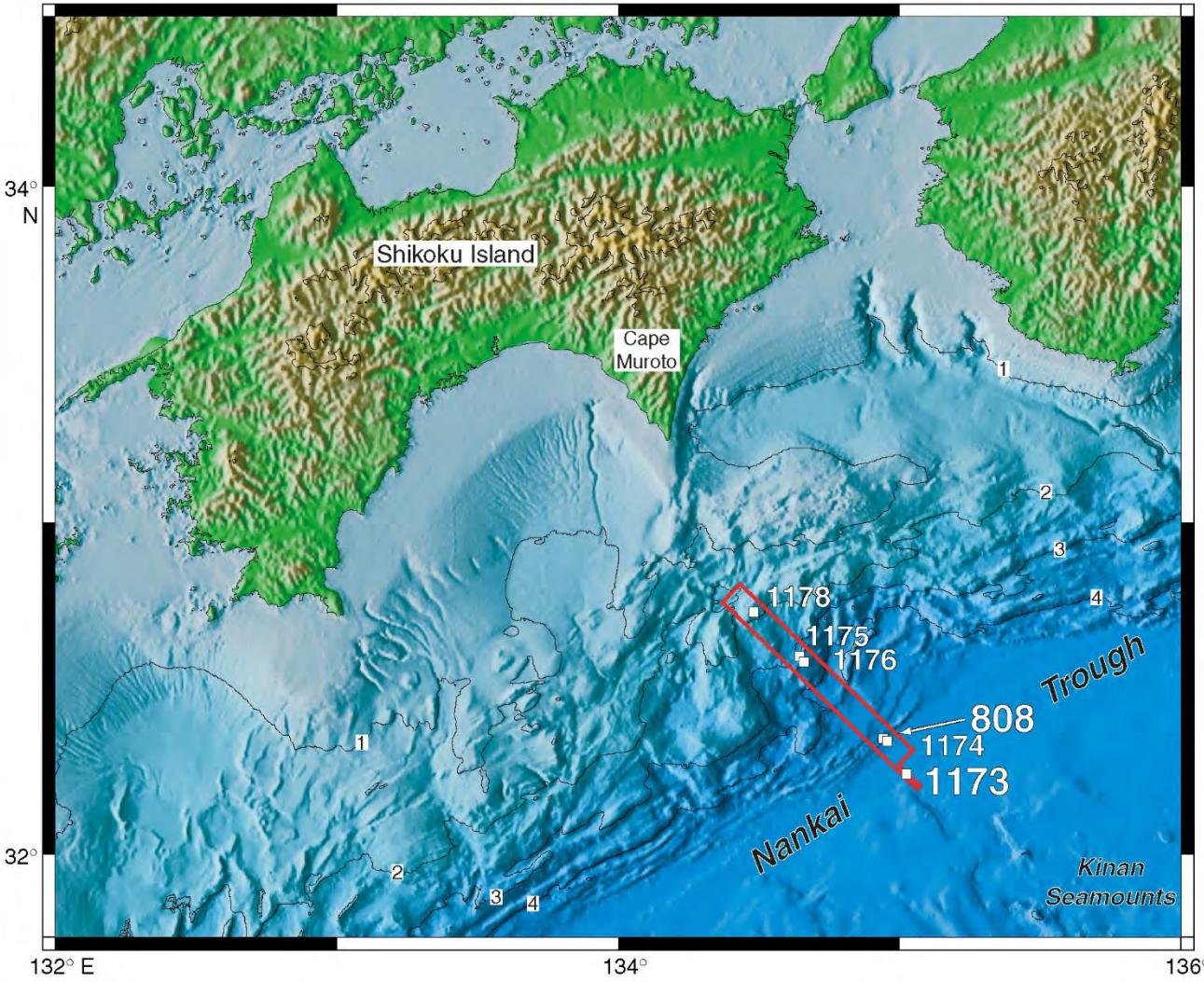

Shipboard Scientific Party, 2002. Chapter 1, Summary. In Proceedings of the ODP, Initial Reports, Leg 196

http://www-odp.tamu.edu/publications/196_IR/chap_01/chap_01.htm

Giappone (Nankai Trench)

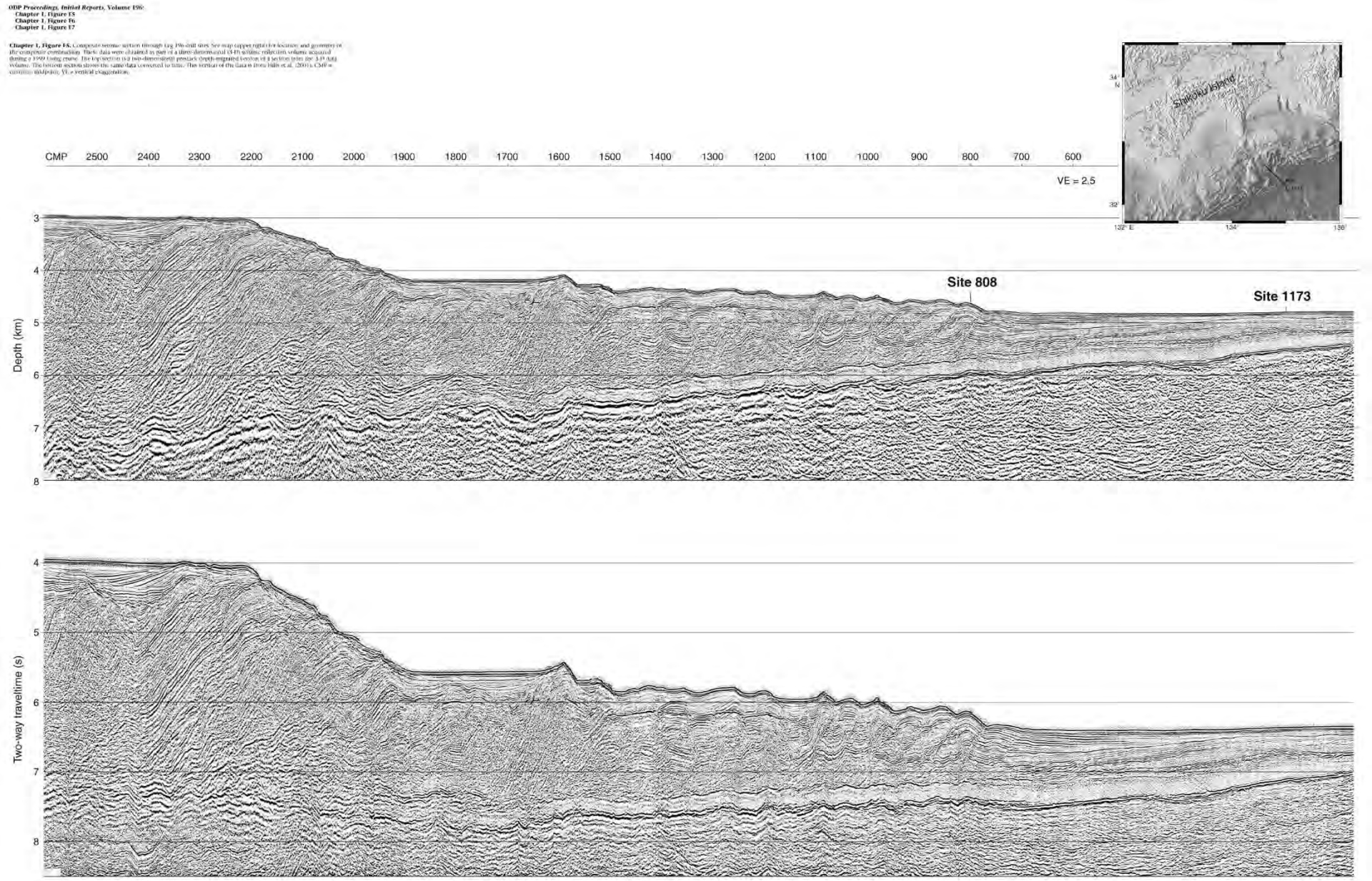

Mikada, H., Becker, K., Moore, J.C., Klaus, A., et al., 2002 Proceedings of the ODP, Initial Reports, Leg 196, 2002. Oversized Materials http://www-odp.tamu.edu/publications/196_IR/196TOC.HTM

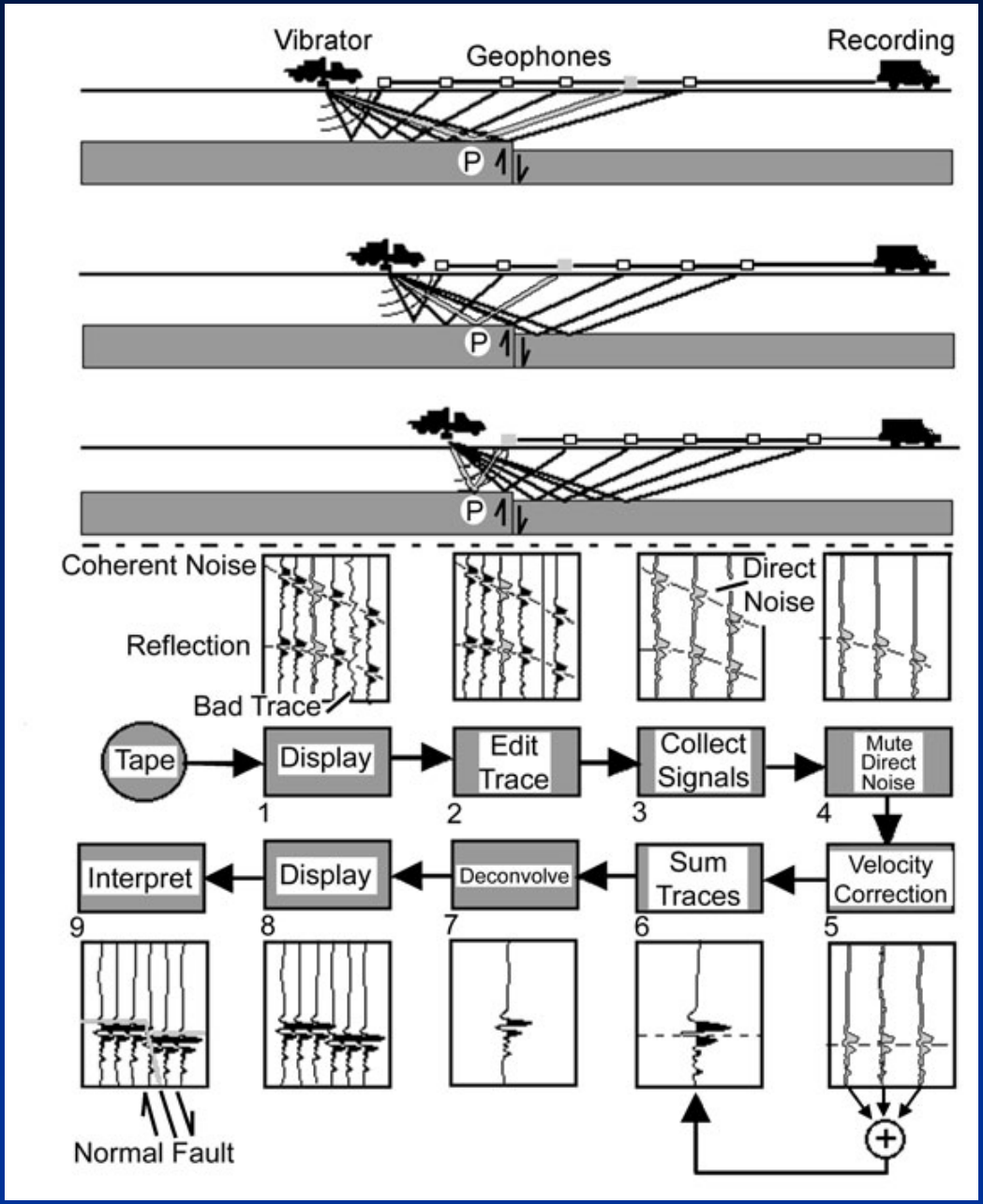

Da van der Pluim & Marshak, 2004

Figure F4. Seismic depth section across Sites 1173, 1174, and 808 (Hills et al., 2001). The section is composed of a northwest-trending segment of seismic line 215 through Site 1173, with a diagonal transition to line 281 that passes near Sites 1174 and 808. CDP = common depth point, VE = vertical exaggeration.

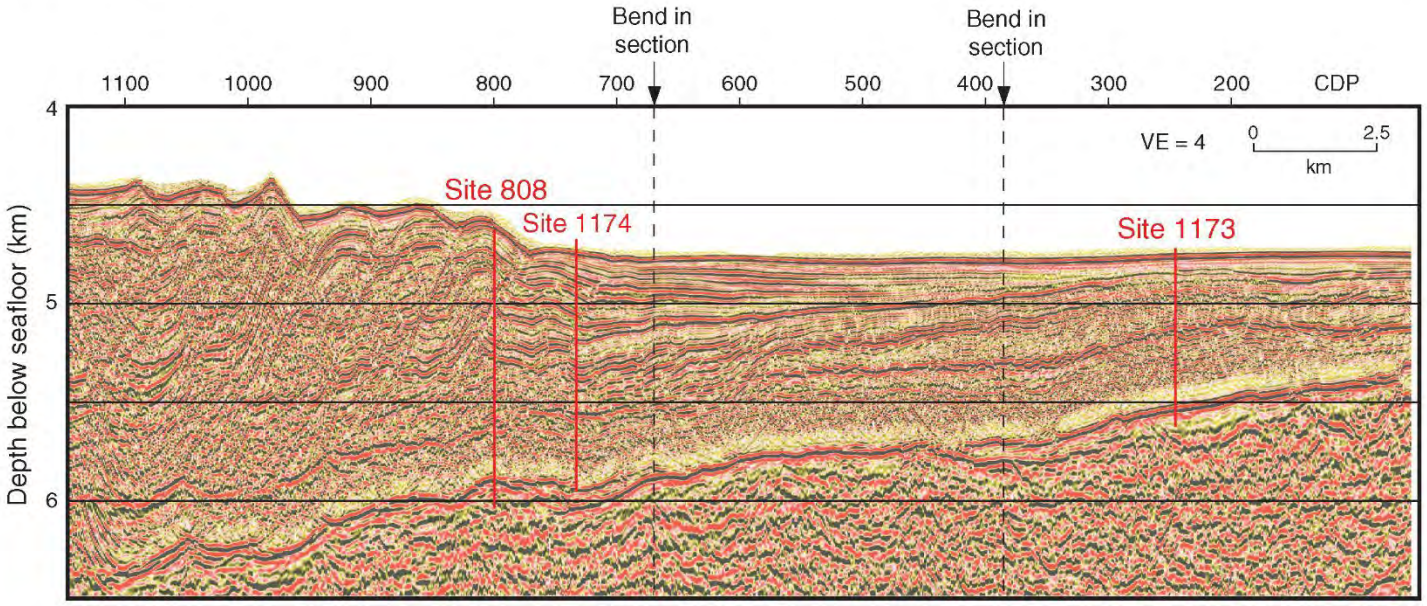

koku Basin to the imbricate thrust zone. liagonal transition to line 281 that passes

Shipboard Scientific Party, 2002. Chapter 1, Summary. In Proceedings of the ODP, Initial Reports, Leg 196 http://www-odp.tamu.edu/publications/196_IR/chap_01/chap_01.htm

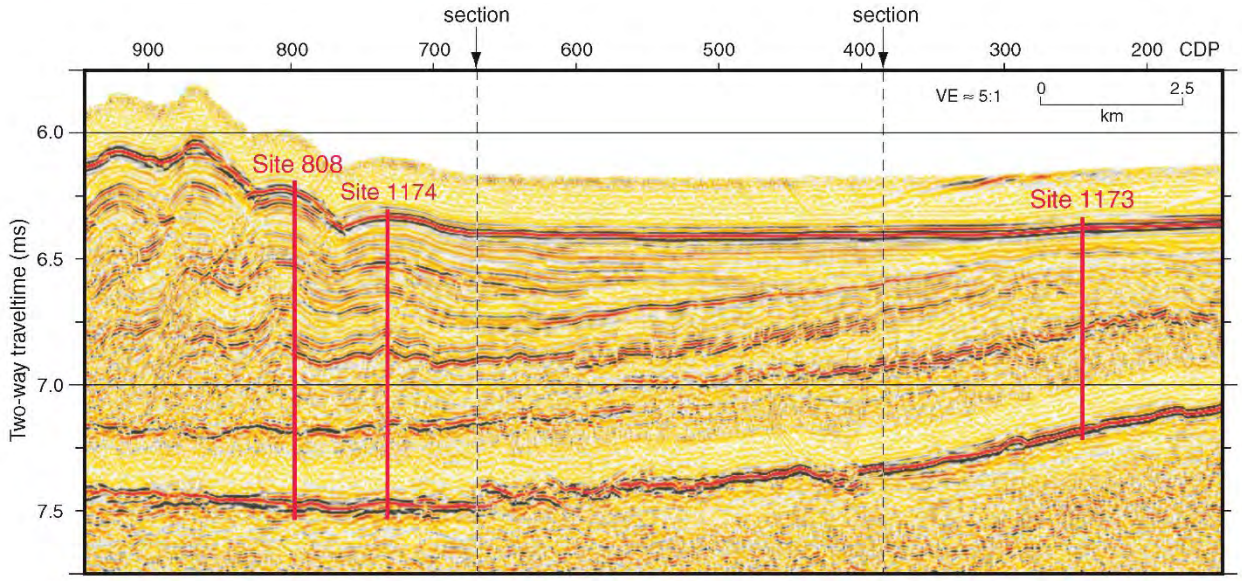

Giappone (Nankai Trench)

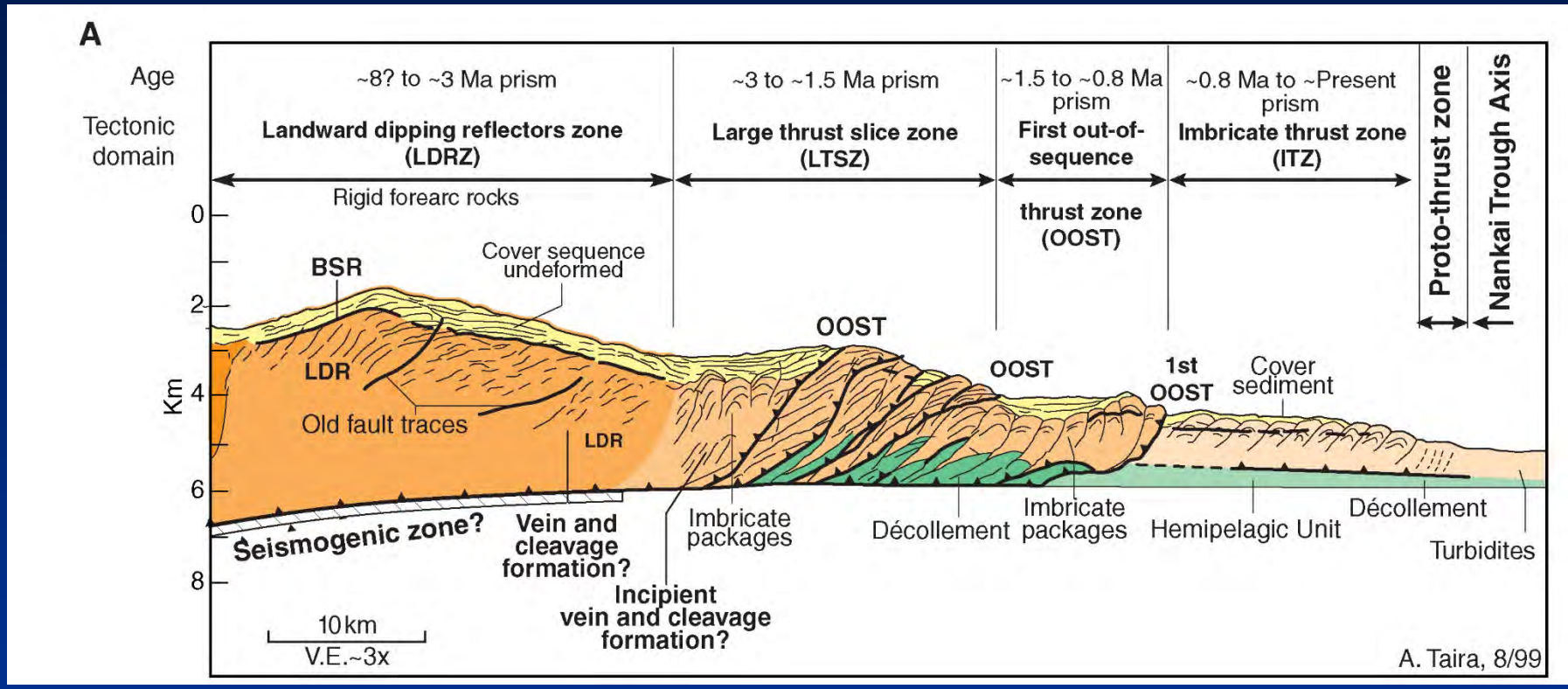

Moore, Taira, Baldauf & Klaus, 2000, ODP Scientific Prospectus Leg 190
http://www-odp.tamu.edu/publications/prosp/190_prs/190toc.html

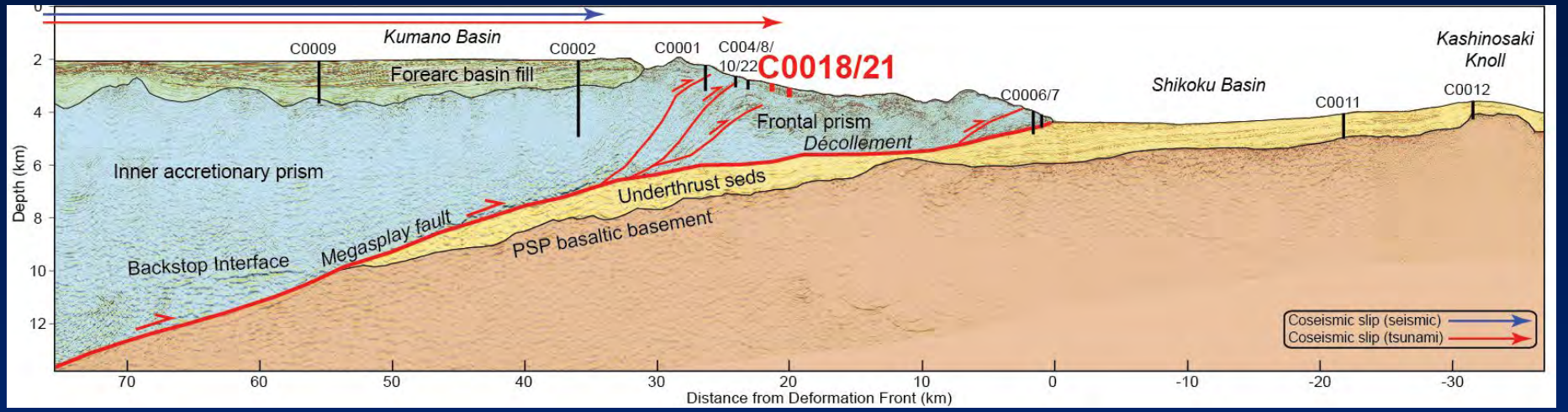

Moore et al., 2014

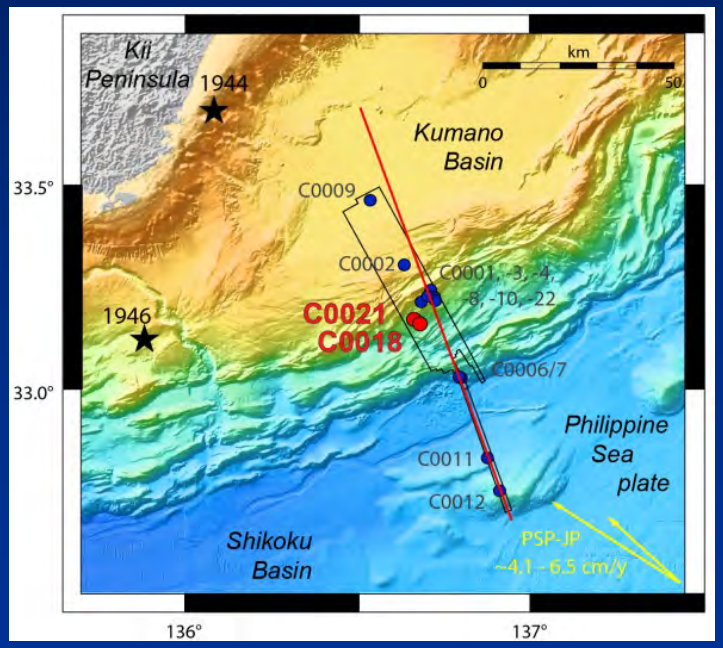

Moore et al., 2014

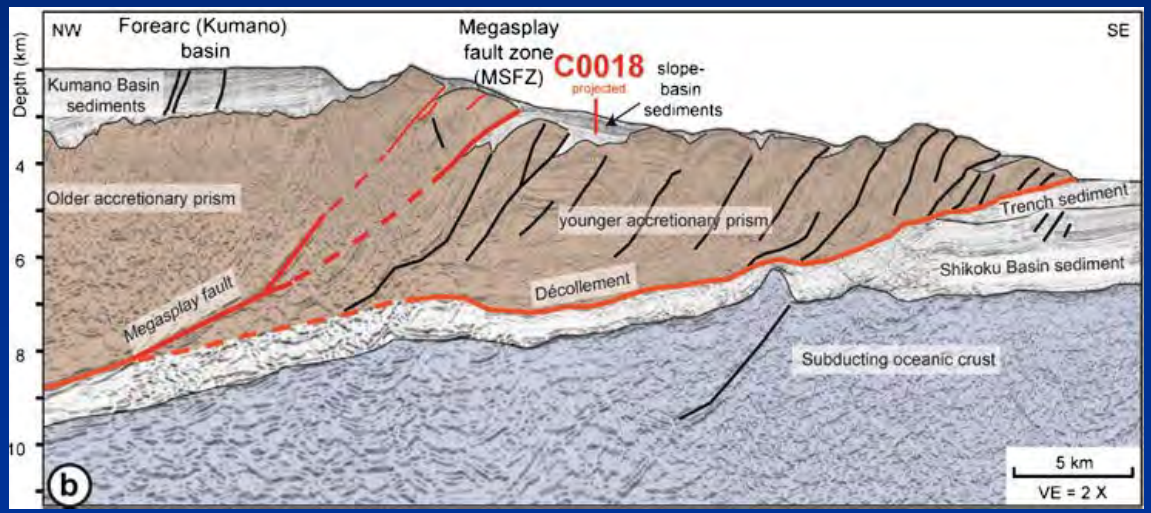

Strasser et al., 2012

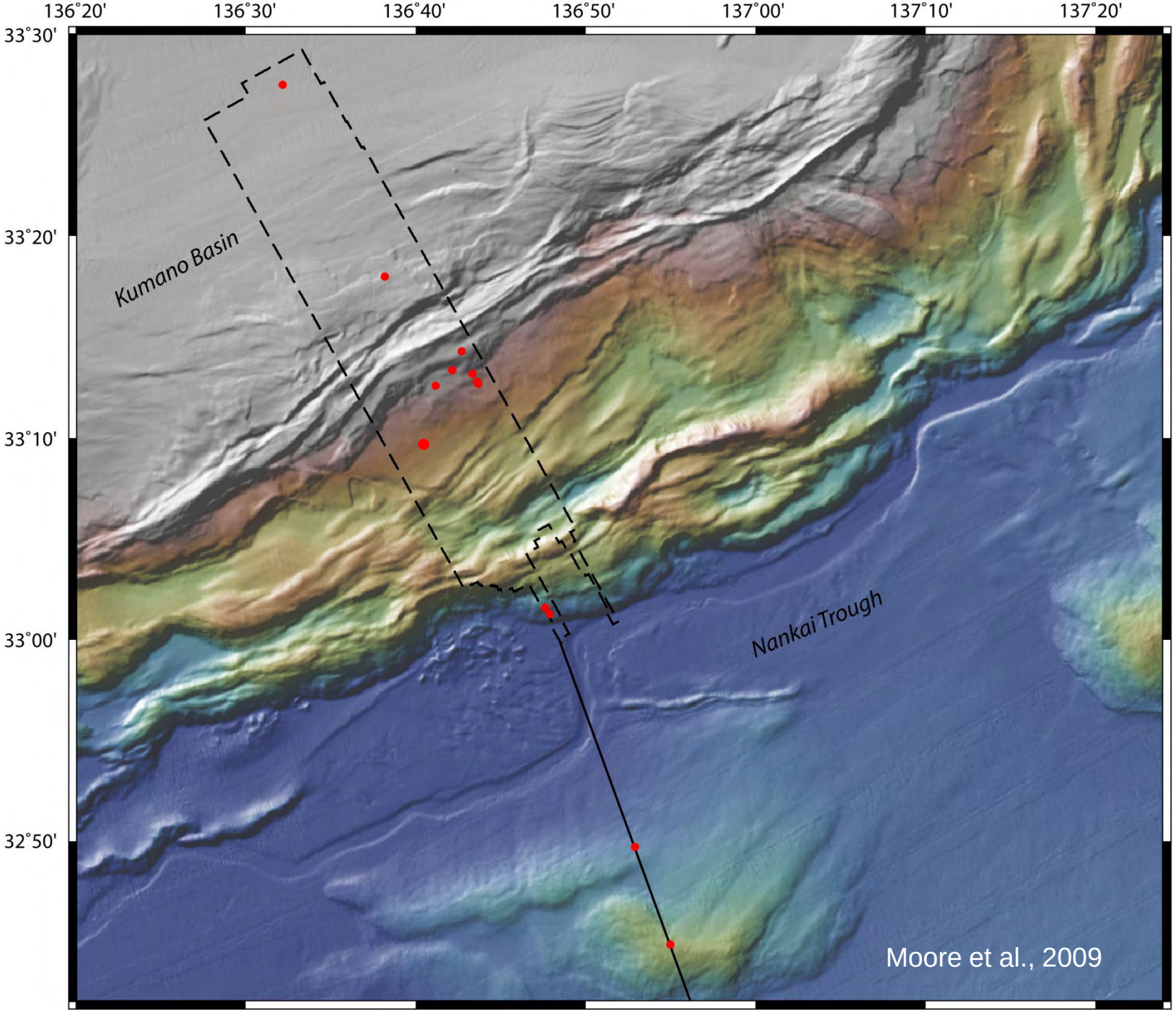
136°20'
136°30'
136°40'
136°50'
137°00'
137°10'
137°20'
33°30'
33°20'
33°10'
33°00'
32°50'
Kumano Basin
Nankai Trough
Moore et al., 2009

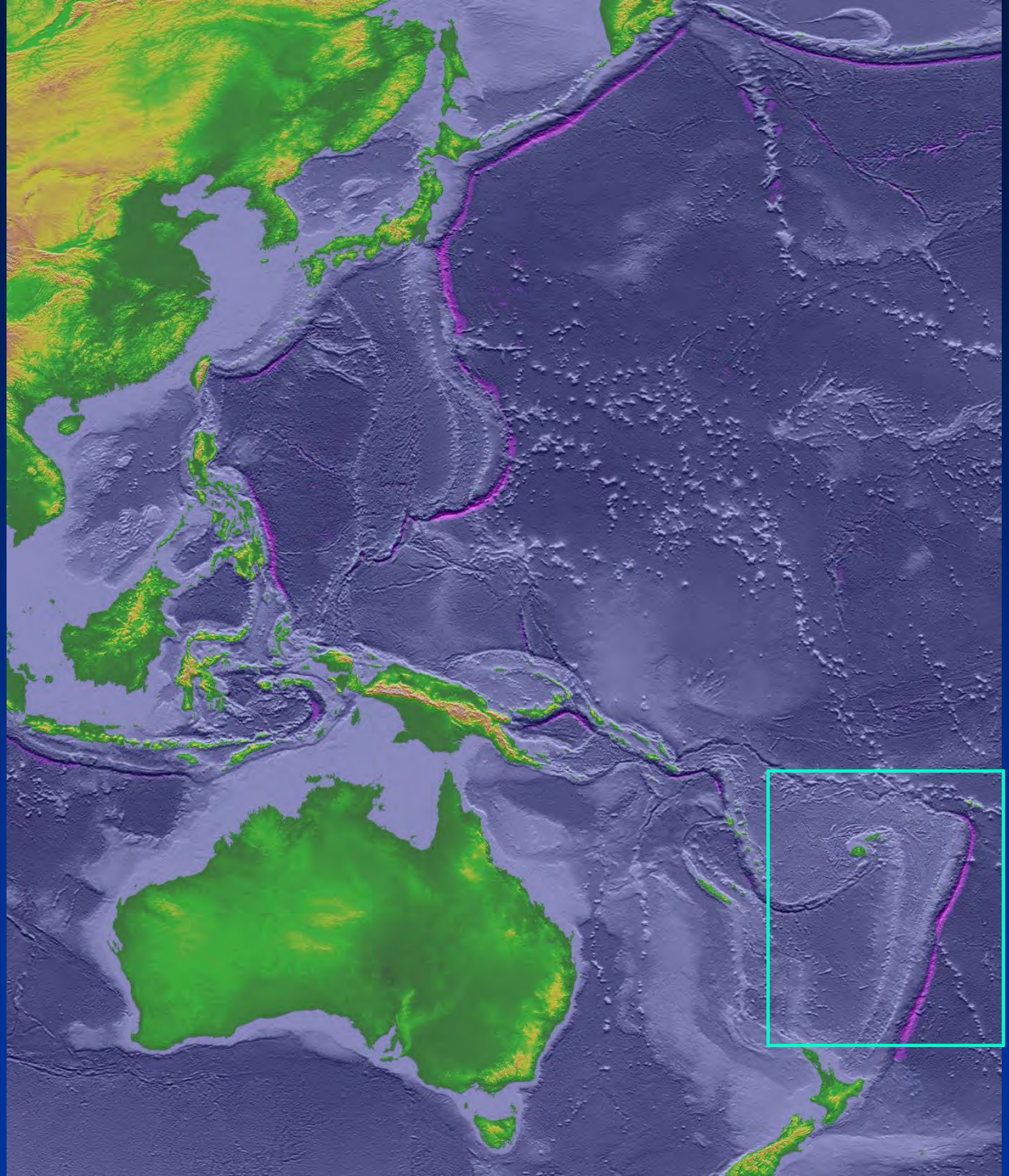

Shaded reliefs e batimetria da NOAA National Centers for Environmental Information (NCEI)

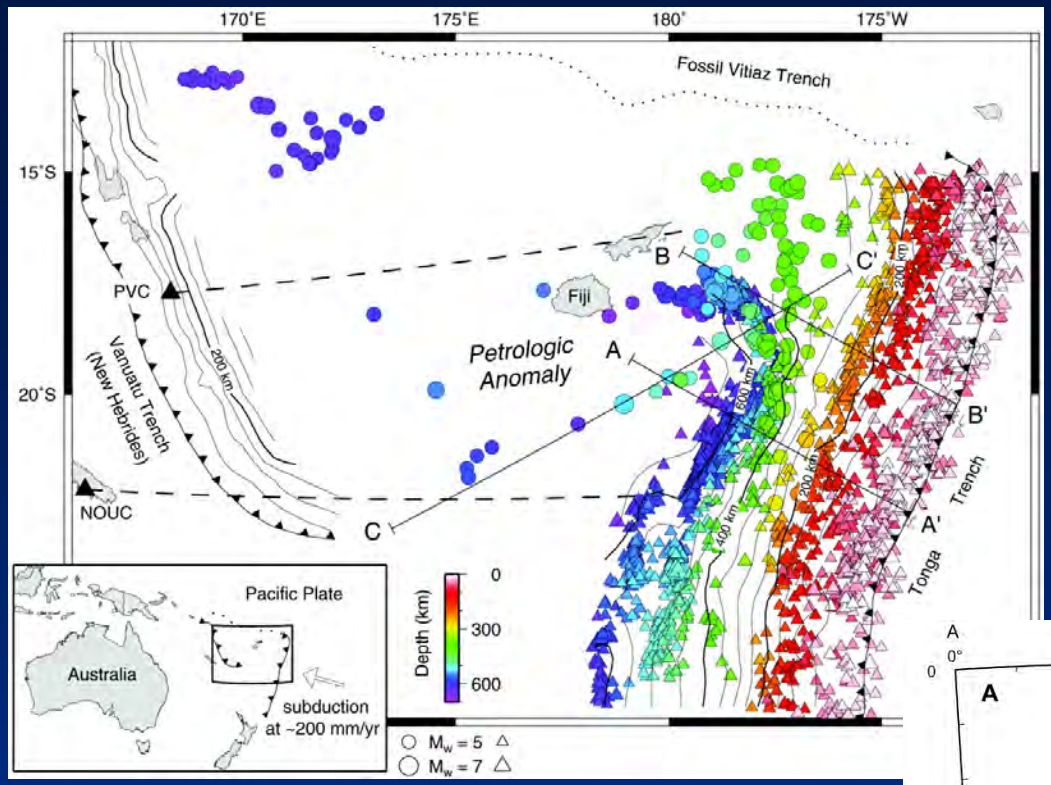

Da Cheng & Brudzinski, 2001

Mappa e tre sezioni crostali-mantelliche mostranti la profondità degli ipocentri dei terremoti a magnitudo ≥ 5 occorsi tra il 1964 e il 1999 nelle Tonga Fiji.

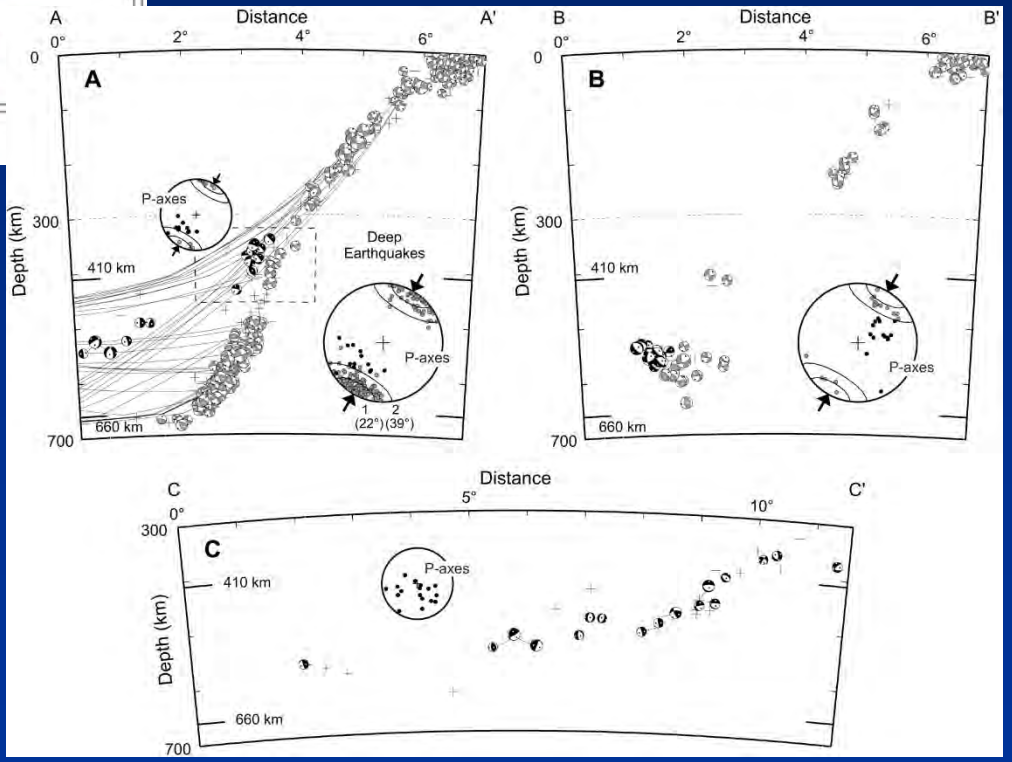

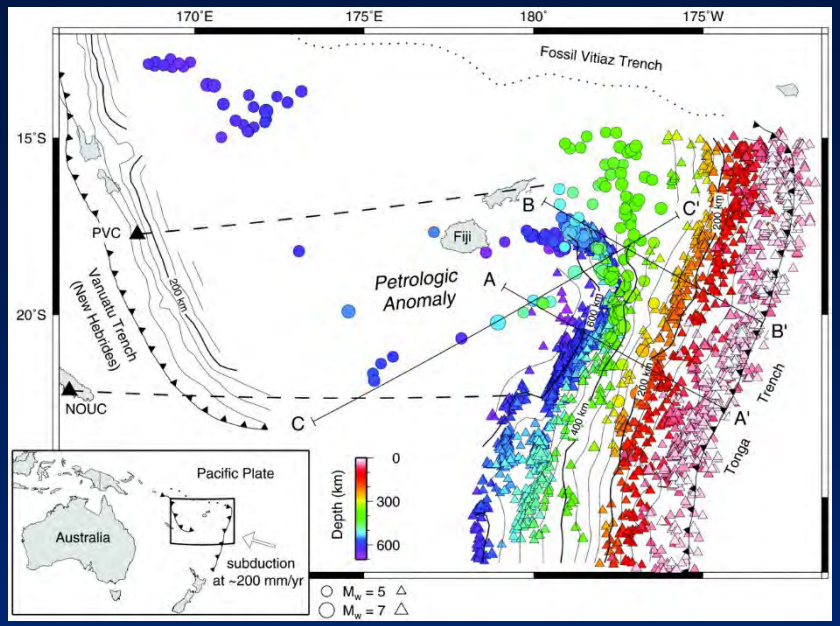

Ricostruzione 3D della sismicità sotto alla fossa-retroarco di Tonga

Da Cheng & Brudzinski, 2001

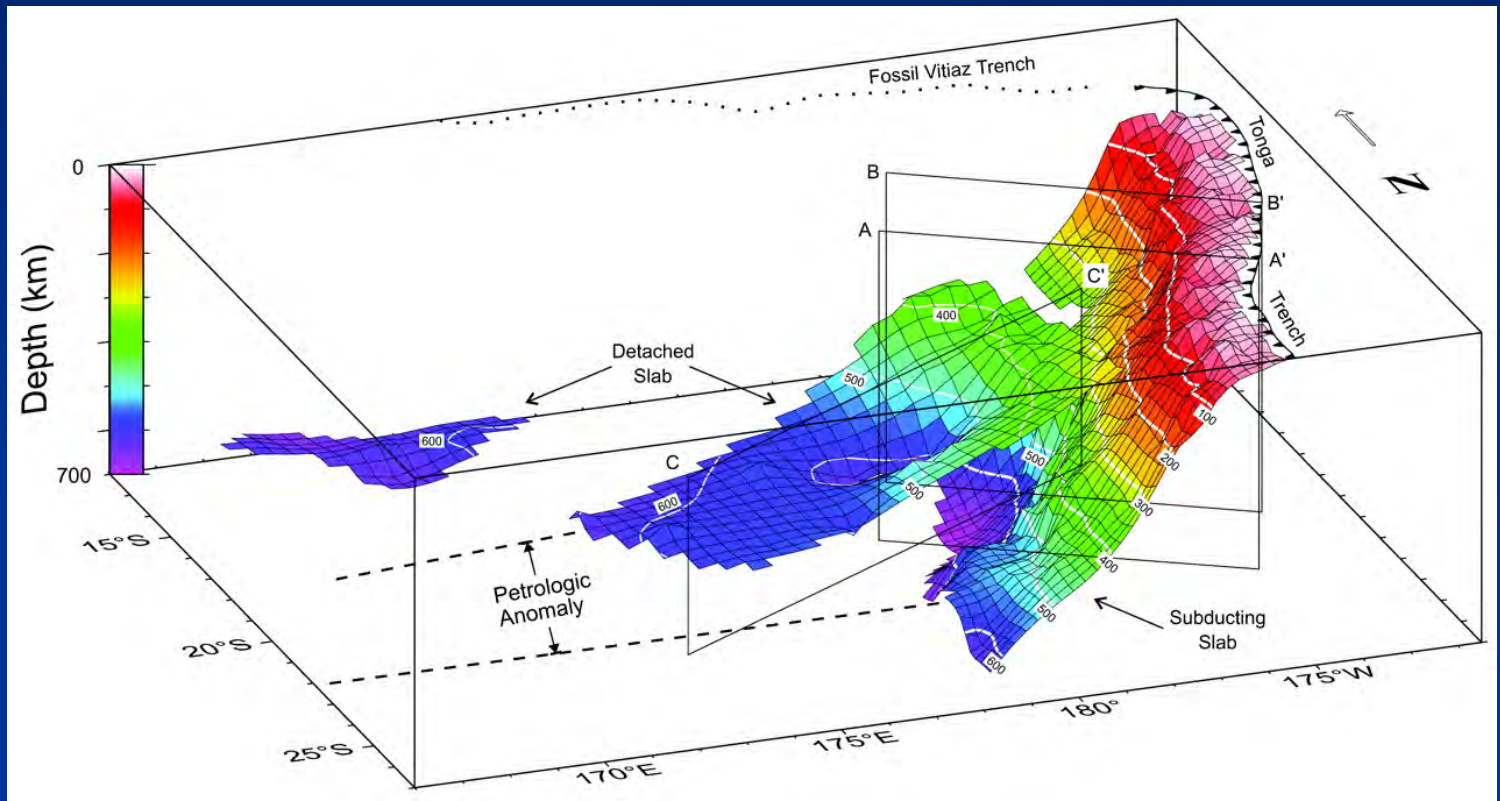

Prismi di accrezione: cordillera-andino

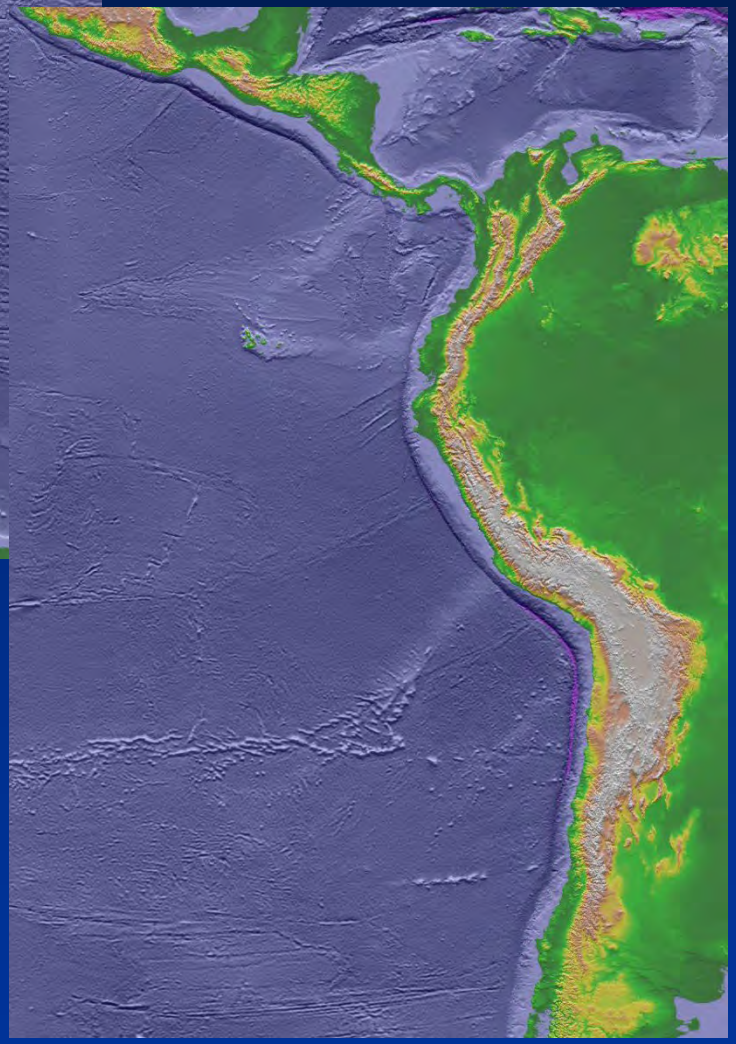

Shaded reliefs e batimetria da NOAA National Centers for Environmental Information (NCEI)

Shaded reliefs e batimetria da NOAA National Centers for Environmental Information (NCEI)

Prismi di accrezione

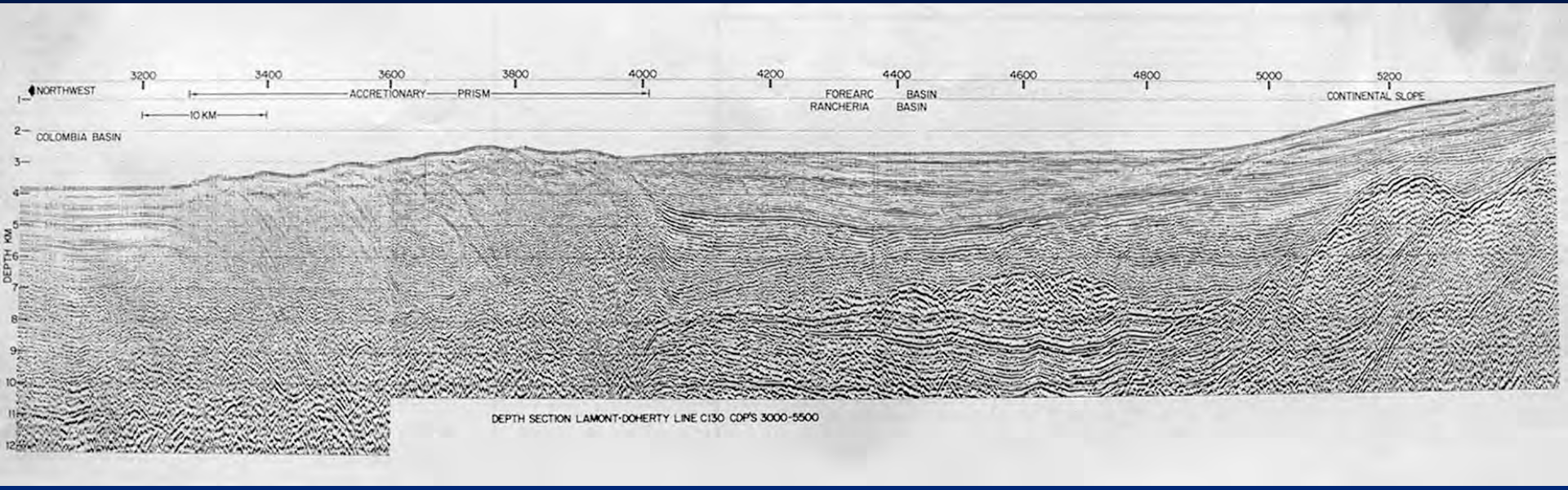

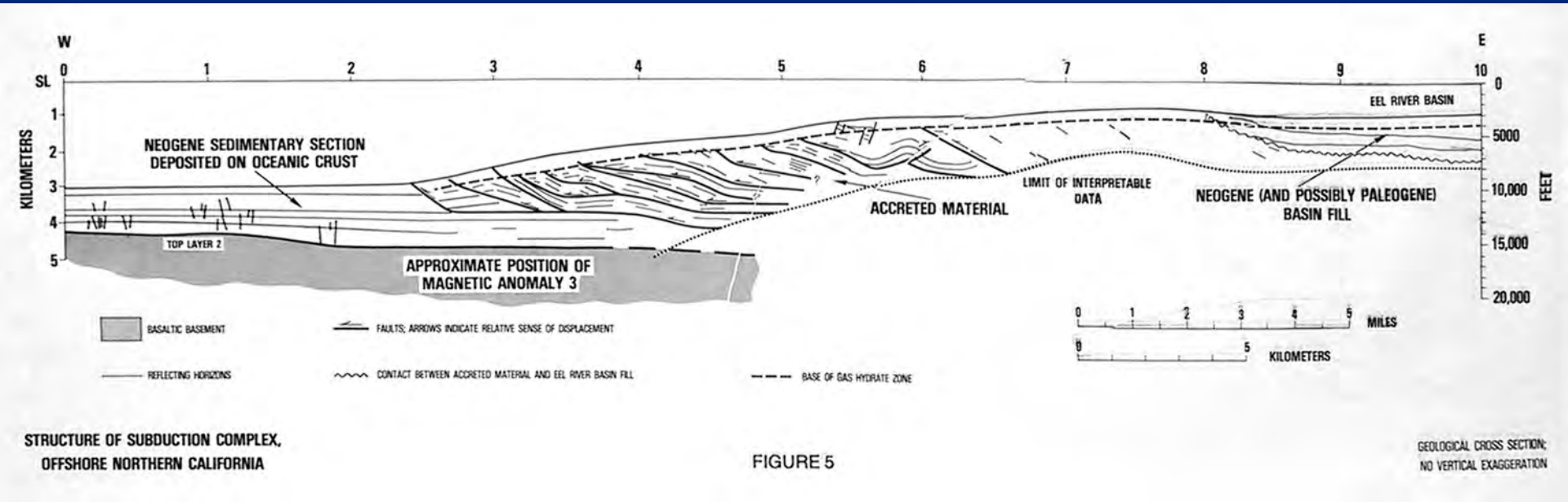

STRUCTURE OF SUBDUCTION COMPLEX, OFFSHORE NORTHERN CALIFORNIA

FIGURE 5

GEOLOGICAL CROSS SECTION; NO VERTICAL EXAGGERATION

Tipo cordillera o andino

Da Bally (ed.), 1985

Prismi di accrezione

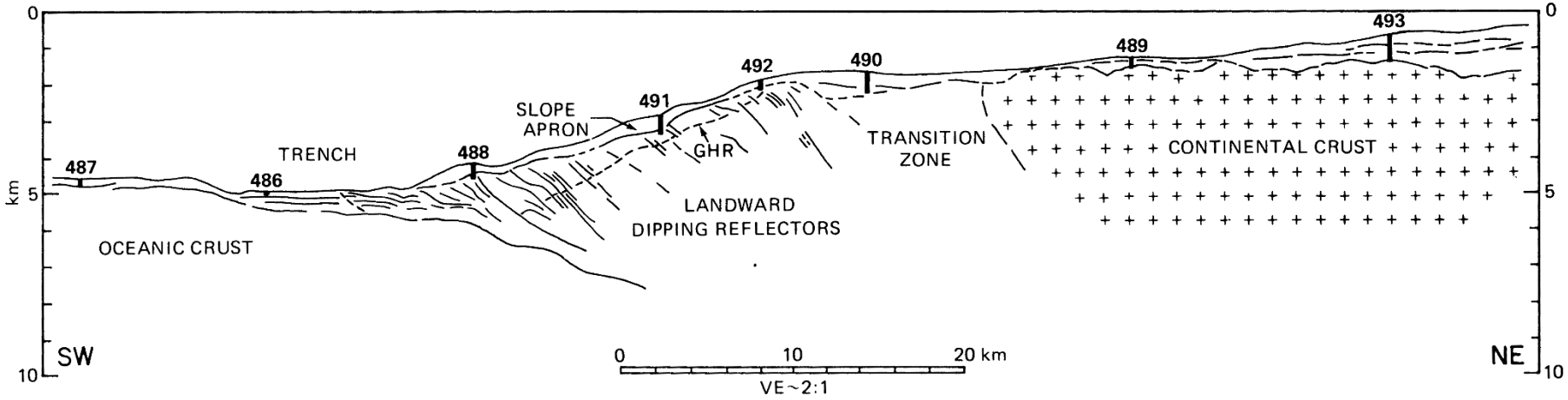

Figure 7. Cross section across the Middle America Trench off Southern Mexico in the Leg 66 drilling area (Moore and others, 1982). Vertical exaggeration (VE) is about 2:1.

Da Moore & Lundberg, 1986

Tipo cordillera o andino

https://commons.wikimedia.org/wiki/File:Tectonic_plates_boundaries_detailed-en.svg

Da Horton, 2018

Da Armijo et al., 2015

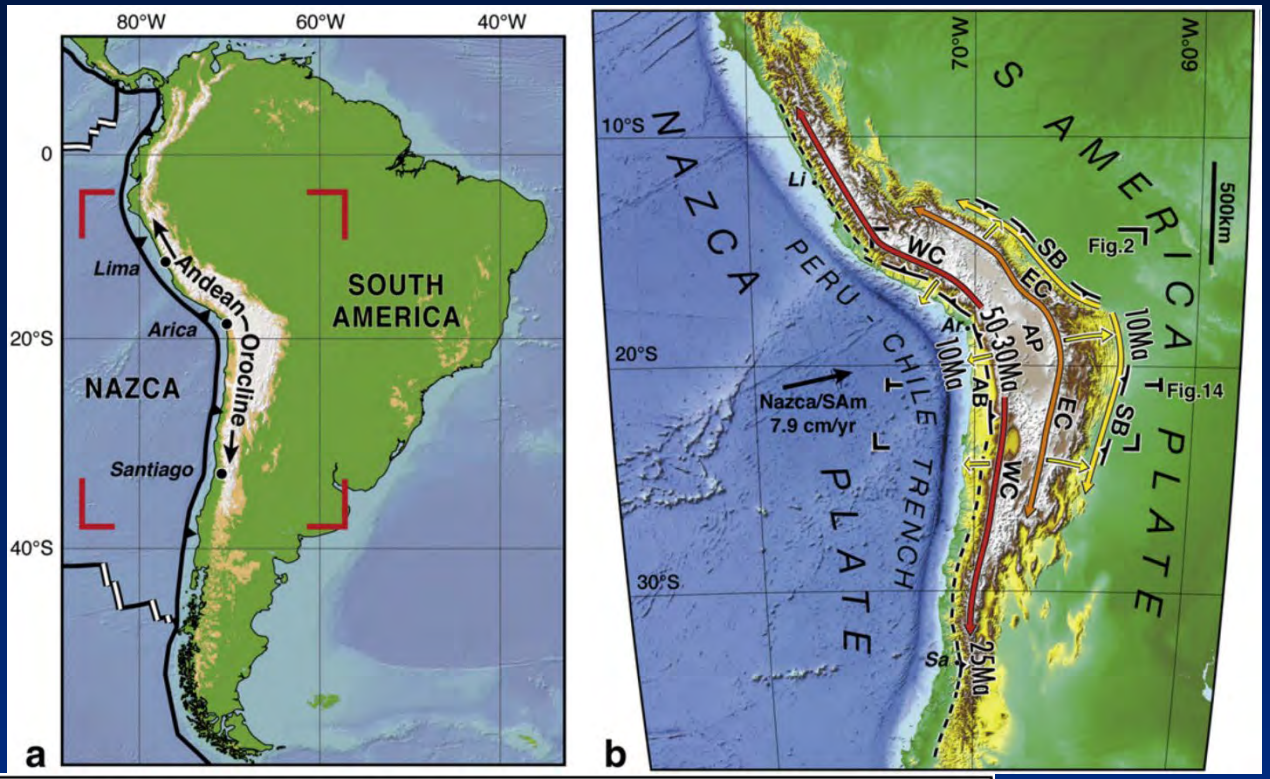

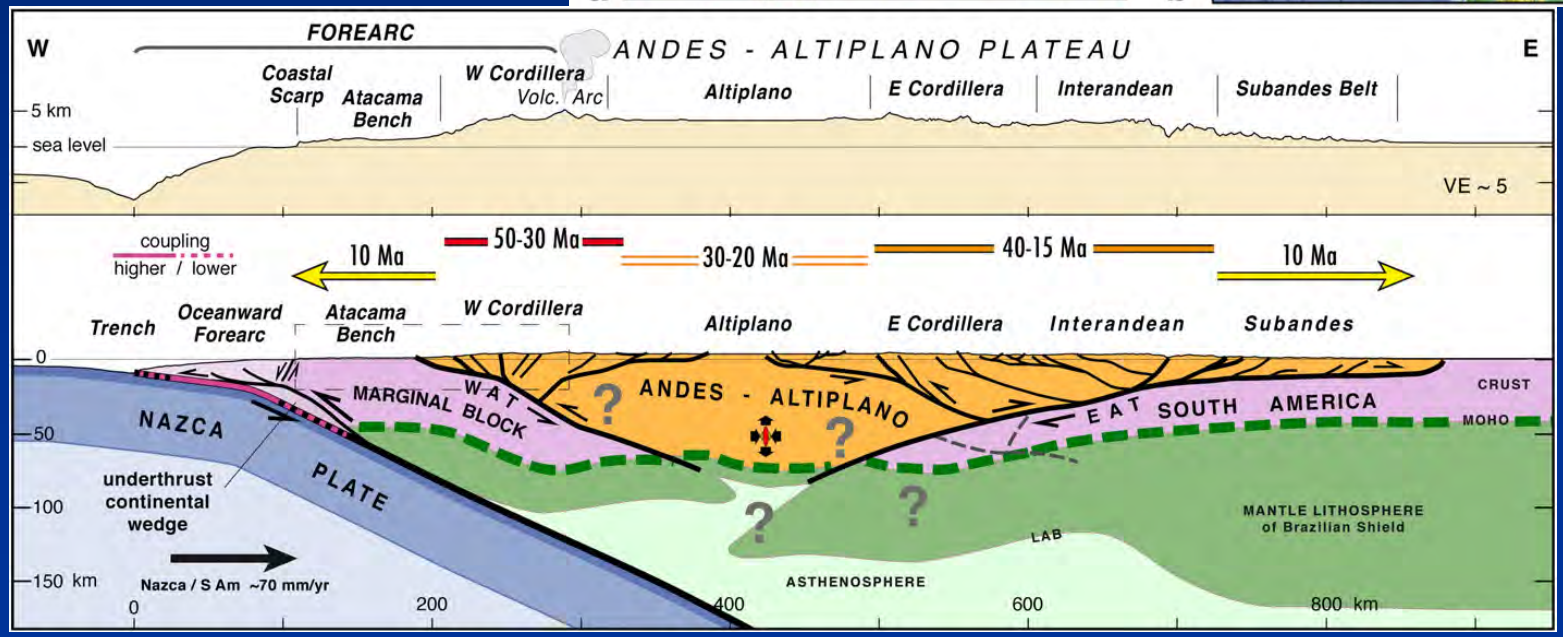

Da Armijo et al., 2015

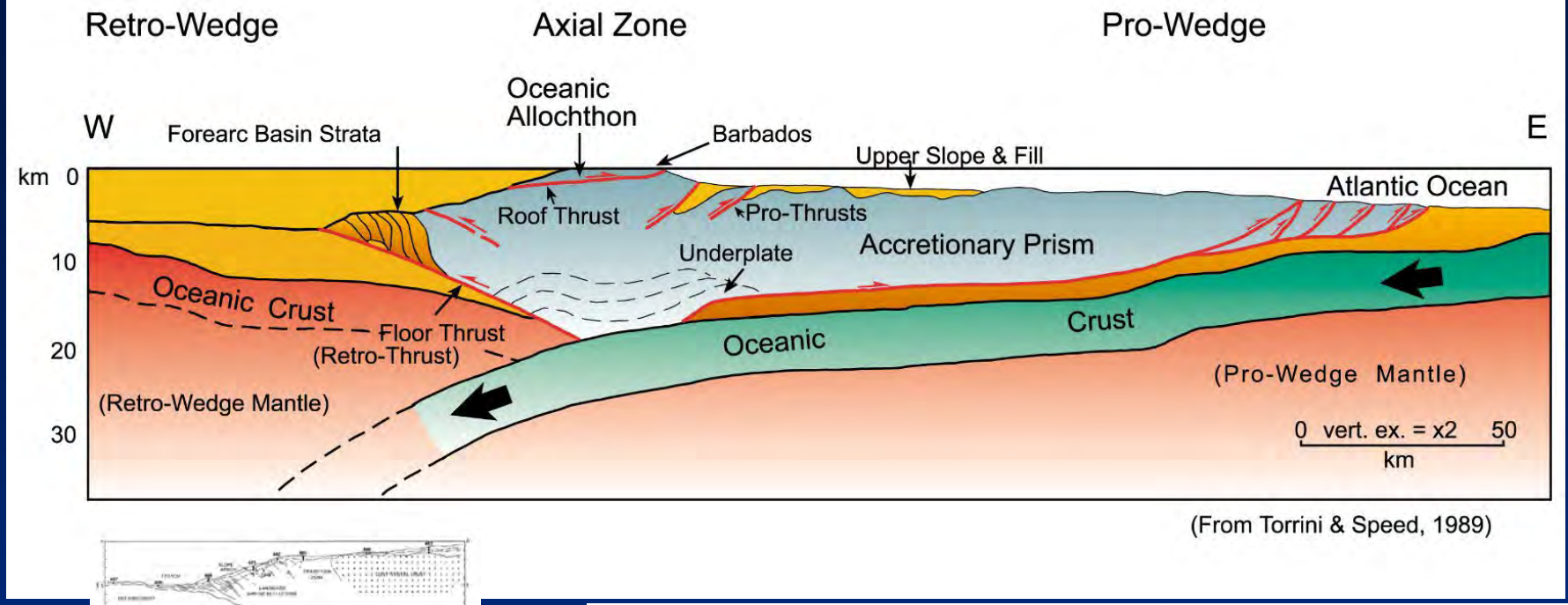

Da Armijo et al., 2015; Moore and Lundberg, 1986

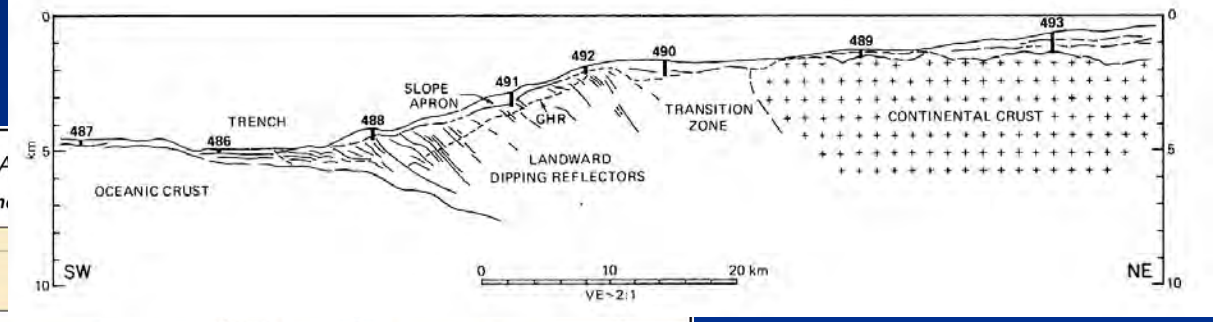

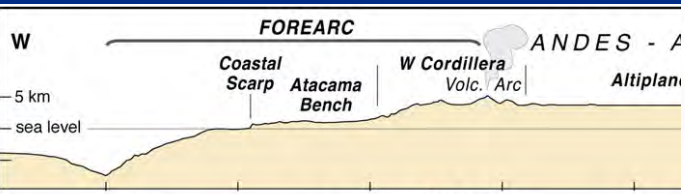

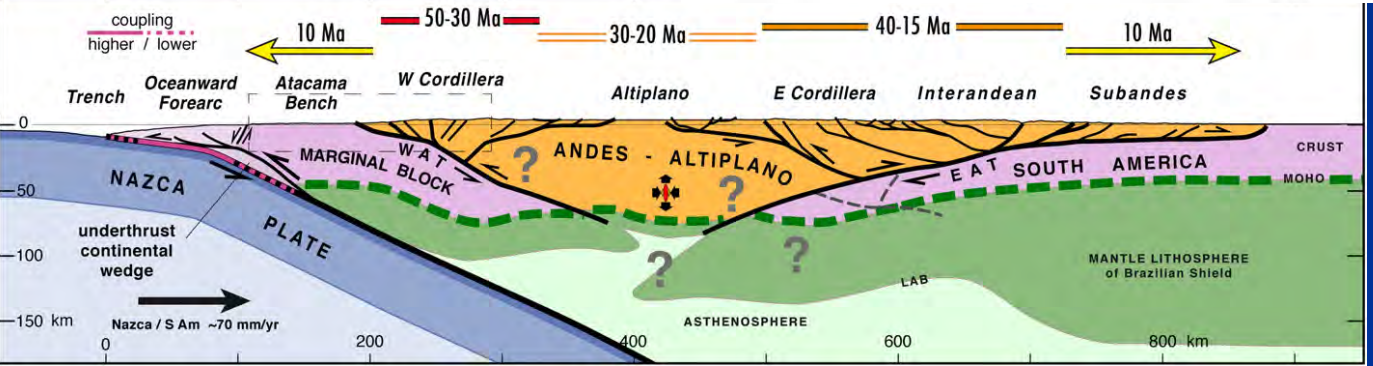

Prismi di accrezione: i due tipi

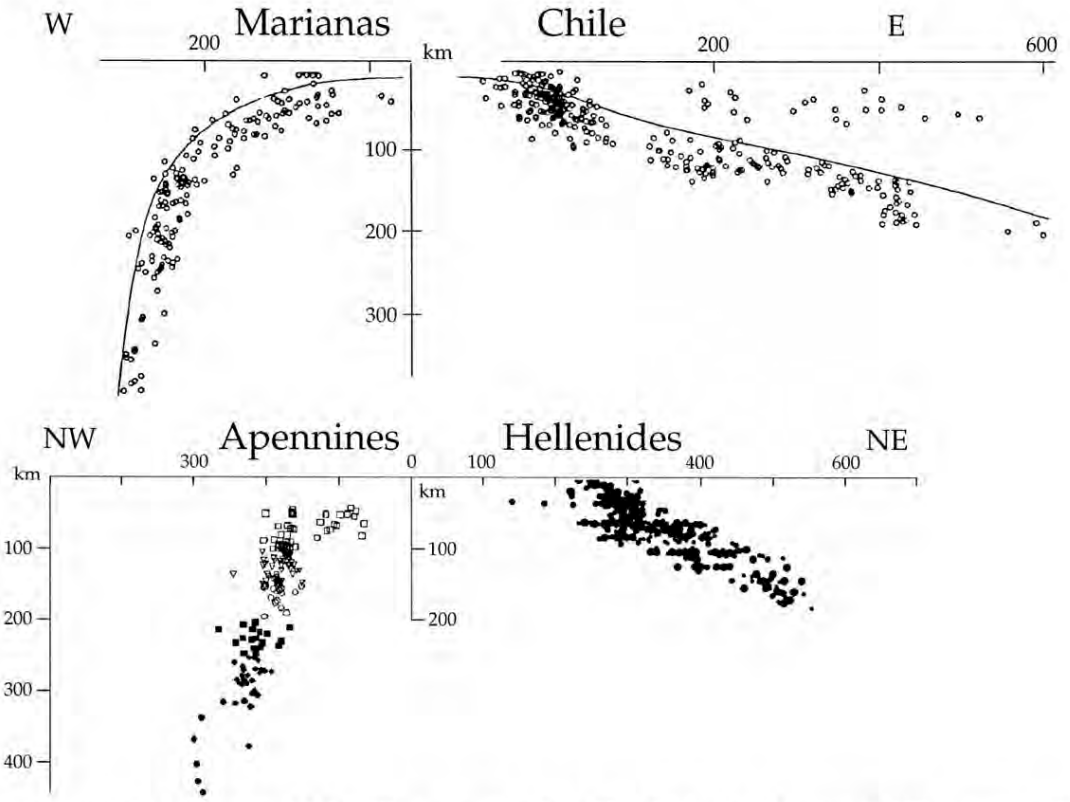

Fig. 3. Ipocenters of the Marianas and Chile subduction zones in the Pacific (after Isacks and Barazangi, 1977), compared with the seismicity of the Apennines (Selvaggi and Chiarabba, 1995) and Hellenides (Papazachos and Comninakis, 1977) opposed subduction zones. The Pacific asymmetry is present also in the central Mediterranean subduction zones where the Ionian oceanic lithosphere is subducting contemporaneously both underneath the Apennines and the Hellenides. Location of the sections in Fig. 2.

Da Doglioni et al., 1999

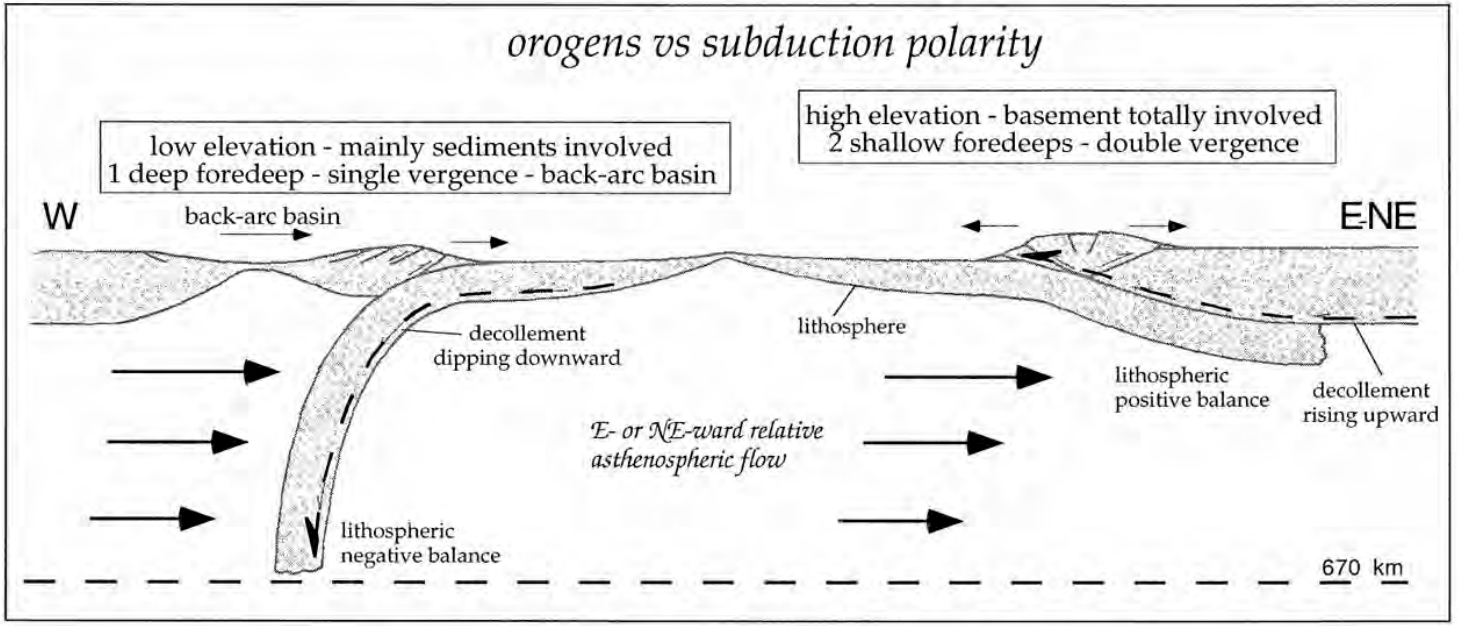

Fig. 5. W-directed subduction zones are steeper and deeper with respect to the E–NE- or NNE-directed subduction zones. Note that the decollement plane of the eastern plate is warped and subducted in case of W-directed plane, whereas it ramps toward the surface in the E–NE-directed subduction, enabling the uplift of deep seated rocks: this asymmetry may be explained by the 'westward' drift of the lithosphere relative to the mantle and controls the strong differences in morphology, structure and lithology of the related thrust belts.

Da Doglioni et al., 1999

Active Back-Arc Basins (BAB) of the World

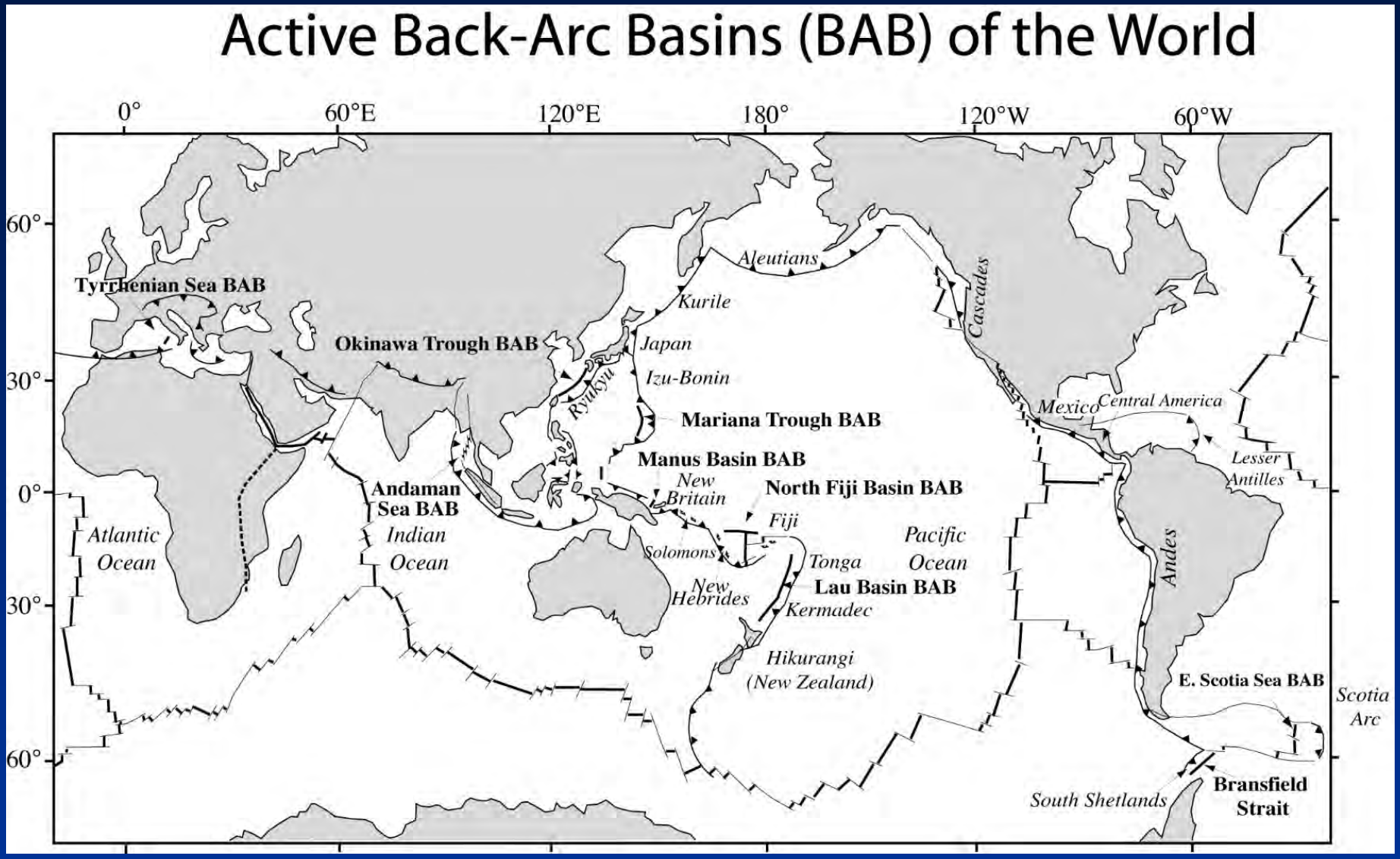

Da Wikipedia e da Guinot & Segonzac, 2017

Foreland system: flessura della litosfera

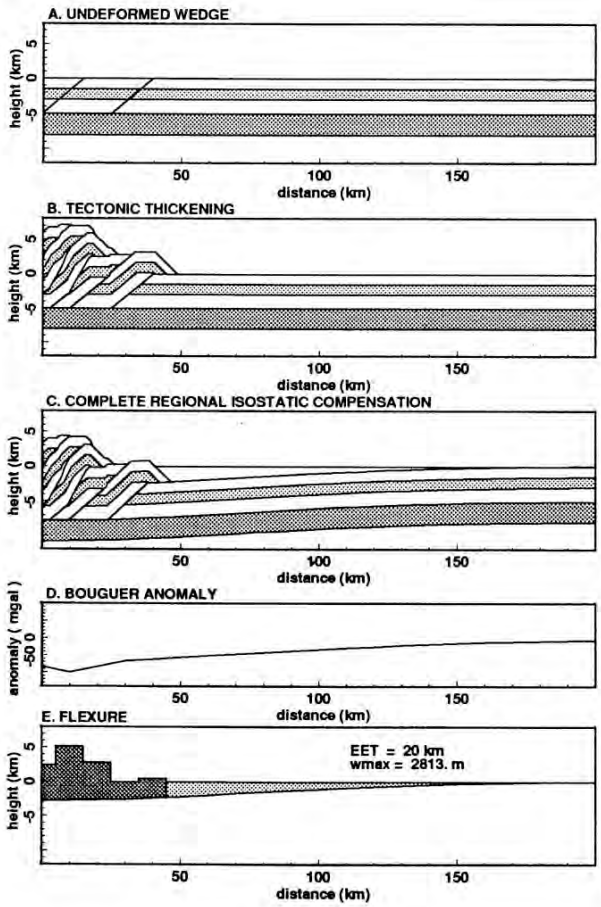

Figure 2-1. Effect of thrust loading on lithospheric response. Regional isostasy results in depression filled with sediments, a) initial situation, b) emplacement of thrust sheets onto the craton, c) flexural response to thrust mass loading, d) associated Bouguer gravity anomaly, e) flexure in (c) calculated with thrust load and sediment load on lithosphere with 20 km effective elastic thickness (EET), quantified after Price [1973].

Da Zoetemeijer, 1993

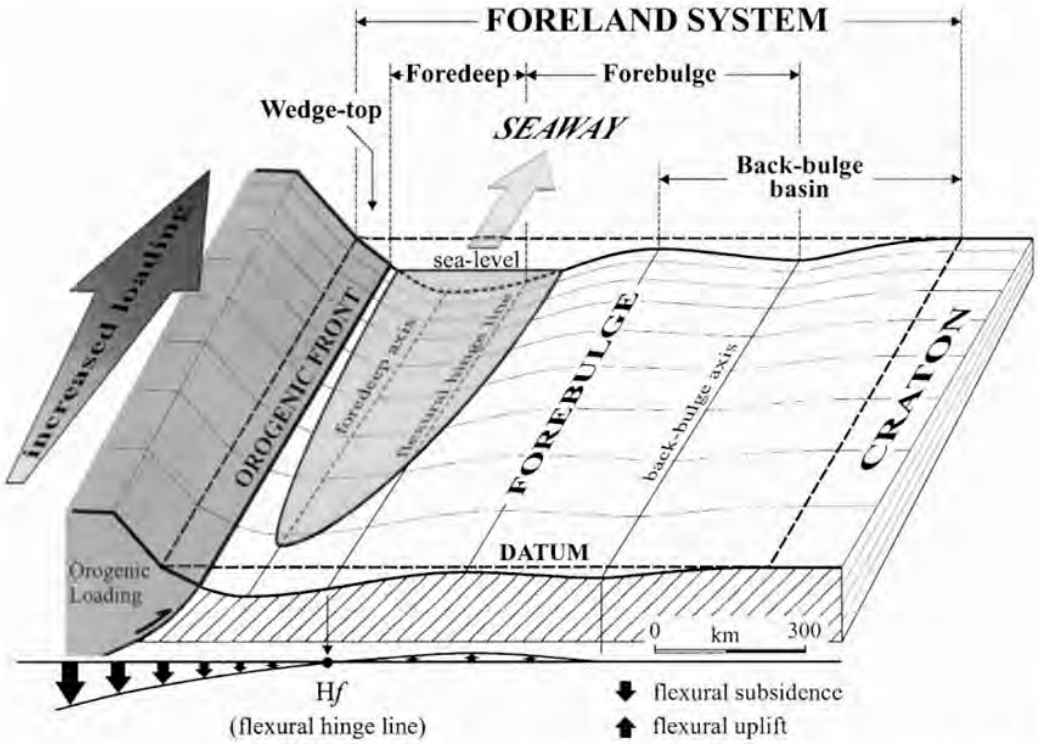

Fig. 3. Configuration of the foreland system during orogenic loading with strike variability. The magnitude of the flexural deflection is proportional to the degree of loading. Four depozones may be differentiated, i.e. wedge-top, foredeep, forebulge and back-bulge. We refer to the wedge-top and foredeep as the proximal sector, and to the forebulge and back-bulge as the distal sector. The proximal and distal sectors of the foreland system are separated by the flexural hinge line. The topographic elevation of the adjacent craton, approximated with a horizontal plane, is taken as a datum. The base-level of deposition within the foreland system may be in any position (below, above or superimposed) relative to the datum, although surface processes on the craton (sedimentation, erosion) tend to adjust the datum to the base-level.

Da Catuneanu et al., 2000

Cunei sedimentari sin-tettonici: la Pianura padana

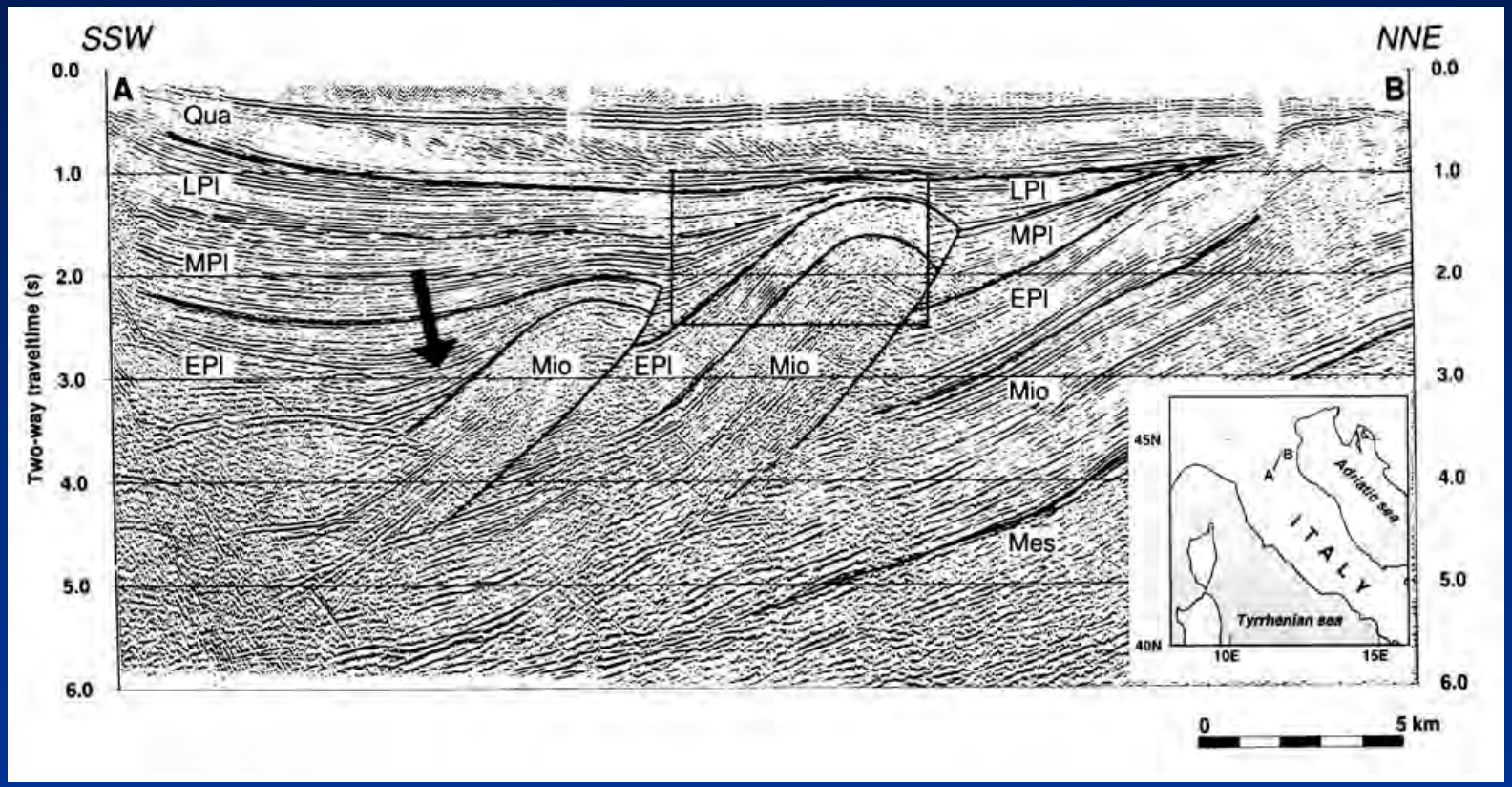

Da Zoetemeijer, 1993

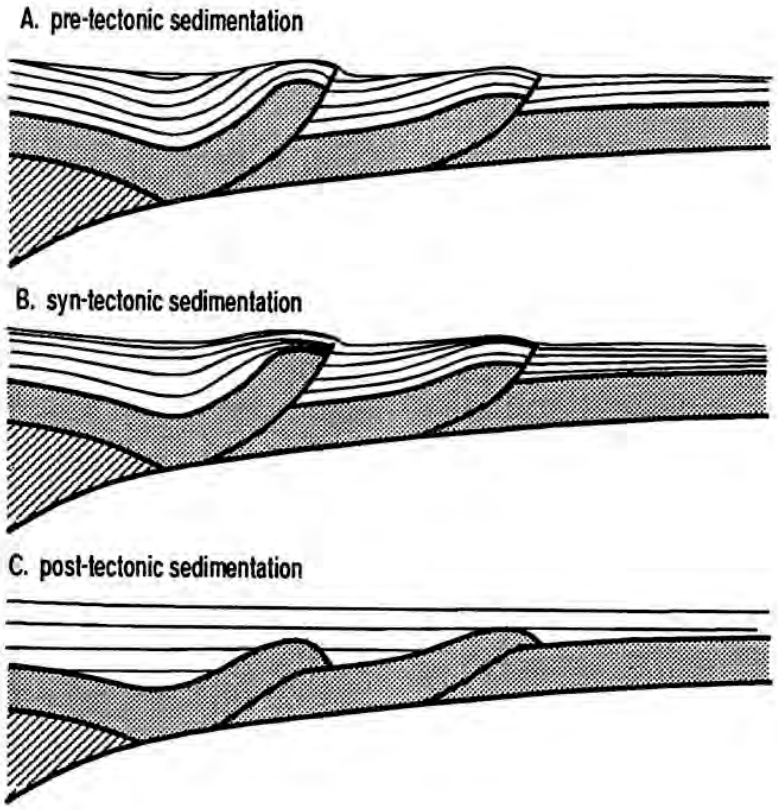

Figure 4-2. Schematic representation of possible basin configurations with sediment deposition (a) before, (b) during, and (c) after thrust interference (modified from Ricci Lucchi, 1986).

Da Zoetemeijer, 1993